

PORT OF WEIPA

# ▶ APPENDIX C

## Sediment budget



# Port of Weipa: Sustainable Sediment Management Assessment

Sediment Budget

Report No. P007\_R03F1



# Port of Weipa: Sustainable Sediment Management Assessment




## Sediment Budget

Report No. P007\_R03F1

September 2018

North Queensland Bulk Ports Corporation Ltd

Version	Details	Authorised By	Date
D1	Unreviewed Draft	Andy Symonds	30/08/2018
D2	NQBP Reviewed Draft	Andy Symonds	14/09/2018
F1	Final	Andy Symonds	28/09/2018

Document Authorisation		Signature	Date
Project Manager	Andy Symonds		28/09/2018
Author(s)	Andy Symonds, Anna Symonds		28/09/2018
Reviewer	Dr Paul Erfemeijer		20/09/2018

### Disclaimer

*No part of these specifications/printed matter may be reproduced and/or published by print, photocopy, microfilm or by any other means, without the prior written permission of Port and Coastal Solutions Pty Ltd.; nor may they be used, without such permission, for any purposes other than that for which they were produced. Port and Coastal Solutions Pty Ltd. accepts no responsibility or liability for these specifications/printed matter to any party other than the persons by whom it was commissioned and as concluded under that Appointment.*

## CONTENTS

<b>1. Introduction</b> .....	<b>1</b>
1.1. Background .....	1
1.2. Report Structure .....	1
1.3. Project Overview .....	1
1.4. Port of Weipa.....	3
<b>2. Local Conditions</b> .....	<b>10</b>
2.1. Gulf of Carpentaria .....	10
2.2. Sediment Characteristics .....	10
2.3. Water Quality Data .....	12
2.4. Sediment Sources .....	16
2.5. Sediment Transport.....	16
2.5.1. Longshore Transport .....	18
2.5.2. Wave Resuspension Relationships .....	20
2.5.3. Sediment Resuspension Calculations .....	24
<b>3. Sediment Budget</b> .....	<b>28</b>
3.1. Approach .....	28
3.2. Regional Sediment Budget .....	32
3.3. Local Sediment Budget .....	37
3.3.1. Transport from DMPA.....	46
<b>4. Summary and Conclusions</b> .....	<b>48</b>
<b>5. References</b> .....	<b>50</b>

## FIGURES

Figure 1. NQBP's SSM Assessment framework. ....	3
Figure 2. Location of the Port of Weipa. ....	6
Figure 3. Close up of the Port of Weipa Inner Harbour area. ....	7
Figure 4. Variable design depths (m LAT) in the Port of Weipa South Channel. ....	8
Figure 5. Variable design depths (m LAT) in the Port of Weipa Inner Harbour. ....	9
Figure 6. Inferred sediment composition for the Weipa region. ....	11
Figure 7. Location of the water quality monitoring sites, along with key port infrastructure. ....	14
Figure 8. SSC data in the Inner Harbour (WQ1 & WQ4). ....	15
Figure 9. SSC data in Albatross Bay (WQ2 & WQ5). ....	15
Figure 10. SSC data in the Amrun region (WQ3 & WQ3b). ....	15
Figure 11. Location of longshore transport wave extraction points. ....	19
Figure 12. Relationship between $H_s$ (at Albatross Bay WRB) and SSC in Albatross Bay (WQ5). ....	21
Figure 13. Relationship between $H_s$ (at Albatross Bay WRB) and SSC in the Inner Harbour (WQ1). ....	21
Figure 14. Relationship between $H_s$ (at Albatross Bay WRB) and SSC at Amrun Port (WQ3b). ....	22
Figure 15. Relationship between $H_s$ (at the Albatross Bay WRB) and the mass of sediment resuspended in Albatross Bay. ....	23
Figure 16. Relationship between $H_s$ (at the Albatross Bay WRB) and the mass of sediment resuspended in the Amrun region. ....	23
Figure 17. Processed SSC data at WQ5 (Albatross Bay). ....	26
Figure 18. Processed SSC data at WQ1 (Embley River). ....	27
Figure 19. Plots showing the sedimentation/erosion, time $H_s$ was above 2 m and total rainfall (May to April) for 2009 to 2018 (PCS, 2018a). ....	29
Figure 20. Sediment cells for regional sediment budget. ....	30
Figure 21. Sediment cells for local Port of Weipa sediment budget. ....	31
Figure 22. Modelled SSC during relatively calm wave conditions in the wet season ( $H_s = 0.54$ m, Direction = $290^\circ$ ). Regional sediment cells are superimposed. ....	34
Figure 23. Modelled SSC during TC Nora in the wet season ( $H_s = 3.5$ m, Direction = $270^\circ$ ). Regional sediment cells are superimposed. ....	35
Figure 24. Modelled SSC during a spring tide with calm wave conditions in the dry season ( $H_s = 0.25$ m, Direction = $90^\circ$ ). Regional sediment cells are superimposed. ....	36
Figure 25. Regional sediment budget for a typical year. Values represent annual resuspension mass. ....	37
Figure 26. Modelled peak spring current speed in Albatross Bay during a flooding tide. ....	40
Figure 27. Modelled peak spring current speed in Albatross Bay during an ebbing tide. ....	41
Figure 28. Local sediment budget for the Port of Weipa for a typical year. Values represent annual net transport (i.e. loss or gain of sediment). ....	42
Figure 29. Modelled bed level change around the Port of Weipa over a 3 month dry season period. ....	43
Figure 30. Modelled bed level change around the Port of Weipa over a 3 month cyclonic wet season period. ....	43
Figure 31. Modelled bed level change around the Port of Weipa over a 3 month typical wet season period. ....	44
Figure 32. Transect locations for Port of Weipa local sediment budget. ....	45
Figure 33. Bed level change resulting from sediment at the Albatross Bay DMPA over the cyclonic wet season. ....	47

## TABLES

Table 1. Historic in-situ dredging volumes at the Port of Weipa (Advisian, 2018). .....	4
Table 2. Typical maintenance dredging volume estimate, declared depth, design depth and footprint for the dredged areas at the Port of Weipa (Advisian, 2018). .....	5
Table 3. Longshore drift calculations.....	18
Table 4. Albatross Bay ambient sediment mass and resuspension rate quantity.....	25
Table 5. Regional annual sediment budget for typical and cyclonic years.....	33
Table 6. Local annual sediment budget for typical and cyclonic years. ....	39
Table 7. Gross and net sediment transport rates and directions around the Port of Weipa. ....	44
Table 8. Loss of sediment from Albatross Bay DMPA and gain in the South Channel.....	47

## APPENDICES

### Appendix A – Numerical Model Development

## Executive Summary

North Queensland Bulk Ports Corporation (NQBP) and Rio Tinto Alcan (RTA) commissioned Port and Coastal Solutions (PCS) who, along with its sub-consultants Water Modelling Solutions and DAMCO Consulting, are undertaking a series of studies to understand whether sedimentation can be managed at the Port of Weipa and at Amrun Port, to avoid or reduce the need for maintenance dredging. The studies form part of NQBP/RTA's Sustainable Sediment Management (SSM) assessment at the Ports, which is aimed at answering the questions regulators have regarding ongoing maintenance dredging.

**Aim:** The aim of this study was to understand the natural sediment transport processes which occur in the Weipa (and Amrun) regions. This includes understanding the source of the sediment, sediment transport pathways, processes controlling the sediment transport and the development of a quantitative sediment budget.

**Local Conditions:** The dominant process which is resulting in sedimentation in the dredged areas at the Port of Weipa (and Amrun Port) is wave action. The wave conditions control the mass of sediment resuspended along the open coastline and within Albatross Bay and the tidal currents subsequently transport the suspended sediment. The sediment will be transported until the bed shear stresses are sufficiently low for the sediment to be deposited (i.e. either the wave energy and tidal current speed have reduced or the sediment has been transported to a sheltered location). The tidal currents also appear to be an important driver within the Inner Harbour area of the Port of Weipa, driving transport by bed load or localised resuspension which can in turn result in localised accretion within the channel.

**Wave Resuspension Relationships:** To better understand the relationship between wave activity and turbidity, numerical modelling simulations were undertaken for a range of wave conditions. The results show an approximate exponential relationship at all locations, with the Suspended Sediment Concentration (SSC) highest in Albatross Bay and lowest in the Inner Harbour region of the Port of Weipa. The increase in SSC is relatively gradual up to a significant wave height ( $H_s$ ) of 2 m, and much more rapid when the  $H_s$  increases beyond this.

**Resuspension Calculations:** Two approaches were adopted to estimate the natural resuspension of fine-grained sediment from the Albatross Bay region and assess the differences between the two approaches. The first approach estimated the annual resuspension through statistical analysis of measured turbidity data, while the second approach estimated annual resuspension using a calibrated sediment transport model. The two approaches provided similar (less than 10% difference) natural annual resuspension estimates for the Albatross Bay region, with the first estimating 38 Mt/yr and the second 35 Mt/yr. The similarity between the two approaches provides confidence that the sediment transport model is able to provide a reliable estimate of the quantitative sediment budget for the region.

**Sediment Budget:** The quantitative sediment budget has been presented at both a regional and a local Port of Weipa scale. The budget shows the following:

- approximately 45 Mt/yr of sediment is resuspended at the Weipa and Amrun regional scale (covering 10,000 km<sup>2</sup>, approximately 130 km along the coast and 80 km offshore) during a typical year and 70 Mt/yr during a cyclonic year;
- the majority of sediment which is suspended at the Weipa and Amrun regional scale is from the local resuspension of existing fine-grained sediment. Wave action drives the resuspension of existing fine-grained sediment within Albatross Bay and along the open coast to the north and south, while tidal currents and locally generated wind waves drive resuspension within the estuaries;



- there is limited input of new sediment to the sediment budget in the Weipa and Amrun regions (less than 1% of the total annual resuspension mass), with the main sources of new fine-grained sediment being from cliff erosion and river discharges/overland flow;
- there is limited net residual transport of sediment (less than 10% of the gross sediment transport in the Port of Weipa local region) and as such the sediment budget is generally balanced. The suspended sediment is typically either transported north and south along the open coastline, or offshore (west) and onshore (east) in Albatross Bay and the adjoining estuaries;
- significant sedimentation occurs in the South Channel of the Port of Weipa, which is mainly due to the resuspension of existing fine-grained sediment within Albatross Bay due to wave action. The suspended sediment is then repeatedly transported backwards and forwards past the channel with 2 – 3% of the total (gross) suspended sediment becoming trapped. Sedimentation occurs predominantly during the wet season due to the increased SSC resulting from larger waves, with limited sedimentation during the dry season when wave conditions are calm and there is little resuspension of sediment from the seabed; and
- limited sedimentation occurs within the dredge areas of the Inner Harbour at Weipa. The results suggest that during cyclonic years some sedimentation can occur at the eastern end of the approach channel and the northern area of the departure channel.

**Transport from Dredge Material Placement Area:** Numerical modelling was also undertaken to better understand the potential for resuspension from the Albatross Bay Dredge Material Placement Area (DMPA) and the fate of any sediment which was resuspended at the DMPA. The modelling showed that sediment placed at the Albatross Bay DMPA only has the potential for significant resuspension during large wave events. It is expected that if the DMPA was not there then the natural seabed sediment would be resuspended, resulting in a similar mass of sediment being suspended (i.e. the DMPA is not significantly increasing the natural resuspension that would occur in the area). Less than 5% of the sediment eroded from the Albatross Bay DMPA was subsequently deposited within the South Channel, with the remaining sediment being thinly distributed within Albatross Bay. This shows how the sediment lost from the Albatross Bay DMPA becomes redistributed across Albatross Bay and is subsequently re-assimilated back into the ambient seabed sediment.

**Implications:** The sediment budget shows that due to the regular reworking of existing fine-grained sediment within Albatross Bay due to wave conditions in the wet season, there is expected to be regular annual sedimentation in the South Channel. As long as the South Channel remains deeper than the adjacent natural seabed, (i.e. remains as a navigable channel) it will act as a sediment sink with sedimentation likely to continue. As such, if no maintenance dredging is undertaken, then ongoing sedimentation in the South Channel will pose a significant risk to Port operations and safety as the sedimentation will result in the South Channel becoming shallower than the declared depth.

## 1. Introduction

### 1.1. Background

North Queensland Bulk Ports Corporation (NQBPC) and Rio Tinto Alcan (RTA) commissioned Port and Coastal Solutions (PCS) who, along with its sub-consultants Water Modelling Solutions and DAMCO Consulting, are undertaking a series of studies to understand whether sedimentation can be managed at the Port of Weipa and at Amrun Port, to avoid or reduce the need for maintenance dredging. These studies form part of NQBPC/RTA's Sustainable Sediment Management (SSM) assessment at the Ports, which aims to answer the questions regulators have regarding ongoing maintenance dredging. The studies being undertaken by PCS as part of the SSM assessment are as follows:

- **Bathymetric Analysis:** the aim of this study is to analyse historic bathymetric data, quantify previous bathymetric changes at the ports and define the natural processes which have caused the changes;
- **Sediment Budget:** the aim of this study is to understand the sediment transport processes which naturally occur at the Ports. This includes understanding the source of the sediment, sediment transport pathways, processes controlling the sediment transport and the development of a quantitative sediment budget;
- **Bathymetric Model:** the aim of this study is to develop interactive predictive sedimentation models for the two Ports. These models will allow future sedimentation predictions to be made for the dredged areas of the Ports which will allow NQBPC/RTA to understand future maintenance dredging requirements at the Ports; and
- **Engineered and Technological Solutions:** the aim of this study is to assess the availability, practicality and feasibility of engineered or technological solutions that could be implemented to reduce sedimentation in the dredged areas of the Ports. The results from this study will then be used to determine whether there are feasible solutions to avoid or reduce the need for maintenance dredging at the Ports.

Each study is being undertaken for both Ports, with separate reports prepared for each of them. **The present report is for the sediment budget study at the Port of Weipa.**

### 1.2. Report Structure

The report herein is set out as follows:

- an introduction to the study is provided in Section 1.
- a summary of the sediment transport conditions for the region is given in Section 2;
- the sediment budget is presented in Section 3; and
- a summary of the findings is detailed in Section 4.

Unless stated otherwise, levels are reported to Lowest Astronomical Tide (LAT). Zero metres LAT is equal to Chart Datum (CD) at the Port of Weipa. Volumes presented throughout are *in-situ* cubic metres.

Wind and wave directions are reported as the direction the wind/waves are coming from in degrees clockwise from True North. Current direction is reported as the direction the current is going to in degrees clockwise from True North.

### 1.3. Project Overview

NQBPC undertakes regular maintenance dredging of the channels and berths at the Port of Weipa to ensure there is sufficient depth for vessels to safely travel to and from the berths (further detail of the historic maintenance dredging is provided in Section 1.4). The sediment

which has historically been removed by maintenance dredging, has been relocated to an offshore dredge material placement area (DMPA) located in Albatross Bay (Figure 2).

NQBP has current State and Commonwealth approvals to support maintenance dredging and at-sea placement of the dredged sediment at the Port of Weipa. The current 10-year permit was issued in 2010. Since then, the process to obtain new long-term sea dumping permits in Queensland has become more onerous.

A Maintenance Dredging Strategy (MDS) has been developed for the ports that are situated within the Great Barrier Reef World Heritage Area (GRBWHA) (TMR, 2016), which provides a framework for the sustainable, leading practise management of maintenance dredging. The MDS has provided a new benchmark in maintenance dredging planning and permitting across all port sectors and it is likely that it will set a national standard for maintenance dredging at all Australian Ports.

A particular aspect that studies are required to inform – derived from the London Protocol, which forms the basis for Australia’s Sea Dumping Act 1981 – is to define whether sedimentation at ports can be managed to avoid or reduce the need for maintenance dredging. Environmental regulators are particularly focused on the following questions:

1. Can sedimentation be managed at the Port to avoid or reduce the need for maintenance dredging?
  - Where do sediments accumulate in the Port and at what volumes and rates?
  - What causes sedimentation in the Port?
  - Does sedimentation at the Port pose a risk to port operations and safety?
  - Why does the Port need to undertake maintenance dredging?
2. If maintenance dredging must occur has there been a comprehensive assessment of whether the material can be beneficially reused?
3. If no beneficial reuse options are available, what would be the most suitable and feasible disposal or placement options?
4. Has a comparative analysis of options been undertaken, which considers human health, social values, environmental impacts and disproportionate costs?

To answer these questions, NQBP developed a framework as part of the SSM assessment at the Port of Hay Point (Figure 1). This framework was subsequently used to inform the framework developed for the MDS, demonstrating that NQBP have been proactive at developing sound long-term maintenance dredging strategies. The studies included as part of the work currently being undertaken by PCS (including the bathymetric analysis for the Port of Weipa, presented in this report) are aimed at answering the questions posed under point 1. Separate studies will be undertaken by NQBP/RTA to answer the other three questions. The findings from all these SSM studies will feed into the development of new long-term maintenance dredging strategies at the Ports of Weipa and Amrun.

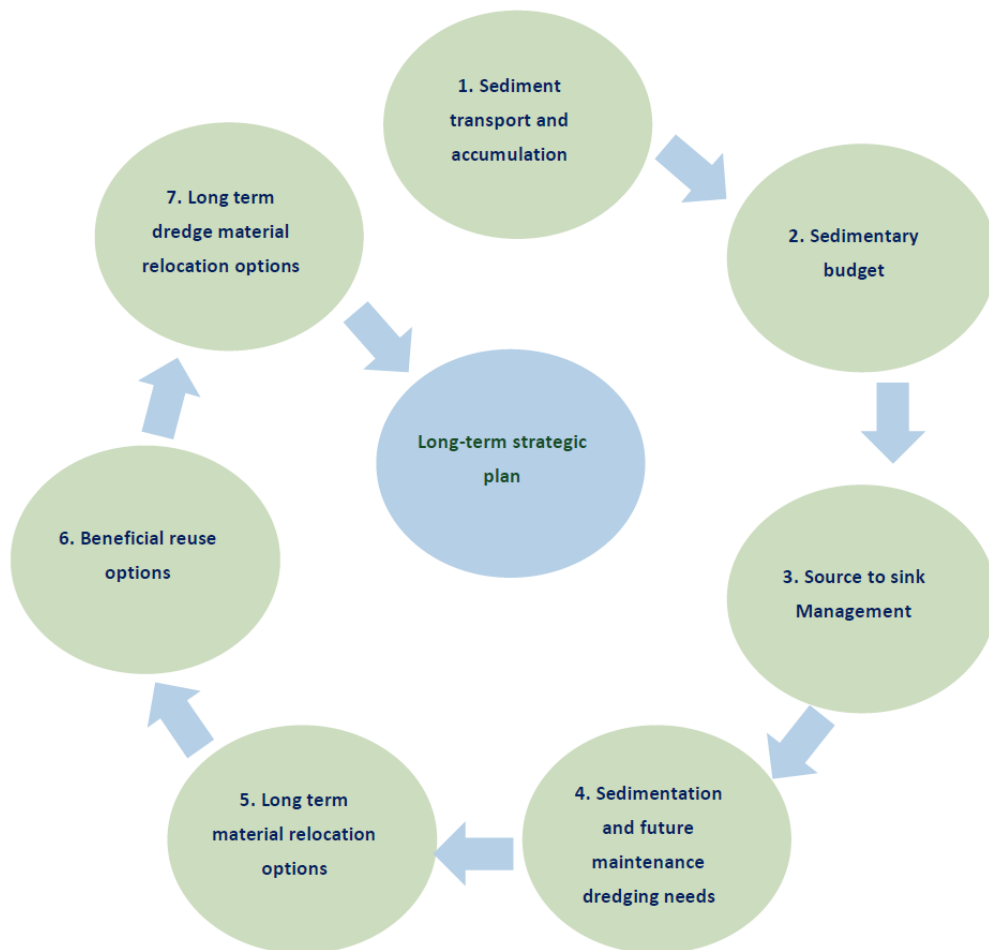


**Figure 1. NQBP's SSM Assessment framework.**

## 1.4. Port of Weipa

The Port of Weipa is located in the Gulf of Carpentaria, on the north-west coast of the Cape York Peninsula in Northern Queensland. The Port is within Albatross Bay, a large embayment, with the wharves and berths located in the Embley River (Figure 2 and Figure 3).

In the 2016/17 financial year, the Port of Weipa handled approximately 36 million tonnes of commodities, including bauxite (>95%), fuel, cattle and general cargo. Rio Tinto Alcan (RTA) currently operates most of the port facilities for the export of bauxite (aluminium ore) from the nearby RTA mine.

The Port of Weipa consists of:

- a main shipping channel in Albatross Bay called South Channel (Figure 2); and
- an Inner Harbour which is within the Embley River and consists of four shipping berths (Lorim Point East and West, Humbug Wharf and Evans Landing) and the Approach and Departure Channels (Figure 3).

Several capital dredging campaigns have been undertaken at the Port of Weipa since the early 1960's, with the most recent capital works undertaken in 2012:

- 1961-63: the South Channel was first dredged across the inner half of Albatross Bay, with the natural South Channel being deepened to a depth of 8.2 m below Low Water Datum (approximately equivalent to the Lowest Astronomical Tide (LAT));
- 1980's: the South Channel was deepened and extended to a length of 14.5 km;
- 2006: the South Channel was widened and deepened (GHD, 2005). Due to variable sedimentation within the South Channel the design depth<sup>1</sup> was increased from the uniform depth of -12.2 m LAT in some areas (see Figure 4 for depths following capital dredging) and due to the deepening, the channel also had to be widened to ensure the batter slopes were stable; and
- 2012: the South Channel was extended by 2.4 km with a design depth of -12.2 m LAT (PaCE, 2011).

The Port has approximately 622 hectares of channels, swing basins and berths where depths are maintained by maintenance dredging. NQBP currently has a 10 year Sea Dumping Permit for the Port of Weipa which allows for an average of 1,200,000 m<sup>3</sup> of sediment to be removed by maintenance dredging per annum, although this includes a contingency for events such as cyclones and so is not realised on an annual basis. Since 2002, maintenance dredging at the Port has been undertaken annually by the Trailing Suction Hopper Dredge (TSHD) Brisbane, with volumes ranging from approximately 300,000 m<sup>3</sup> to 980,000 m<sup>3</sup> (although the 980,000 m<sup>3</sup> dredged in 2002 was because dredging had not been undertaken in 2001). Prior to 2002, maintenance dredging was typically undertaken every two years. The majority of the historic maintenance dredging at the Port of Weipa has been towards the western end of the South Channel, with limited maintenance dredging occurring in the Inner Harbour. A summary of the historic dredging works is provided in Table 1 and the average volumes removed (2012 to 2016) are detailed in Table 2.

The fact that the Port requires annual maintenance dredging relates to the fact that regular sedimentation occurs. In addition to the regular sedimentation, it has also been observed that extreme events such as tropical cyclones (TCs) can result in significant increases in the sedimentation and therefore increased maintenance dredging requirements at the Port. To reduce the risk of increased sedimentation from a TC resulting in operational or safety issues at the Port, the maintenance dredging has typically been scheduled immediately after the wet season (when TCs occur) and the design depths have been adjusted over time based on the variable sedimentation that occurs in the Port (Figure 4 and Figure 5). In addition, the Dynamic Under Keel Clearance (DUKC) system, by OMC International, is in operation at the Port of Weipa to ensure safe vessel navigation and to help optimise port operations.

**Table 1. Historic in-situ dredging volumes at the Port of Weipa (Advisian, 2018).**

Year	Type of Dredging	Volume of in-situ Material removed (m <sup>3</sup> )
2002	Maintenance	976,585
2003	Maintenance	463,513
2004	Maintenance	621,650
2005	Maintenance	803,098
2006	Capital and Maintenance	2,976,868
2007	Maintenance	711,000
2008	Maintenance	774,100
2009	Maintenance	553,457
2010	Maintenance	832,779

<sup>1</sup> the design or dredge depth is the depth that engineers have selected as suitable for the safe and efficient operation of the Port at all tidal levels with natural sedimentation also factored in. The declared depth is the depth designated by the harbour master and reflects the shallowest depth within the area.

2011	Maintenance	470,820
2012	Capital and Maintenance	927,057
2013	Maintenance	644,525
2014	Maintenance	394,523
2015	Maintenance	368,384
2016	Maintenance	504,071
2017	Maintenance	297,301
2018	Maintenance	591,875

**Table 2. Typical maintenance dredging volume estimate, declared depth, design depth and footprint for the dredged areas at the Port of Weipa (Advisian, 2018).**

Port Area	Volume Estimate (m <sup>3</sup> )	Declared Depth (m below LAT)	Design Depth <sup>1</sup> (m below LAT)	Footprint (ha)
South Channel	465,000	11.1	12.1 to 14.1	256
Approach Channel	24,000	7.3	7.3	272.5
Departure Channel	12,000	11.1	11.1 to 11.8	138.3
Evans Landing	500	9.4	9.4	0.5
Humbug	500	9.5	9.5	0.86
Lorim Point	500	12.3	12.3	2.45
Tug Berth	500	9.0	9.0 <sup>2</sup>	2.12

<sup>1</sup> in some areas the design depth is variable due to natural variability in the sedimentation that occurs. The design depths are shown in Figure 4 and Figure 5.

<sup>2</sup> although the design depth at the Lorim Point Tug Berths is -9 m LAT it has not been dredged to that depth (currently around -5 m LAT) and due to the existing depths, the TSHD Brisbane is not able to dredge the area and so bed levelling has been used to maintain the depths to -5 m LAT.



Figure 2. Location of the Port of Weipa.



Figure 3. Close up of the Port of Weipa Inner Harbour area.



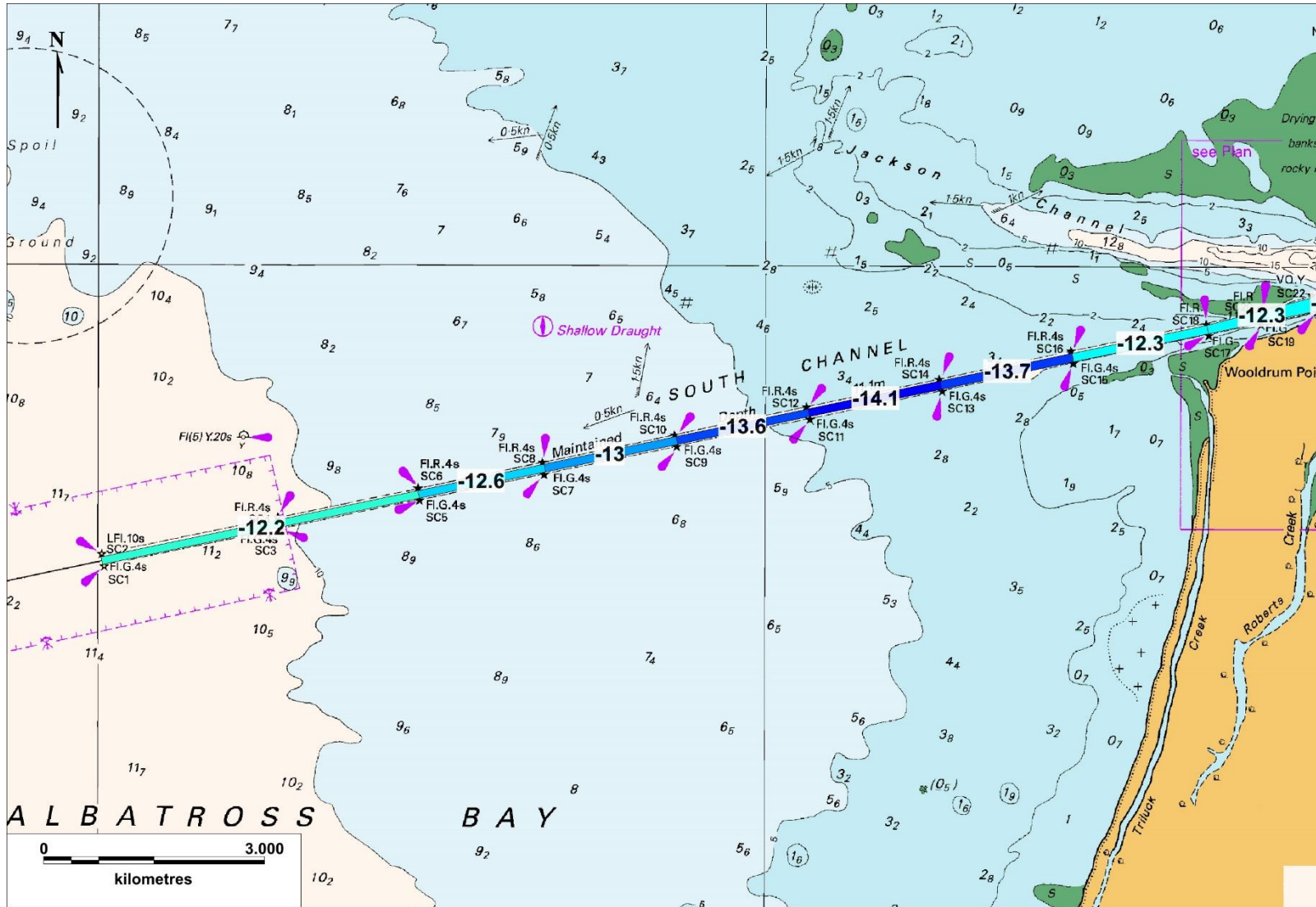


Figure 4. Variable design depths (m LAT) in the Port of Weipa South Channel.

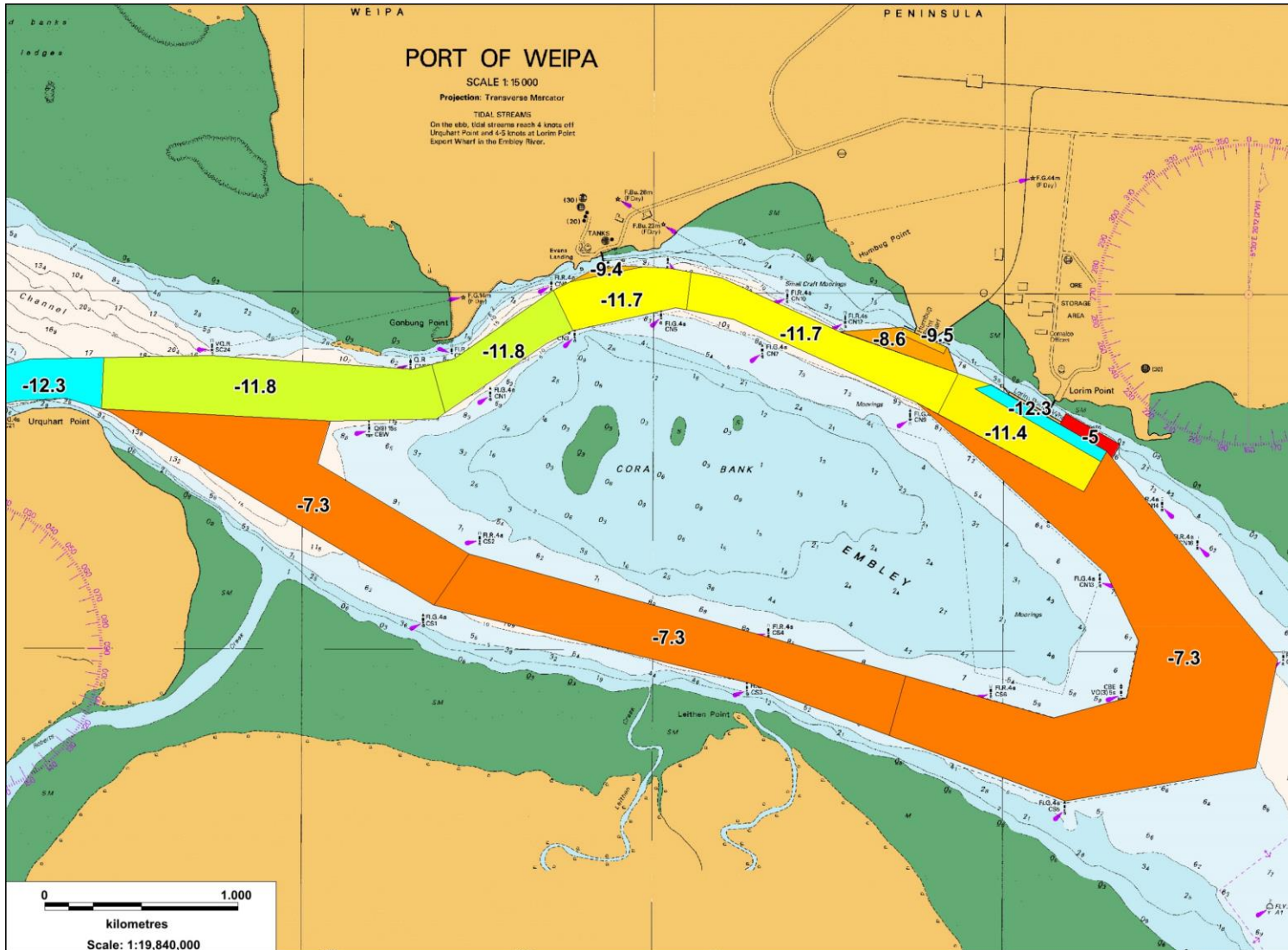


Figure 5. Variable design depths (m LAT) in the Port of Weipa Inner Harbour.

## 2. Local Conditions

### 2.1. Gulf of Carpentaria

Weipa is located within the Gulf of Carpentaria on the western side of the Cape York Peninsula, approximately 250 km south of the northern tip. The Gulf of Carpentaria is an epicontinental sea (a shallow sea on top of a continent), which means that the seabed in the gulf is the continental shelf of Australia. As a result, the Gulf is a relatively shallow sea throughout (maximum depths in the order of 60 m).

The east coast of the Gulf of Carpentaria is subject to mesotidal and relatively low wave energy conditions. Due to the limited fetch in the Gulf of Carpentaria the wave climate is characterised by calm wave conditions in the dry season (when the wind direction is offshore) while locally generated wind waves and larger cyclonic waves can occur during the wet monsoonal period.

### 2.2. Sediment Characteristics

Exploration for commercial deposits of bauxite in the Gulf of Carpentaria in the early 1970's involved a number of marine surveys that included seismic and borehole data from the inner shelf environments offshore of Weipa (e.g. Bates et al., 1971). Results from the drilling showed that the surface sediment typically comprised of Holocene marine muds with thicknesses of less than 1 m north of Duyfken Point (Figure 2) to more than 6 m in parts of Albatross Bay (Hudson, 1995). Based on information from available literature, the deposits which typically occur along the eastern shoreline of the Gulf of Carpentaria can be categorised by water depths as follows:

- Depths of less than 20 m: sands and sandy muds are present on top of older sediment (pre-Holocene). Typically, sands are present along the open coast down to 10 m water depth, while in sheltered embayments such as Albatross Bay silts and clays are present (Michaelsen, 1994); and
- Depths of 20 to 60 m: relict alluvial (river) sands and gravels are common on the seafloor (Hudson, 1995).

In the Gulf of Carpentaria from Weipa north, there is little evidence for the accumulation of significant volumes of terrigenous sediment on the present day inner shelf, suggesting limited sources of new sediment to the system (Hudson, 1995).

The sediment composition information from the literature agrees well with the findings from recent sediment sampling undertaken in the region as part of the impact assessment for Amrun Port and the ongoing maintenance dredging requirements at the Port of Weipa. Based on the available information as well as findings from the bathymetric analysis and observations during the site visit (PCS, 2018a) a sediment composition map has been developed for the region (Figure 6). The map shows the following:

- the majority of Albatross Bay is made up of sandy/clayey silt;
- the ebb tidal deltas and some upstream areas of the main channels in the Pine, Mission and Embley Rivers are made up of predominantly silty sand;
- the main channels of the Pine, Mission and Embley Rivers close to the river mouths are made up of predominantly sand, with some sandy gravel present in the Embley River where the current speeds are highest (it is likely that sandy gravel will be present in the other rivers, but there are no samples available to confirm this);
- the nearshore areas along the open coast and the southern side of Albatross Bay is predominantly sandy sediment; and
- the offshore region (deeper than 15 to 20 m) is predominantly made up of silty sand.

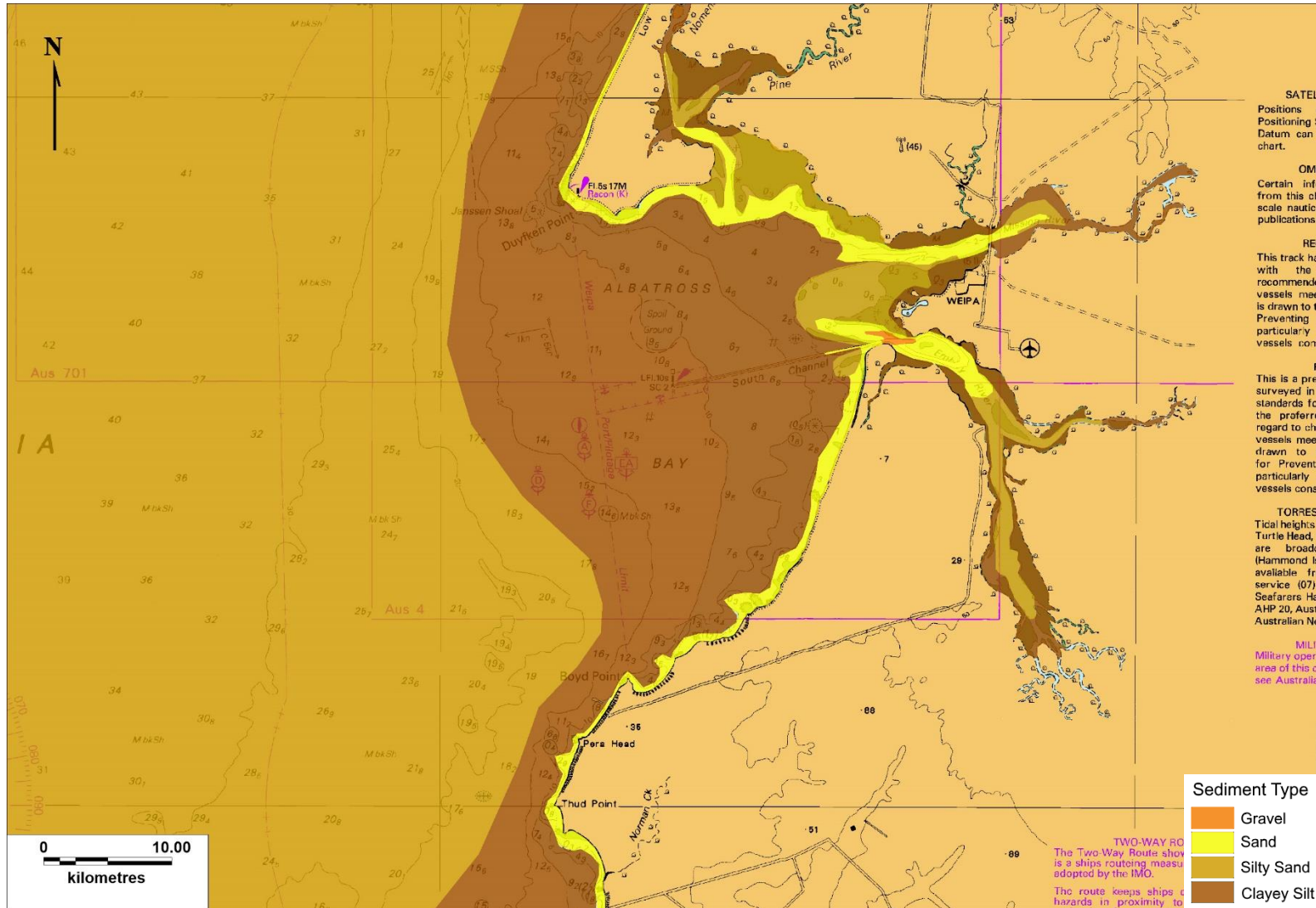


Figure 6. Inferred sediment composition for the Weipa and Amrun regions.

### 2.3. Water Quality Data

Additional measured water quality data are available for the Port of Weipa and Amrun Port regions since the previous conceptual sediment transport understandings at the two Ports were developed (PCS, 2018a & 2018b).

Turbidity data have been measured using self-logging backscatter probes which take 250 samples over an eight second period and record in Nephelometric Turbidity Units (NTU). The instruments were serviced (i.e. loggers cleaned, data downloaded and batteries replaced) every six weeks. Site specific correlations between NTU and the suspended sediment concentration (SSC) have been developed by James Cook University (JCU) by undertaking concurrent turbidity measurements and water samples and then subsequently analysing the water samples in the laboratory to determine the mass of sediment and therefore the SSC.

Water quality data are available at five sites (Figure 7) from the middle of January 2018 to the middle of July 2018<sup>2</sup>. It should be noted that the site at WQ3 was moved in March 2018 to WQ3b as this site had been used for previous water quality monitoring and was considered preferential over WQ3. The data has been used to provide an indication of how the water quality varies spatially and temporally in the region, with the different regions discussed below (Figure 8 to Figure 10).

- **Embley River, Inner Harbour (WQ1 & WQ4):** within the Inner Harbour region of the Embley River there is a clear tidal signal in the SSC, with higher SSC during spring tides and lower SSC during neap tides. In addition, during periods with larger waves and increased SSC in Albatross Bay the peaks in SSC within the Inner Harbour also increase. The SSC in the Inner Harbour has regular large fluctuations, with the largest peaks occurring on the flooding tide suggesting that the highest SSC is either due to suspended sediment being imported from Albatross Bay or the high current speeds during the flooding tide locally resuspending sediment in the Inner Harbour area.
- **Albatross Bay, South Channel (WQ2 & WQ5):** in Albatross Bay, the SSC is strongly influenced by the wave activity, with SSC generally only exceeding 100 mg/l during periods with larger waves. During calm periods, there is a tidal signal in the SSC, with higher SSC during spring tides and lower SSC during neap tides.
- **Amrun Region, Boyd Head and Pera Head (WQ3 & WQ3b):** the SSC in the Amrun region generally appears to be lower than the SSC within Albatross Bay (especially at site WQ3b, adjacent to Pera Head, where SSC is very low). Similar to Albatross Bay, the SSC is influenced by the wave activity although with the limited data available at these sites it isn't possible to determine the influence of wave activity during smaller wave events.

The SSC data at WQ5 provides the most continuous dataset out of the five sites. Data are available for the majority of the time from January 2018 until July 2018, including approximately three months of the wet season and four months of the dry season. The data show a clear change in the SSC in Albatross Bay between the wet and dry seasons, with the SSC in the wet season being higher than in the dry season. The wet season is characterised by peaks in SSC (more than 100 mg/l, with larger events exceeding 1,000 mg/l) due to the larger wave conditions with periods of lower SSC between due to calm wave conditions. In contrast, the dry season is characterised by low SSC (peaks of up to 10 mg/l during neap tides and 30 mg/l during spring tides) varying due to the spring-neap cycle (higher SSC during spring tides when tidal currents are higher) and when wave activity increases the peaks can increase up to approximately 100 mg/l.

The measured data in the Inner Harbour (WQ1 and WQ4) shows limited variation between the wet and dry seasons. At WQ4 the data during the wet season (up to April 2018) shows more variability in the peaks in SSC (peaks exceeding 500 mg/l) compared to the dry season

<sup>2</sup> Due to errors in the data and instrument loss the data return is variable between the five sites.

(peaks of up to 200 mg/l). However, the data also show that when the instrument was retrieved and redeployed in the middle of April the SSC dropped from 300 mg/l to 100 mg/l over the 24 hours that the instrument was out of the water. It is possible that the instrument was either deployed in a slightly different location where the SSC was lower or that following servicing/changing of the instrument a less noisy and lower turbidity signal was recorded. As such, although initial review of the data suggest that the SSC was higher in the wet season, it was probably only noticeably higher during the large wave events in the wet season. The data at WQ1 indicate the opposite to the data at WQ4, with lower SSC in the wet season and higher SSC in the dry season which is surprising. It is expected that during periods when the wave conditions in Albatross Bay are calm, the SSC would be lower in the wet season compared to during the dry season due to the strong easterly to south-easterly winds during the dry season causing small wind waves in the estuaries which would increase resuspension. However, during periods of the wet season with large waves and increased SSC in Albatross Bay it is expected that increased peaks in SSC would also occur within the Inner Harbour area of the Embley River due to suspended sediment being imported during the flooding tide. As a result, the measured data collected at WQ1 up to the 15<sup>th</sup> March 2018 is not considered to be reliable and has not been used further in the assessment.



**Figure 7. Location of the water quality monitoring sites, along with key port infrastructure.**

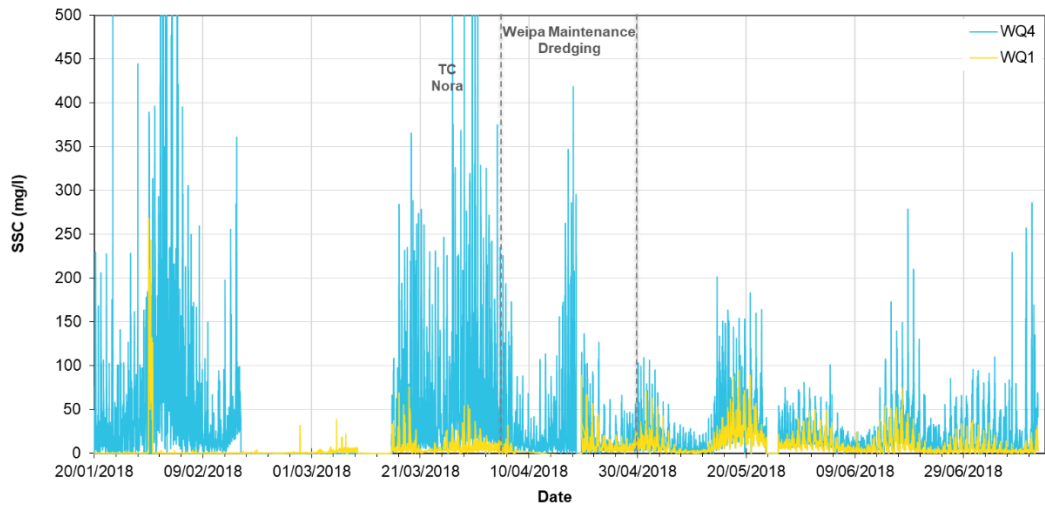


**Figure 8. SSC data in the Inner Harbour (WQ1 & WQ4).**

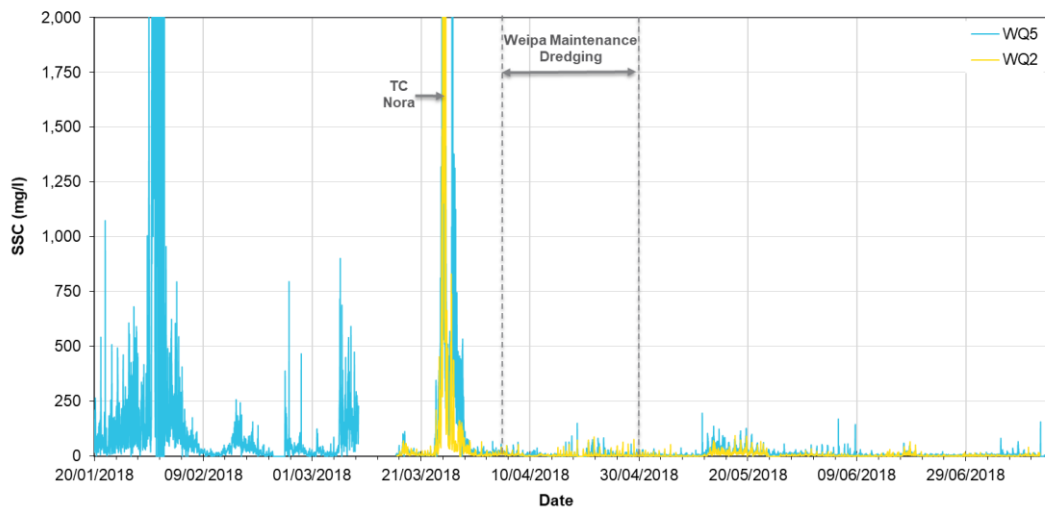


**Figure 9. SSC data in Albatross Bay (WQ2 & WQ5).**

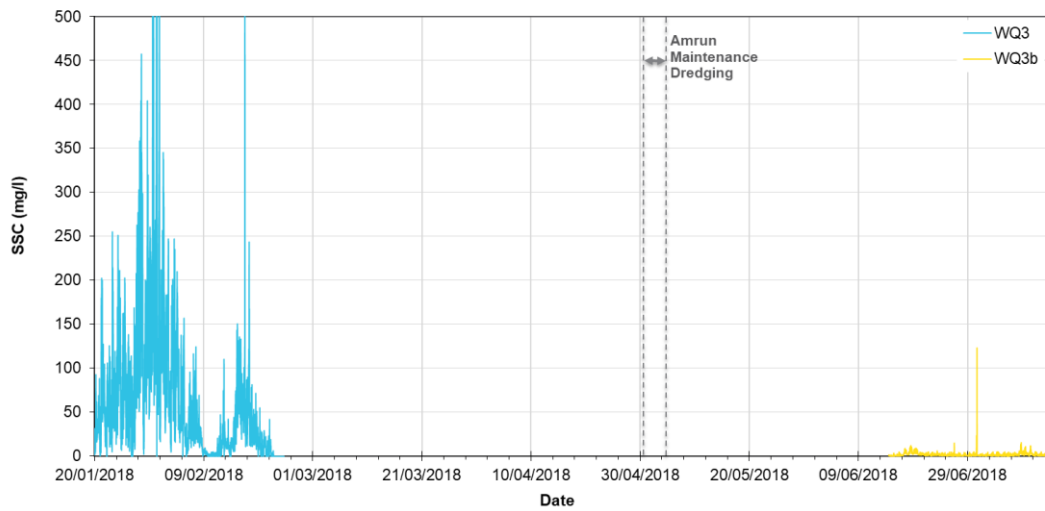


**Figure 10. SSC data in the Amrun region (WQ3 & WQ3b).**



## 2.4. Sediment Sources

In order to develop a sediment budget, it is important to understand the sources of sediment which contribute to sediment transport in the region. There are two types of sediment sources:

- **sources of new sediment:** for the Weipa (and Amrun) region the main sources of new sediment to the marine system are from cliff erosion and river discharge/overland flow, although there will also be small inputs from the erosion and reworking of carbonate reefs; and
- **sources of existing sediment:** for the Weipa (and Amrun) region the main source of existing sediment which contributes to the sediment transport is from the surface sediment on the seabed, although the sediment in the estuaries, particularly in shallow intertidal areas, will also contribute.

Analysis of measured water quality data by PCS (2018a) indicates that heavy rainfall does not result in a significant increase in SSC in the Embley and Hey Rivers. Based on this and the fact that the rivers which connect to Albatross Bay all have relatively small catchments due to the flat topography of the land, it is expected that any sediment inputs from river discharge and overland flow in the Weipa and Amrun region will be small. In addition, due to the limited amount of coral in the region (RTA, 2011), the input of sediment from the erosion and reworking of carbonate reefs is also expected to be small. As such, neither of these two sources will be considered as part of the sediment budget.

The input of new sediment to the marine environment from cliff erosion can be estimated based on existing information. The erosion rate of the cliffs between Boyd Point and Thud Point was estimated to be in the order of 0.5 m/yr (WorleyParsons, 2008). The approximate length of coastline where the distinctive kaolinite cliffs with a bauxite surface layer occur is approximately 9 km between Boyd Point and Thud Point as well as a 7 km stretch to the north of Boyd Point. If we assume an average height for the cliffs of 10 m then we can calculate that cliff erosion results in an input of approximately 75,000 m<sup>3</sup>/yr of sediment to the marine environment. If we assume an average dry density for the eroded sediment of 1.6 t/m<sup>3</sup> (Van Rijn, 1993) and that the majority of the sediment is fine grained clay (assume 80% clay and silt, 20% sand and gravel) then we can calculate that cliff erosion results in the input of approximately 100,000 t/yr of silt and clay to the marine environment and 25,000 t/yr of sand and gravel. It is important to note that the erosion rate adopted is only an estimate and is based on the best available information. The quantum of the sediment input from cliff erosion could therefore be assumed to be larger or smaller than the value presented. However, this would not alter the sediment budget as the input is small relative to the sediment already in the system (discussed below).

The primary source of sediment which contributes to the increased turbidity observed in Albatross Bay and in the Amrun region is from sediment which is already present on the seabed. Sediment sampling in the region found that out to depths of between 15 and 20 m below LAT a thin silt and clay surface layer of 0.1 to 0.5 m thickness was present with firm clays underneath. If we assume that a 0.3 m thick surface layer of silt and clay is present throughout Albatross Bay down to Thud Point, extending out to 18 m below LAT (based on sediment sampling the surface sediment starts to be sandy in deeper water than this), then there is in the order of 300 Mm<sup>3</sup> of fine grained silt and clay available for resuspension in this region (excluding the estuaries). As this sediment is loosely consolidated the dry density would be in the order of 0.7 t/m<sup>3</sup> (McCook et al, 2015), which gives approximately 200 Mt of fine-grained sediment in the Weipa and Amrun region available for regular resuspension.

## 2.5. Sediment Transport

The findings of the recent bathymetric analyses at the Port of Weipa (PCS, 2018a) and Amrun Port (PCS, 2018b) can be used to help understand the dominant sediment transport processes in the region. The key findings are summarised below:

- the majority of the historical sedimentation at the Port of Weipa has occurred in the South Channel with limited sedimentation in the Inner Harbour. The sedimentation within the South Channel has been spatially variable, with the highest rates occurring between Beacons SC14 and SC10, where the channel design depth is deepest. Sediment sampling in the South Channel correlates well with the findings of the bathymetric analysis, with the sediment composition changing from predominantly sand and gravel close to the mouth of the Embley River (where limited regular sedimentation has occurred), to predominantly silt and clay between SC16 and SC14 (and beyond to SC2) where regular sedimentation has occurred. The historical sedimentation in the South Channel has been highest at the sides of the channel, with the propeller wash from laden vessels leaving the Port either limiting the sedimentation or in some areas resulting in erosion;
- in the Inner Harbour area of the Port of Weipa the relatively high tidal current speeds limit deposition of fine-grained sediment in most areas. In the limited areas where sedimentation has occurred the sediment typically deposited has been predominantly composed of sand. In general, the sedimentation is thought to be due to the localised process of the existing shallow sand banks (mainly Cora Bank) encroaching on the channel, as a result of either bed load or suspended load transport driven by the tidal currents. In addition, the propeller wash resulting from vessel operations in the Inner Harbour was found to have resulted in erosion of the seabed at the berths at Lorim Point Wharf and around the eastern bend of the approach channel; and
- at Amrun Port the bathymetric analysis showed that the berth pocket has been subject to regular ongoing sedimentation, with the sediment deposited being predominantly silt and clay. The sedimentation has been due to the resuspension of the loosely consolidated fine-grained surface layer of sediment by wave action and the subsequent transport of this sediment in suspension by the tidal currents. The tidal currents flow approximately parallel with the shoreline which means that suspended sediment can be transported across the berth pocket on both the flood and ebb tide. The berth pocket has a high trapping efficiency as it is relatively narrow (70 to 110 m) in the direction of the dominant tidal currents and deep relative to the natural seabed (-16.2 m LAT compared to -11 to -12 m LAT). As such, any sediment which is deposited in the berth pocket is unlikely to be naturally resuspended.

At the Port of Weipa it was found that there was a positive correlation between the significant wave height ( $H_s$ ) and sedimentation, with the three years when the  $H_s$  was above 2 m for the most time, corresponding with the three years when the most sedimentation was observed in the South Channel. In addition, the year when the most erosion occurred in the South Channel corresponds with the only year when the  $H_s$  was never above 2 m. These findings also correlate with numerical modelling results (see Appendix A for details of the numerical modelling) which show that the area of the South Channel where the deposition starts to occur corresponds with where the current speeds start to reduce away from the entrance of the Embley River (see Section 3.3 for further details), potentially allowing fine-grained sediment to be deposited and not be resuspended on the subsequent tide.

The findings indicate that the dominant process resulting in sedimentation in the dredged areas at the Port of Weipa (and Amrun Port) is wave action. The wave conditions control the mass of sediment resuspended along the open coastline and within Albatross Bay and the tidal currents subsequently transport the suspended sediment. The sediment will be transported until the bed shear stresses are sufficiently low for the sediment to be deposited (i.e. either the wave energy and tidal current speed have reduced or the sediment has been transported to a sheltered location). The tidal currents also appear to be an important driver within the Inner Harbour area of the Port of Weipa, potentially driving transport by bed load or localised resuspension which can result in localised areas of accretion within the channel.

### 2.5.1. Longshore Transport

There is the potential for the longshore transport of sediment on the shorelines which are exposed to wave action. Based on visual observations during an aerial survey of the region as well as sediment samples collected at Amrun Port, which found the median grain size to be 0.6 mm (WorleyParsons, 2013), these shorelines are typically characterised by sandy sediment. Previous longshore transport calculations were undertaken for the shoreline at Amrun Port and found that the net transport was in a northerly direction (although some storm events did result in a net southerly transport of sediment) and the majority of the transport occurred during cyclonic storm events (WorleyParsons, 2008). The average volume of sediment transported by a storm event was estimated to be 16,000 m<sup>3</sup> based on 16 historical cyclones (WorleyParsons, 2008).

For the present study, longshore transport calculations were undertaken for a year with a typical wet season (2016) and for a year with a wet season which included a cyclone (TC Nora) (2018). Wave conditions were modelled using the MIKE Spectral Wave model (see Appendix A for further details) and wave conditions were extracted at four locations (Figure 11). The Kamphius (1991) method was adopted to calculate the longshore drift as this has often been found to provide the most realistic longshore drift predictions (e.g. Wang et al (2002); and Shanas & Kumar (2014)). A grain size of 0.6 mm has been adopted and the beach slope was calculated based on the available hydrographic charts.

The predicted longshore drift rates are presented in Table 3. The results show that the highest longshore transport rate is at the beach at Amrun Port, with annual net transport rates in a northerly direction of 21,000 to 32,000 m<sup>3</sup>/yr. As expected, the longshore transport rates within Albatross Bay are lower than those on the open coast to the north and south of the bay due to the shallow water in Albatross Bay attenuating some of the wave energy before it reaches the shoreline. The longshore transport rate along the shoreline to the north of Albatross Bay is approximately four times lower than the transport at Amrun and the results show that the net transport direction can vary. This suggests that the shoreline to the north of Albatross Bay is approximately aligned with the direction of the largest waves which means that the gross and net transport rates are relatively low and the net direction can vary due to slight differences in the offshore wave direction.

**Table 3. Longshore drift calculations.**

Location	Northerly Transport (m <sup>3</sup> /yr)	Southerly Transport (m <sup>3</sup> /yr)	Net Transport (m <sup>3</sup> /yr) <sup>1</sup>
<b>Typical Year</b>			
North of Albatross	2,100	-8,600	-6,400
Albatross North	1,800	0	1,800
Albatross South	1,800	-500	1,300
Amrun	23,300	-1,800	21,400
<b>Cyclonic Year</b>			
North of Albatross	12,500	-4,200	8,300
Albatross North	2,600	0	2,600
Albatross South	2,600	-1,000	1,700
Amrun	34,300	-1,800	32,400

<sup>1</sup> positive net transport rates represent transport to the north while negative rates represent transport to the south. Note: to convert the transport rates from m<sup>3</sup>/yr to t/yr multiply by 1.6 (Van Rijn, 1993).

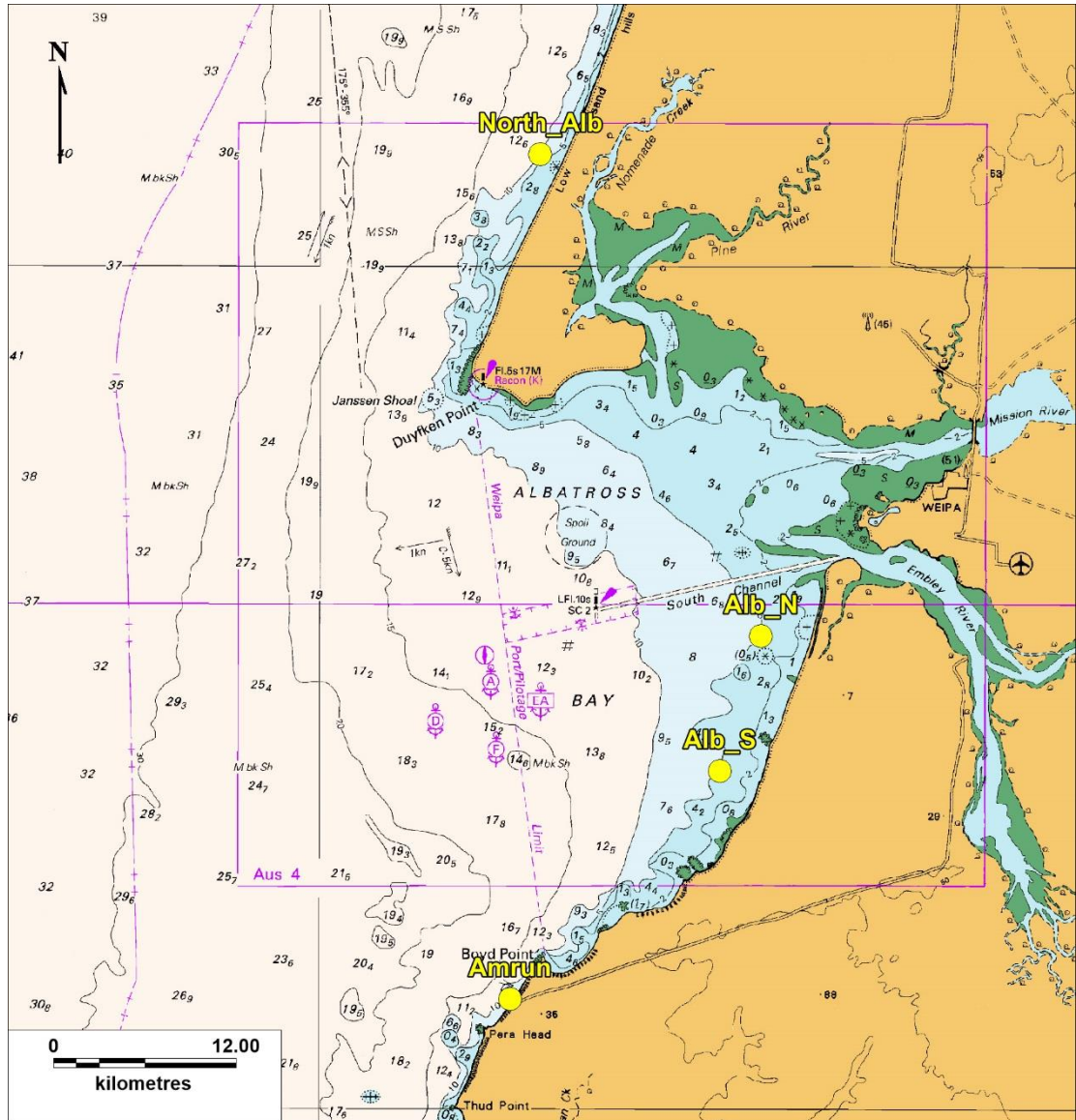


Figure 11. Location of longshore transport wave extraction points.

### 2.5.2. Wave Resuspension Relationships

As noted in Section 2.3, the SSC in Albatross Bay and in the Amrun region is strongly influenced by the wave activity, with data showing that the SSC increases as the wave height increases. Due to the wind and wave conditions within the Gulf of Carpentaria, the local wind conditions at Weipa do not directly relate to the wave conditions and so it is not possible to relate the local wind conditions to SSC. To better understand the relationship between wave activity and SSC a number of numerical modelling simulations (see Appendix A for further details of the numerical model) were undertaken for a range of wave conditions.

The SSC data shows that when the wave conditions are calm there is a spring-neap signal in the SSC data (i.e. higher SSC during spring tides due to the increased tidal current speeds). However, when the wave activity increases the relative importance of the tidal range on the SSC reduces. As such, all simulations have assumed the same tidal conditions, with the peak of the wave event coinciding with spring tides. If neap tides were assumed then similar relationships would be expected but with lower SSC when the wave conditions were small (e.g.  $H_s$  of 1 m and below).

The sediment transport model was configured to simulate an eight-day period which coincided with a representative wet season wave event (wave direction from the west north-west). This typical wave event formed the basis of the model setup for six different synthesised scenarios in which the wave boundary was scaled such that the peak significant wave height ( $H_s$ ) at the Albatross Bay WRB equated to a pre-defined value (every 0.5 m from 0.5 to 3 m). A wet season period was selected as during the dry season the wave conditions are calmer, with the  $H_s$  generally being below 0.5 m and only exceeding 1 m during the peaks of wave events for a few times over the season (e.g. 3 to 4 events per dry season).

Results from model simulations were processed to show how the SSC varies depending on the wave conditions at three locations (Albatross Bay (WQ5), the Inner Harbour (WQ1) and at Amrun Port (WQ3b), see Figure 7 for a map of locations). The relationships are shown in Figure 12 to Figure 14. The plots show an approximate exponential relationship at all locations, with the SSC highest in Albatross Bay and lowest in the Inner Harbour. The increase in SSC is relatively gradual up to an  $H_s$  of 2 m, and much more rapid when the  $H_s$  increases beyond this.

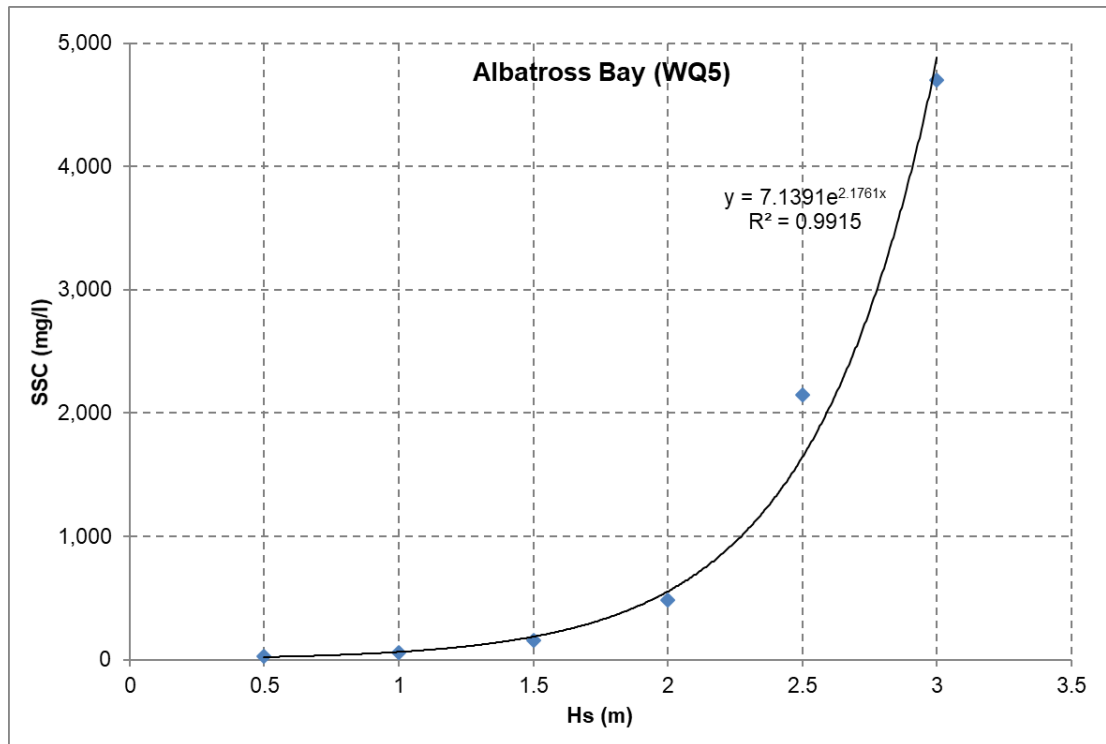


Figure 12. Relationship between H<sub>s</sub> (at Albatross Bay WRB) and SSC in Albatross Bay (WQ5).

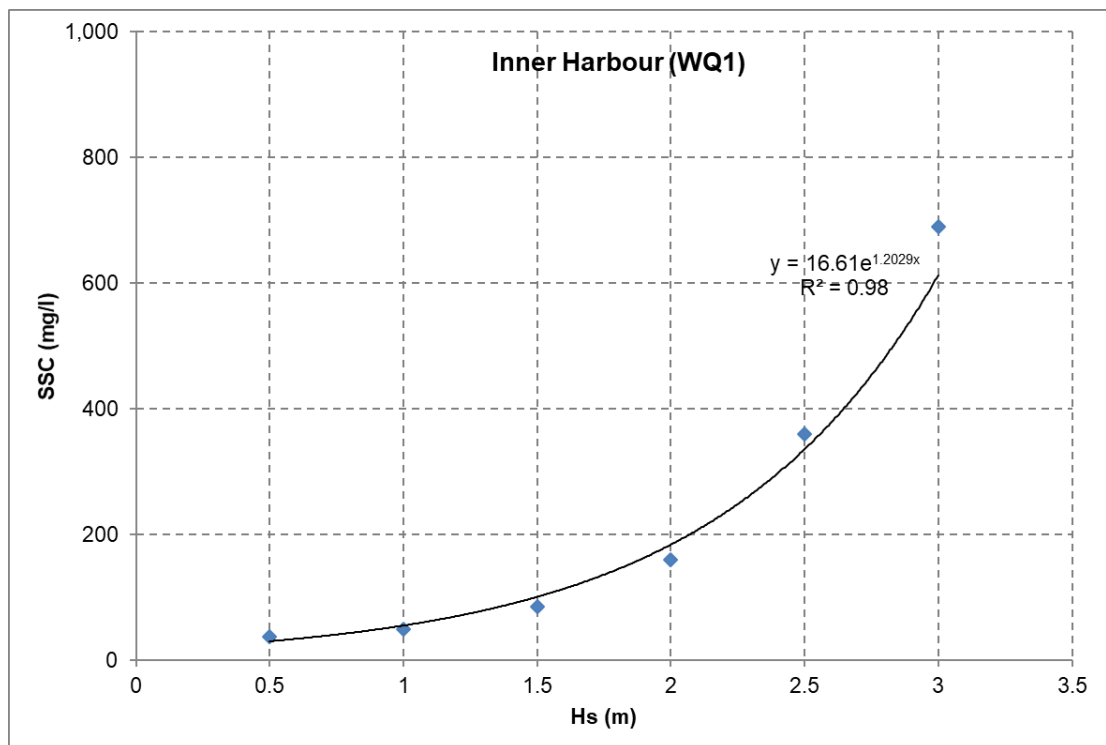


Figure 13. Relationship between H<sub>s</sub> (at Albatross Bay WRB) and SSC in the Inner Harbour (WQ1).

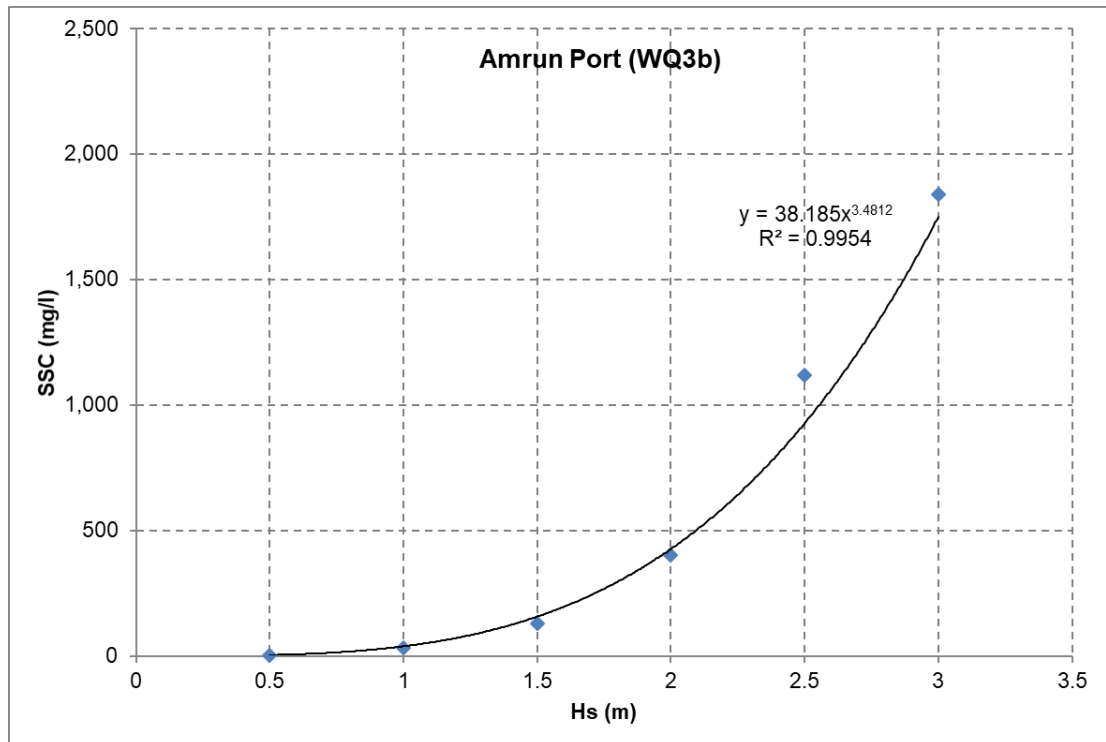


Figure 14. Relationship between  $H_s$  (at Albatross Bay WRB) and SSC at Amrun Port (WQ3b).

The results from the model simulations have also been processed to show how the mass of sediment resuspended by the wave event varies based on the wave conditions. This has been calculated for a region covering all of Albatross Bay (to a depth of approximately -17.5 m LAT) and the three adjoining estuaries (approximate total area of 1,150 km<sup>2</sup>) and for an area 9 km to the north and south of Amrun Port which extends offshore to a depth of -17.5 m LAT (approximate area = 110 km<sup>2</sup>). The relationships are shown in Figure 15 and Figure 16. Like the SSC relationships there is an approximate exponential relationship, with the mass of sediment resuspended increasing significantly when  $H_s$  exceeds 2 m. The reason for the non-linear relationship is firstly because as the wave height increases the spatial area where erosion can occur increases as the waves can resuspend sediment in deeper water (i.e. more of the seabed is subject to erosion) and secondly because the wave energy increases as the wave height increases and so the erosion rate increases as well (i.e. the seabed erodes quicker).

The plots show that the total mass of sediment resuspended in the Albatross Bay region is almost ten times larger than that in the Amrun region, but this is to be expected given that the spatial area is approximately ten times larger (1,150 km<sup>2</sup> compared to 110 km<sup>2</sup>). The modelling predicts that for a spring tide wet season wave event with an  $H_s$  of 2 m approximately 1.5 Mt and 0.2 Mt of sediment is resuspended from within Albatross Bay and the Amrun region, respectively (similar masses would be expected for a neap tide event). This value increases by more than five times when the  $H_s$  increases to 3 m, with approximately 10 Mt and 1.3 Mt being resuspended from within Albatross Bay and the Amrun region, respectively.

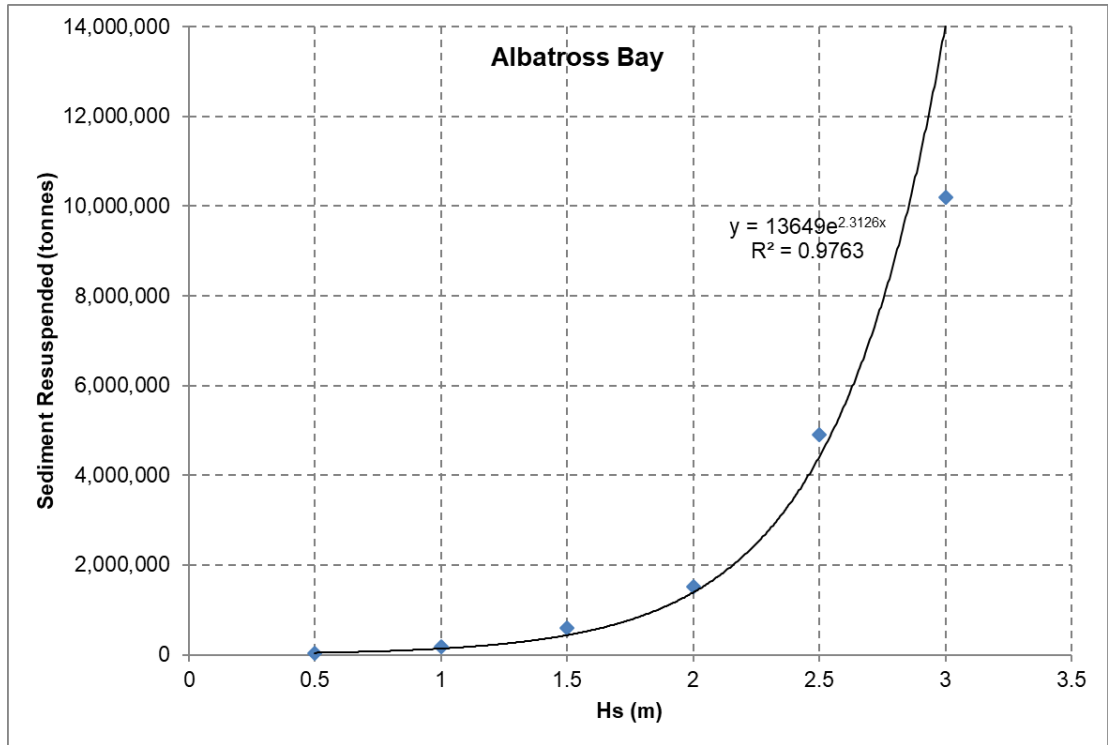


Figure 15. Relationship between  $H_s$  (at the Albatross Bay WRB) and the mass of sediment resuspended in Albatross Bay.

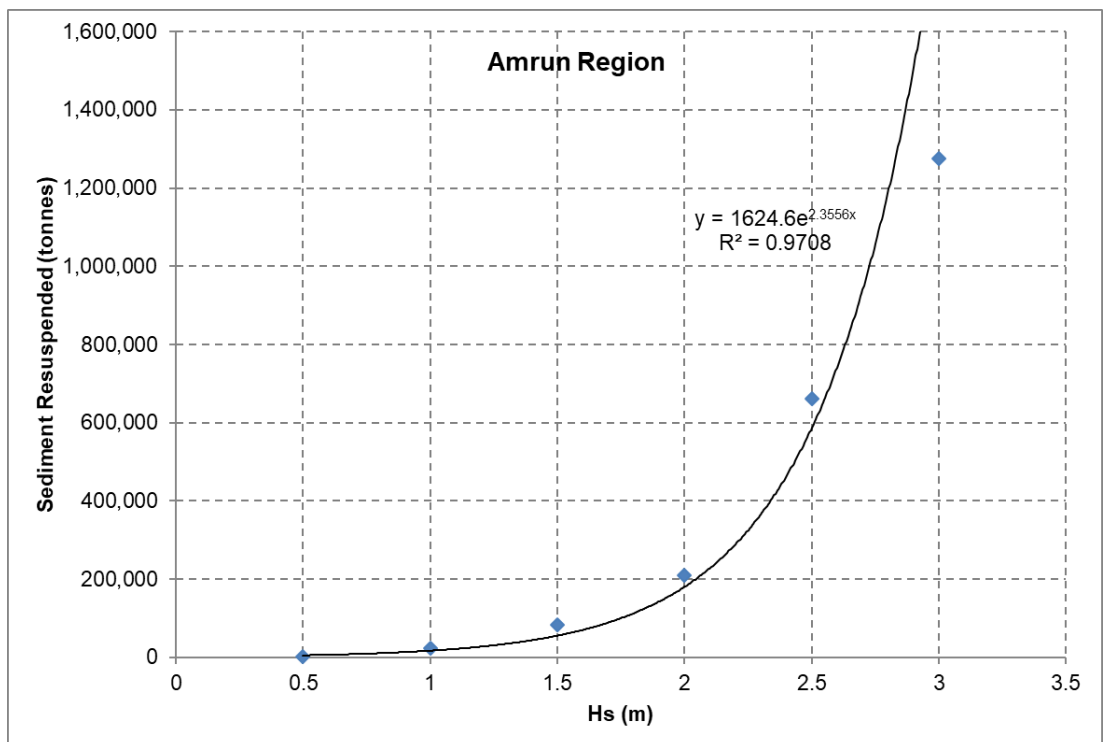


Figure 16. Relationship between  $H_s$  (at the Albatross Bay WRB) and the mass of sediment resuspended in the Amrun region.



### 2.5.3. Sediment Resuspension Calculations

The SSC data collected by JCU since January 2018 has been used as an input for a high-level estimate of the annual resuspension which occurs within Albatross Bay and the adjoining estuaries. It has not been possible to undertake the calculations at Amrun Port as there is insufficient measured turbidity data available at this stage. The same approach for estimating the total mass of sediment resuspended as adopted by BMT WBM (2018) was adopted, this involved the following:

- applying a moving median filter with a 1-hour window to remove spurious short duration spikes in SSC and adopting this filtered data for all subsequent analysis;
- applying a 1-day and 30-day moving average filter to the data to show the amount of natural variation which occurs over varying timescales;
- tidal variations in the SSC signal can be quantified by calculating the sub-daily SSC fluctuations by subtracting the 1-day moving average from the filtered hourly SSC data;
- the average SSC and frequency were calculated for natural resuspension events which were defined as periods when the daily-average SSC exceeded the long-term mean, which was between 2 and 10 times the median value; and
- the annual ambient resuspension was then calculated as follows:

$$\text{Annual Ambient Resuspension} = ((\text{Event Mass} - \text{Median Mass}) \times \text{No. Event per year}) + (\text{Tidal Mass} \times \text{No. of tides per year}).$$
 The units of the annual ambient resuspension rate are in tonnes per year.

This approach makes the assumption that the measured turbidity data collected within Albatross Bay (WQ2 and WQ5) and the Embley River (WQ1 and WQ4) can be considered to be representative of the remainder of Albatross Bay and the other river (the Pine and Mission Rivers), respectively. In addition, the approach implicitly assumes that there is a net balance between upward sediment resuspension fluxes and downward settling fluxes in the region (i.e. there is limited net import or export of suspended sediment from other sources).

Results from the analysis are provided in Table 4 and example processed data along with the statistical information is shown for a site in Albatross Bay and the Embley River in Figure 17 and Figure 18, respectively. The results show that the annual resuspension within Albatross Bay is approximately 34 Mt, while the combined annual resuspension in the Embley, Pine and Mission Rivers is approximately 4 Mt. As such, the combined annual resuspension for Albatross Bay and the adjoining rivers is approximately 38 Mt. For comparison, when scaled to represent the same spatial area as this case, the annual resuspension calculated by BMT WBM (2018) show that the annual resuspension in Albatross Bay can be considered to be high as it is similar to the Port of Cairns (40 Mt) and higher than the other Ports located in the Great Barrier Reef World Heritage Area (Port of Gladstone = 20 Mt; Port of Hay Point = 9 Mt, Port of Mackay = 10 Mt, Port of Abbot Point = 5 Mt and the Port of Townsville = 12 Mt).

These resuspension rates, which are based on the measured turbidity (which was converted to SSC) data, will be compared with the modelled results in Section 3 to ensure continuity between the two approaches.

**Table 4. Albatross Bay ambient sediment mass and resuspension rate quantity.**

Location	Average Depth (m)	Area (km <sup>2</sup> )	Median SSC (mg/l)	Mean SSC (mg/l)	Event SSC (mg/l)	Tidal SSC (mg/l)	Median SSC Load (tonnes)	Mean SSC Load (tonnes)	Event SSC Load (tonnes)	Tidal SSC Load (tonnes)	No. of Events (/yr <sup>-1</sup> )	No. of Tides (/yr <sup>-1</sup> )	Annual Resuspension (tonnes/yr)
Rivers	5	115	8.5	18	33	16	4,888	10,350	18,975	9,200	20	365	3,737,500
Albatross Bay	8	750	7.5	62.5	725	7.5	45,000	375,000	4,350,000	45,000	4	365	33,825,000
<b>Total</b>		<b>865</b>	<b>8</b>	<b>40.25</b>	<b>379</b>	<b>11.75</b>	<b>49,888</b>	<b>385,350</b>	<b>4,368,975</b>	<b>54,200</b>			<b>37,562,500</b>

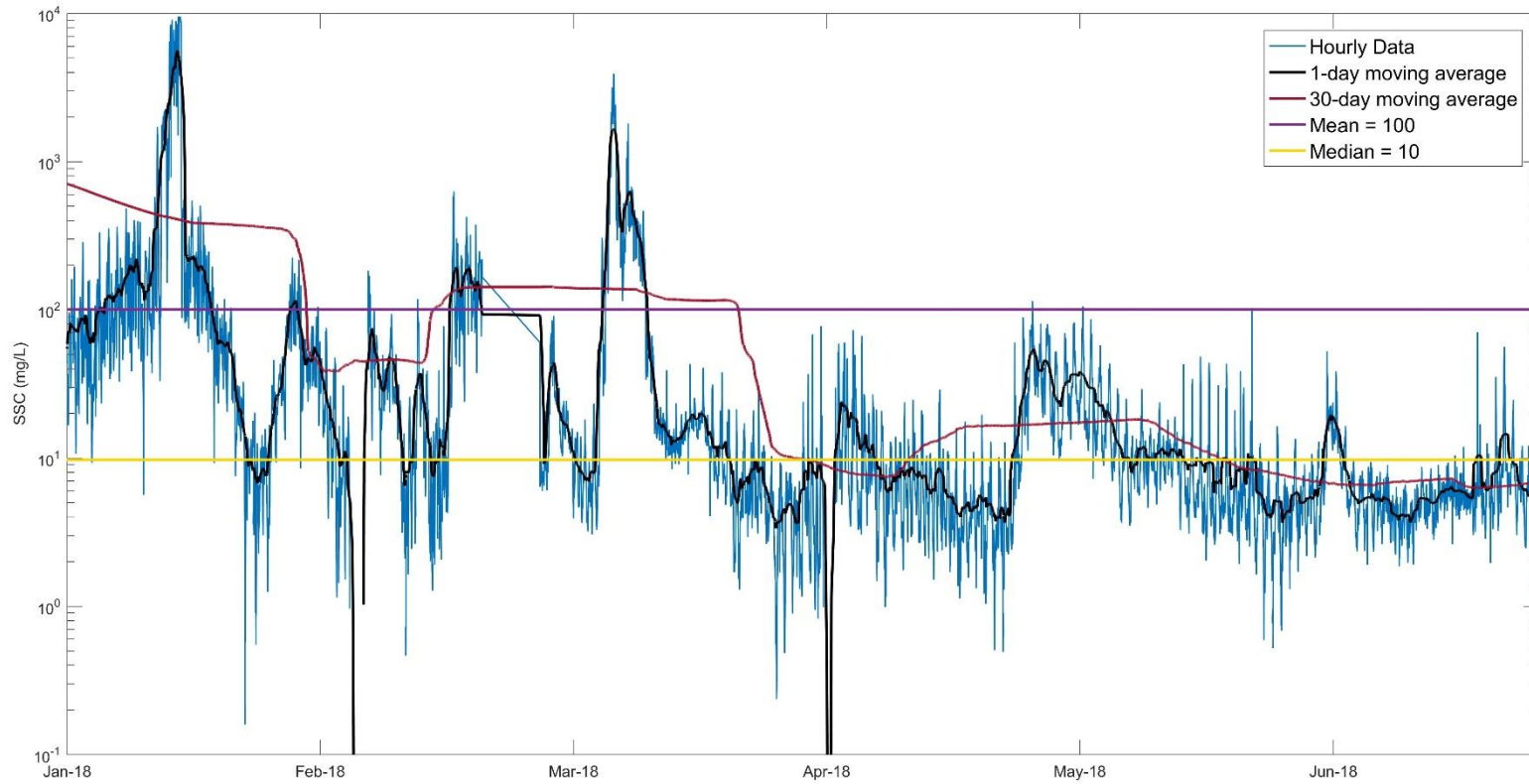


Figure 17. Processed SSC data at WQ5 (Albatross Bay).

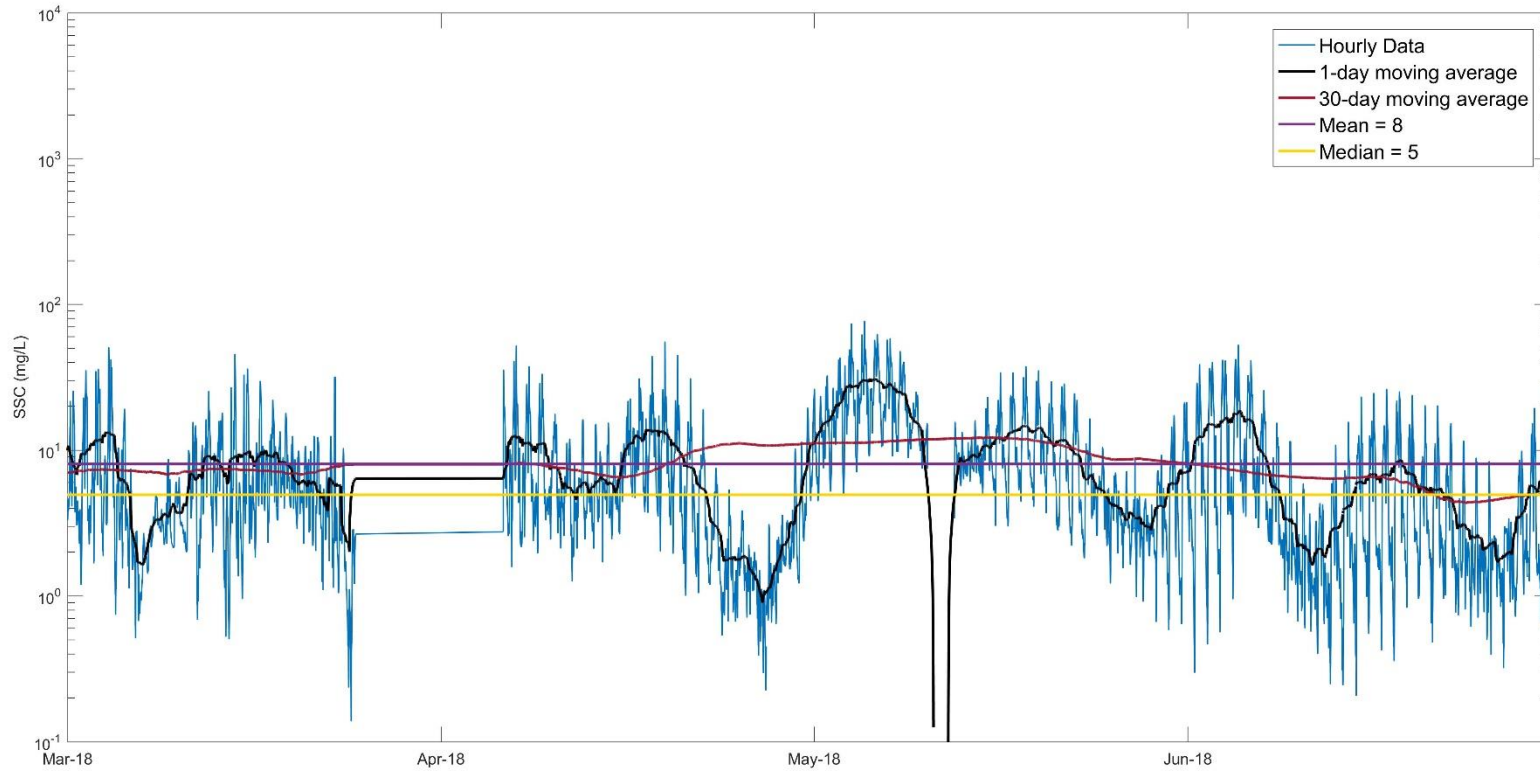


Figure 18. Processed SSC data at WQ1 (Embley River).

### 3. Sediment Budget

The overall aim of this study is to develop a quantitative sediment budget which helps to explain what causes sedimentation at the Port and where the sediment that is deposited within the dredged areas of the Port comes from. As such, both a regional and local Port scale sediment budget has been developed, which includes the gross resuspension of sediment from the seabed as well as the net residual transport of the sediment.

A sediment budget is the balance of sediment which enters and exits a coastal or marine area. As such, the sediment budget analysis consists of evaluating the transport, fluxes, sources and sinks of sediment to help develop a better understanding of the system. Typically, sediment budgets are developed using a series of sediment cells, which represent regions of the coastal/marine environment, and quantifying the relative balance in transport between the cells. The cell can then be defined as being balanced (i.e. the sediment entering and exiting the cell are approximately equal), being a source of sediment (i.e. there is a net loss of sediment from the cell) or being a sediment sink (i.e. there is a net gain of sediment in the cell).

#### 3.1. Approach

For an environment such as the Weipa and Amrun region, which is made up of a combination of cohesive and mixed sediments (which will also display cohesive properties when the percentage of clay is more than about 10% (Van Rijn, 1993)) and is characterised by relatively large SSCs, it is appropriate to develop the budget based on exchanges in mass to and from the water column (i.e. sediment resuspension and subsequent deposition) (ABPmer, 2008).

Two approaches have been adopted to provide an initial high-level estimate of the mass of sediment which is resuspended. The first approach uses the measured turbidity data (which was converted to SSC) (see Section 2.5.3) and the second uses results from the sediment transport model (see Appendix A for further details on the model setup and calibration/validation). The numerical model was run to simulate the sediment transport during the wet and dry season of 2018 (coinciding with the period for which the measured turbidity data were available). The model results were then processed to estimate the annual mass of sediment resuspended from within Albatross Bay and the adjoining rivers. Results from the two approaches for the Albatross Bay and adjoining rivers were:

- **Measured Data:** annual resuspension of **38 Mt**; and
- **Numerical Model:** annual resuspension of **35 Mt**.

The results from the two approaches are within 10% of each other, giving confidence that the numerical model is able to provide a realistic representation of the key sediment transport processes and resultant mass of sediment resuspended in the system. Based on this comparison, along with the model calibration to the available SSC data (detailed in Appendix A), the model is considered to be a suitable tool to assist in defining the sediment budget.

To provide input into the sediment budget, the sediment transport model was setup to represent the following conditions:

- **Typical Wet Season:** a wet season period (November to April) with wave conditions that can be considered to be representative of a typical year. Based on processing of the measured wave data from the Albatross Bay WRB undertaken as part of the Bathymetric Analysis study (PCS, 2018a), the period of Nov 2015 to Apr 2016 was selected as a suitable wet season period as the duration the  $H_s$  was above 2 m was the sixth highest out of ten years (Figure 19) and the year also did not have any wave events where the  $H_s$  exceeded 3 m (i.e. an extreme wave event);
- **Cyclonic Wet Season:** a wet season period (November to April) where a cyclone resulted in large waves. The Nov 2017 to Mar 2018 period was selected as a suitable cyclonic

wet season as TC Nora occurred over this period and the cyclone resulted in the largest recorded  $H_s$  at the Albatross Bay WRB. In addition, the sediment transport model was calibrated using measured turbidity data that was collected over this period (January to March 2018 inclusive) giving confidence that the model is able to represent this type of event; and

- **Typical Dry Season:** a dry season period (May to October) with wind and wave conditions that can be considered to be representative of a typical year. The measured data shows limited variability in the wind and wave conditions for the region during the dry season period due to the dominance and consistency of the prevailing east to south-easterly trade winds during this period. As such, the 2018 dry season has been adopted as there are measured water quality data available for the period which the sediment transport model has been validated for (April to June 2018 inclusive), providing additional confidence that the model is accurately representing the conditions.



**Figure 19. Plots showing the sedimentation/erosion, time  $H_s$  was above 2 m and total rainfall (May to April) for 2009 to 2018 (PCS, 2018a).**

A series of sediment cells were defined based on aspects such as the environmental setting, bathymetry, dominant coastal processes and sediment composition. Sediment cells were defined for both regional and local Port scale sediment budgets (Figure 20 and Figure 21).

Results from the sediment transport model were processed for each of the sediment cells to provide estimates of the following:

- **natural resuspension of sediment:** this has been estimated by calculating the cumulative increase in total mass of sediment in suspension within the cell over the model simulation period. This has also been calculated for the total area covered by the regional and local cells to allow the individual cell values to be checked to ensure no double counting of increases in mass when resuspended sediment is transported into adjacent cells; and
- **net residual transport into/out of the cell:** this has been calculated as the net difference in the mass of sediment between what is transported into the cell and what is transported out of the cell. The value adopted is the final net residual balance at the end of the model simulation.

As such, the sediment budget provides a quantitative estimate of both the gross resuspension and net sediment transport at both a regional and a local Port scale. The regional sediment budget is presented in the following section and the local Port scale sediment budget is presented in the section after.

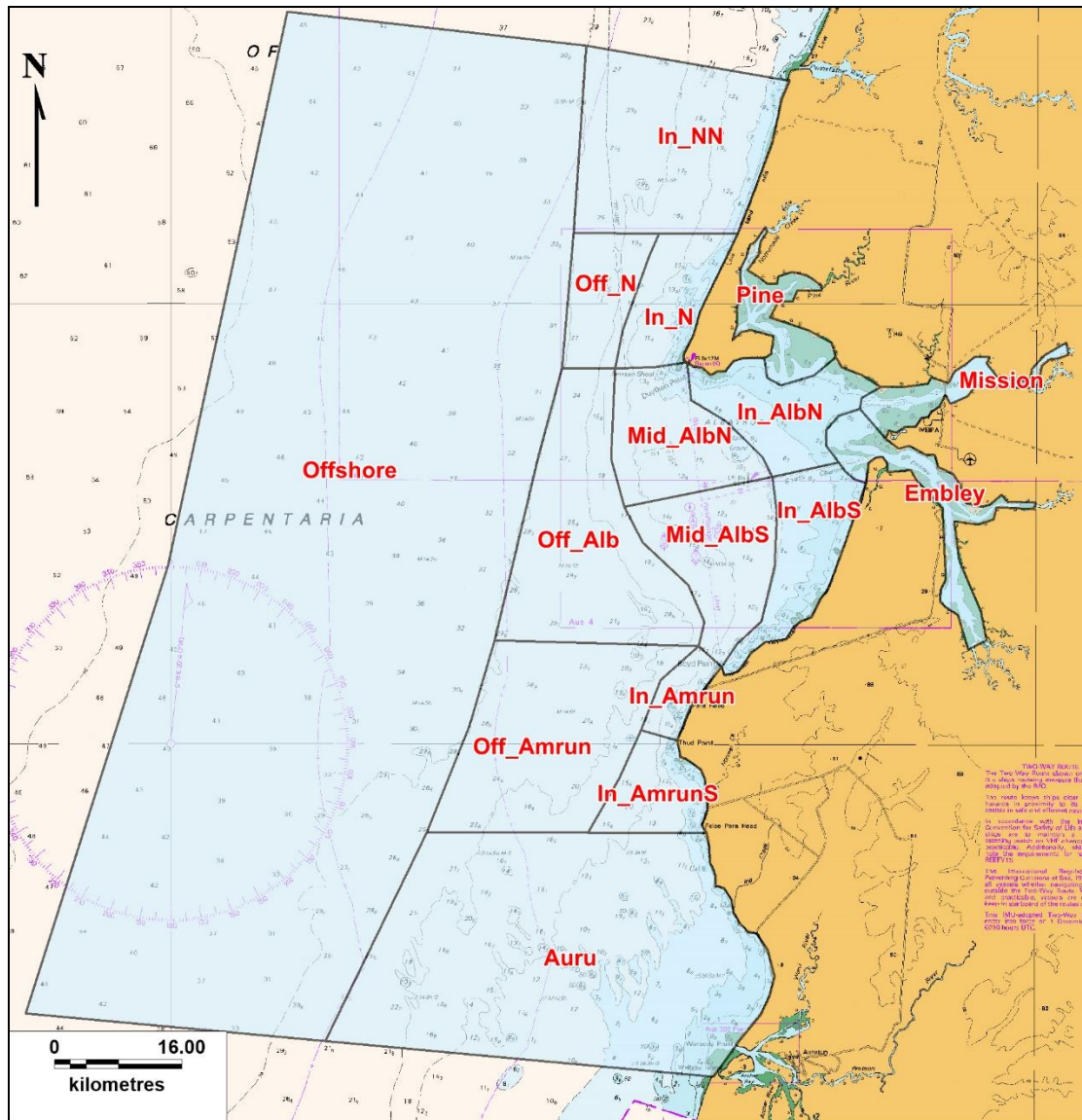


Figure 20. Sediment cells for regional sediment budget.

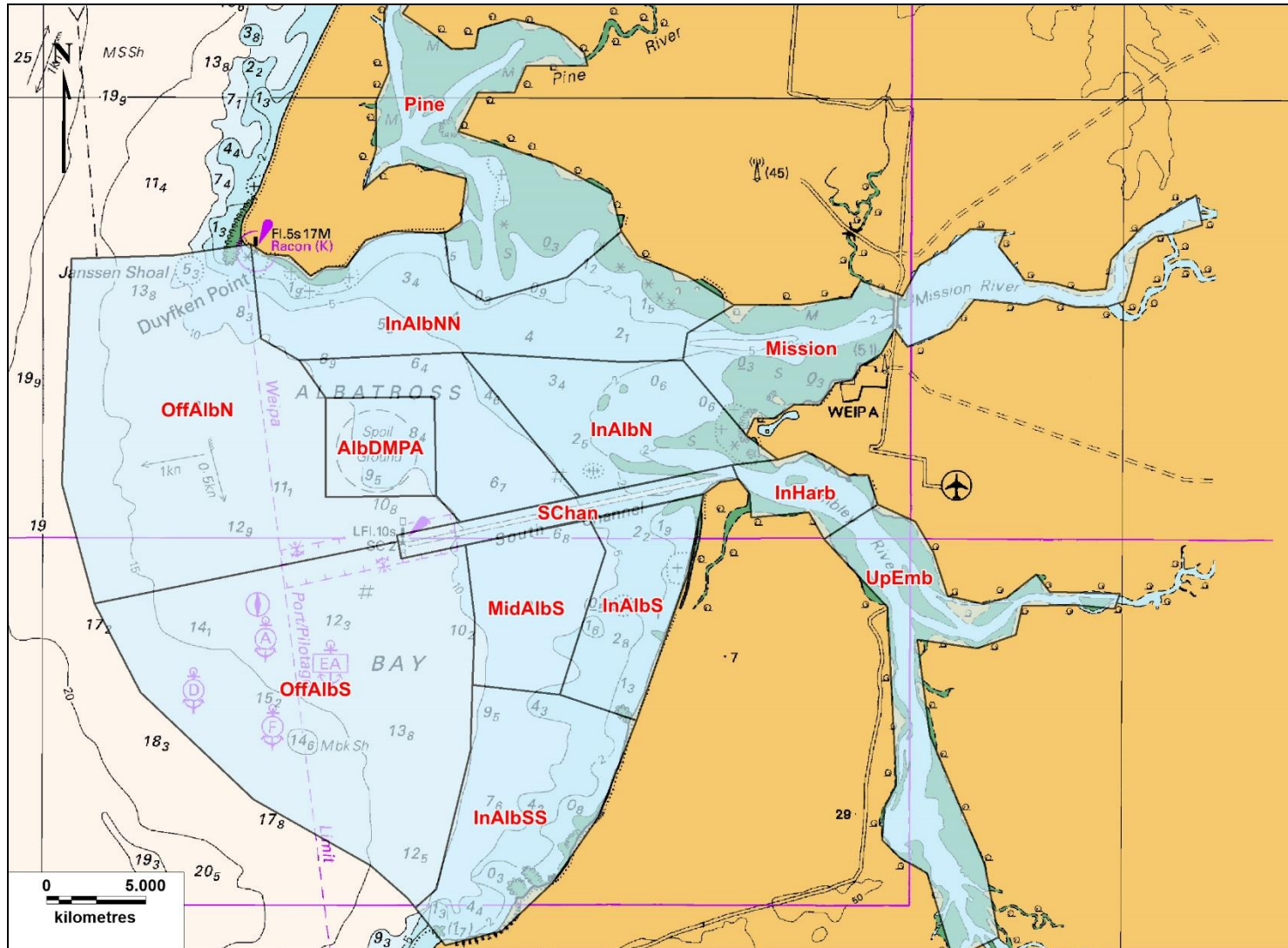


Figure 21. Sediment cells for local Port of Weipa sediment budget.



## 3.2. Regional Sediment Budget

The regional sediment budget has been calculated for an area covering 10,000 km<sup>2</sup> which extends 40 km to the north of Albatross Bay and 50 km to the south of Amrun Port, encompassing a total length of coastline of approximately 130 km and extending offshore to the -50 m LAT contour (approximately 80 km offshore). To show how the SSC varies spatially at this regional scale, and relative to the sediment cells adopted, plots of the modelled SSC for a range of conditions are shown in Figure 22 to Figure 24. The plots show the following:

- during relatively calm wave conditions in the wet season (Figure 22), the SSC is mainly constrained within the inshore sediment cells (i.e. areas shallower than -10 m LAT) and in the estuaries. The shallow embayment areas of Albatross Bay and the area adjacent to Aurukun (sediment cell Auru) are the areas with the most sediment in suspension. Due to the relatively deep water adjacent to the shoreline in the Amrun area there is minimal SSC in this area. The Mid\_AlbS sediment cell has limited SSC compared to the other Mid and Inner sediment cells in Albatross Bay;
- during a tropical cyclone which resulted in large waves (Figure 23), the SSC is generally above 100 mg/l in all areas except for the Offshore sediment cell. The highest SSC is within Albatross Bay where concentrations of more than 1,000 mg/l are present; and
- during a spring tide with calm wave conditions in the dry season (Figure 24), the areas where the SSC is more than 2 mg/l is limited to the estuaries and the areas of Albatross Bay directly adjacent to the estuary mouths. The SSC in the estuaries can be seen to be higher than it was during the wet season plots, this is due to the strong east south-east winds generating small waves within the estuaries, which results in localised resuspension of the intertidal and shallow subtidal mudflats.

The sediment transport model results also show that there is limited net residual transport of suspended sediment in the region. The suspended sediment tends to be circulated around Albatross Bay without significant amounts being lost from the Bay. Along the open coastline, the sediment is typically transported to the north and then back to the south along the shoreline, with minimal onshore/offshore transport. In the estuaries, the suspended sediment is generally transported up and down the estuaries, with some exchange at the estuary mouths with Albatross Bay. As such, the SSC tends to remain elevated until the conditions are calm enough for the suspended sediment to deposit, generally in a similar location to where it was originally resuspended.

The regional sediment budget is shown for a typical year in Figure 25. The sediment cells have been colour coded whereby if the net residual transport is more than 25% of the resuspension in the cell (i.e. there is either an increase or decrease in the mass of sediment in the cell of more than 25% of the sediment resuspended) the cells are coloured either green (sink, gain of sediment) or purple (source, loss of sediment) and if it is less than 25% then the cell is considered to be balanced and is coloured pale blue. Examination of the modelled spatial movement of the suspended sediment over time showed that there was minimal residual transport (this is further discussed in Section 3.3). The budget therefore does not include any arrows to show sediment transport pathways between cells as the lack of any residual transport direction means there can be exchange between all adjacent cells. In addition, due to the magnitude of the annual resuspension (46 Mt/yr taken from Table 5) relative to the sources of sediment from cliff erosion (0.1 Mt/yr) and the transport of sediment by longshore drift (0.03 Mt/yr), these have been excluded from the regional sediment budget, but are included in the local scale budget (see Section 3.3).

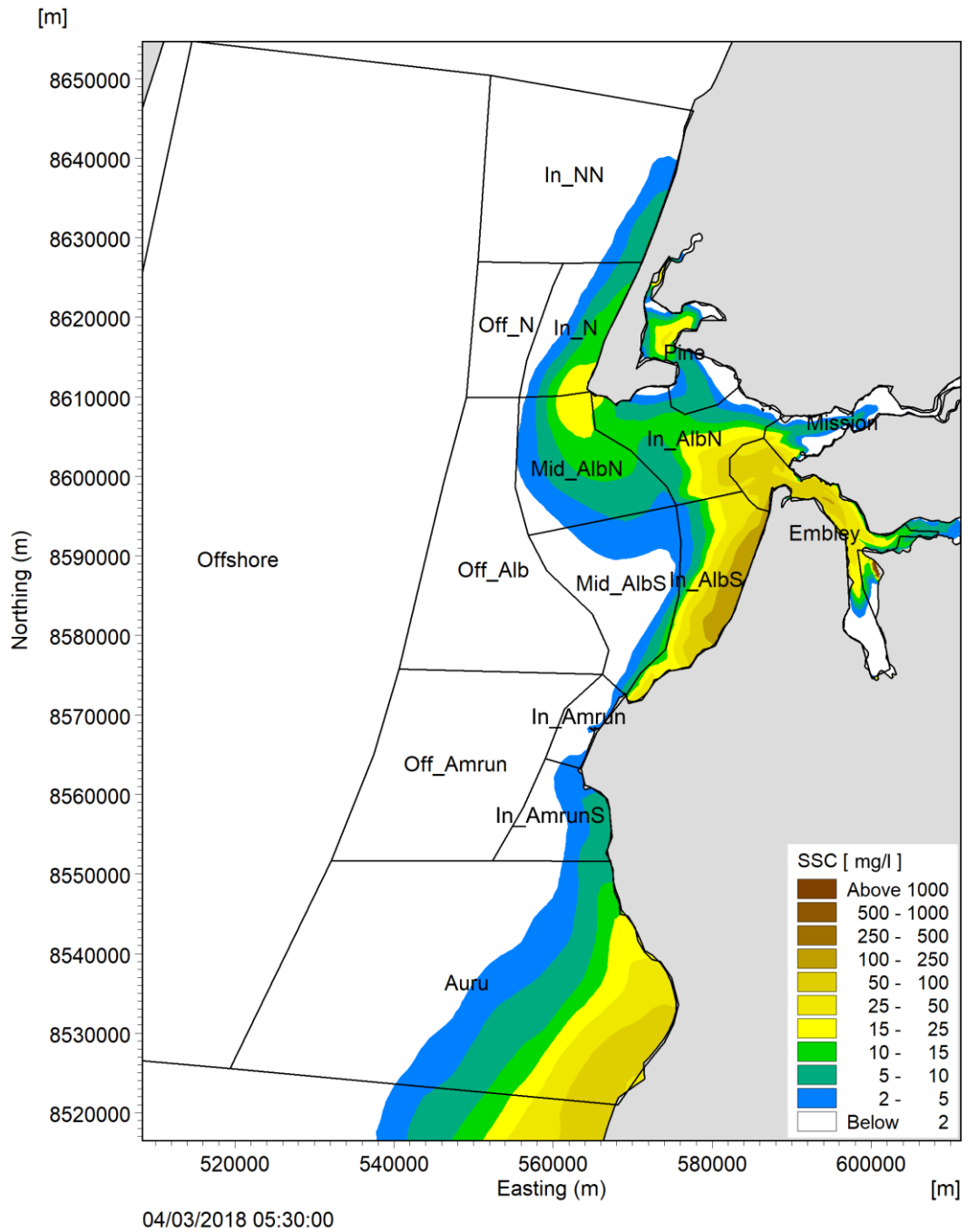
The regional sediment budget for both typical and cyclonic years is shown in Table 5<sup>3</sup>. The table details the natural resuspension of sediment within each cell as well as the net residual

<sup>3</sup> Note: to calculate the value of 35 t presented in Section 3.1, the Cyclonic Year values from the three estuary regions (Pine, Mission and Embley) and the In and Mid Albatross Bay regions (In\_AlbN, Mid\_AlbN, In\_AlbS and Mid\_AlbS) were used.

transport into/out of each cell. The table shows that the total resuspension for a cyclonic year is 50% more than for a typical year, with the majority of this increase occurring in the deeper sediment cells (Mid and Off cells) due to the larger waves during the cyclone resuspending more sediment in deeper water. Although the budgets for both years show a net loss of sediment from the system, it is expected that the budgets overall should be approximately balanced due to the predicted limited net residual transport. The total net loss for both years is approximately equivalent to the loss from the Auru sediment cell. The reason this cell is indicating a relatively large loss is because it is located close to the southern boundary of the numerical model which can remove sediment from the model domain, but does not input new sediment into the model (i.e. any sediment which is transported from the Auru cell to the model boundary when the currents are in a southerly direction will then be lost from the model and will not be transported back to the north when the currents switch to a northerly direction). As such, if we assume that the Auru sediment cell is balanced then the entire regional budget is also balanced during both typical and cyclonic years.

**Table 5. Regional annual sediment budget for typical and cyclonic years.**

Region	Area (km <sup>2</sup> )	Typical Year		Cyclonic Year	
		Resuspension (t)	Net Transport (t)	Resuspension (t)	Net Transport (t)
In_NN	506	2,100,000	100,000	4,500,000	200,000
In_N	153	1,500,000	-100,000	2,200,000	100,000
Off_N	142	700,000	100,000	1,300,000	-100,000
Pine	99	3,300,000	40,000	3,500,000	100,000
Mission	81	2,700,000	200,000	3,000,000	200,000
Embley	142	10,000,000	200,000	11,400,000	400,000
In_AlbN	196	2,100,000	-400,000	2,700,000	-700,000
Mid_AlbN	231	2,700,000	-900,000	4,500,000	-700,000
Off_Alb	502	2,400,000	600,000	4,000,000	-300,000
In_AlbS	189	3,100,000	-700,000	4,700,000	-700,000
Mid_AlbS	254	2,600,000	1,300,000	5,600,000	2,300,000
In_Amrun	55	700,000	-100,000	700,000	-300,000
In_AmrunS	128	800,000	-100,000	1,200,000	-100,000
Off_Amrun	525	2,000,000	-100,000	5,500,000	700,000
Auru	1,327	6,900,000	-1,500,000	10,400,000	-2,800,000
Offshore	5,330	2,100,000	-200,000	3,900,000	-300,000
<b>Total</b>	<b>9,860</b>	<b>45,700,000</b>	<b>-1,560,000</b>	<b>69,100,000</b>	<b>-2,000,000</b>



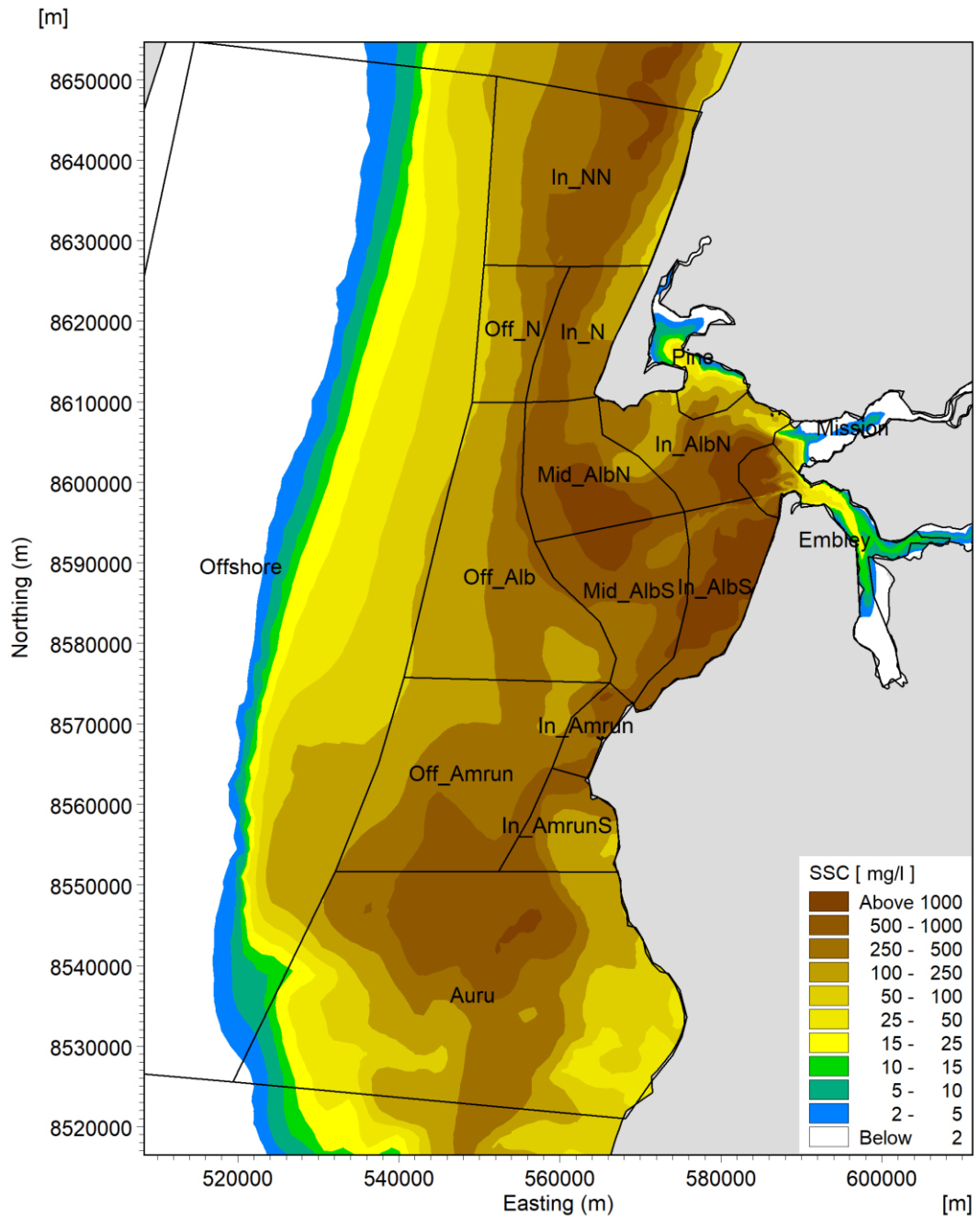
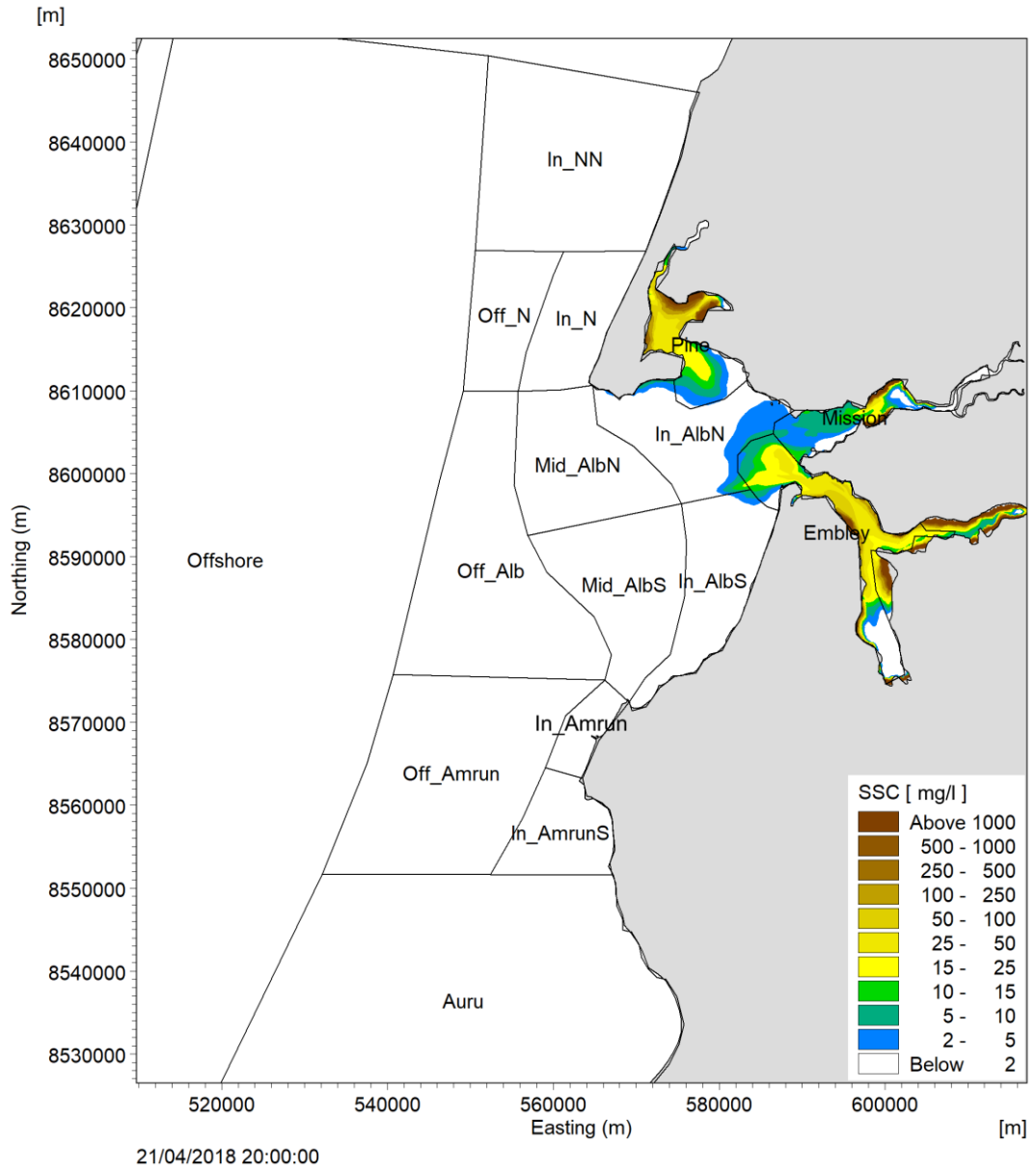


Figure 23. Modelled SSC during TC Nora in the wet season ( $H_s = 3.5$  m, Direction = 270°). Regional sediment cells are superimposed.



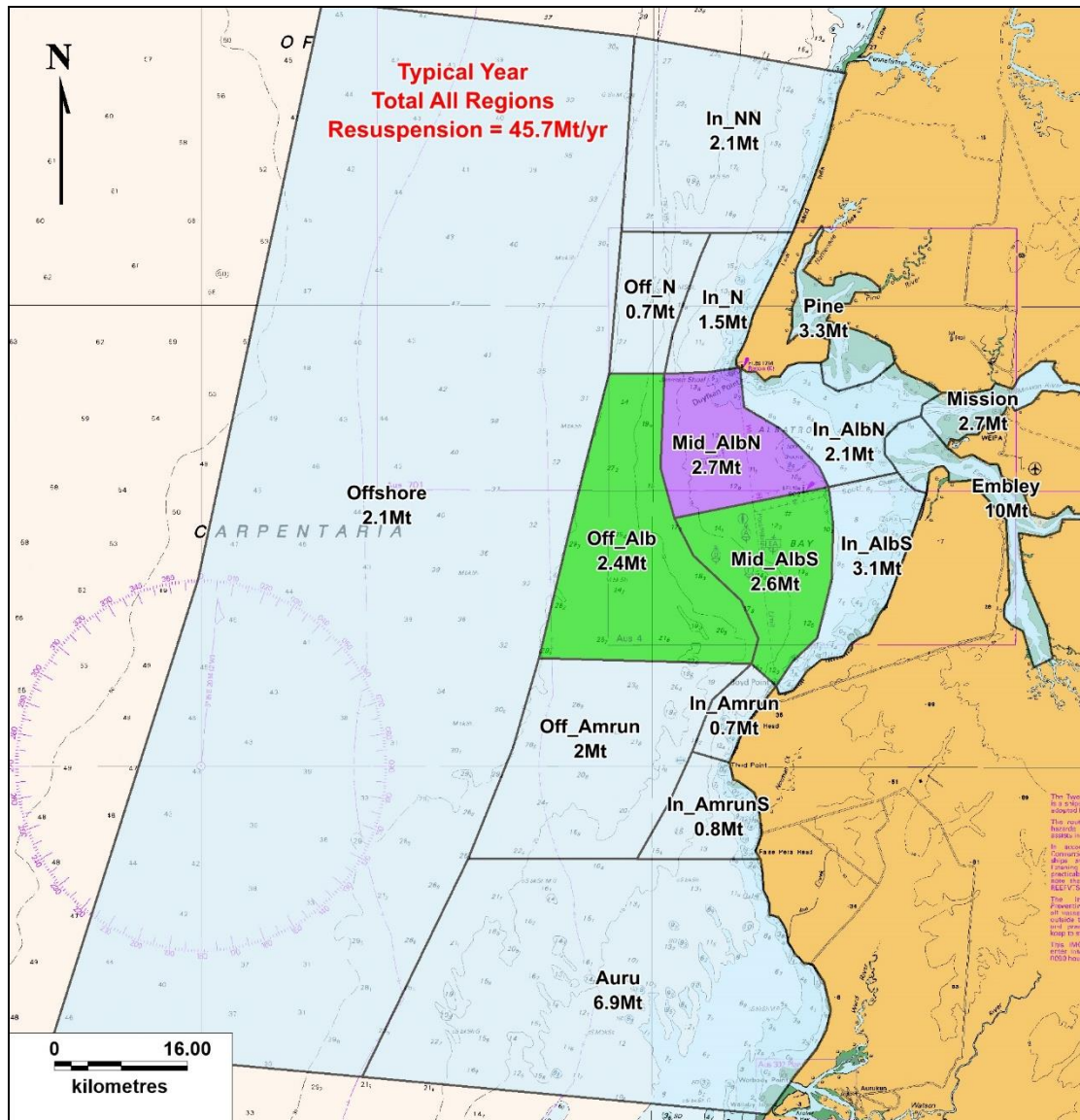


Figure 25. Regional sediment budget for a typical year. Values represent annual resuspension mass.

### 3.3. Local Sediment Budget

As noted in the previous section, the sediment transport model shows that there is limited net residual transport of suspended sediment in the Albatross Bay region. Sediment which is suspended within the Bay is typically transported landwards towards the estuary mouths during the flooding tide and then offshore during the ebbing tide (Figure 26 and Figure 27). The tidal currents within Albatross Bay away from the estuary mouths are generally less than 0.4 m/s, and given the size of the Bay (approximately 25 km east to west and 35 km north to south), these current speeds would not be expected to transport any sediment suspended in the nearshore area to the boundaries of the Bay before the subsequent flood tide started to transport the sediment back landwards. As such, the majority of the sediment which is resuspended within Albatross Bay is transported backwards and forwards by the tidal currents until the tidal current and wave energy is low enough for the sediment to be deposited. This could occur during slack water or when the wave conditions are calm, in which case the sediment would likely be subsequently resuspended again when conditions become more energetic, or it could occur because the sediment has been transported to a

more sheltered location within Albatross Bay (such as the deepest section of the South Channel) in which case the sediment is less likely to be resuspended.

The local sediment budget for a typical year is shown in Figure 28. The sediment cells have been colour coded in the same way as for the regional budget (i.e. increase in mass = green, reduction in mass = purple, and balanced = pale blue). The budget also includes the additional new source of sediment from cliff erosion at the southern end of Albatross Bay and the longshore transport of sand along the shoreline. The budget does not include any arrows to show sediment transport pathways between cells as due to the predicted lack of any residual transport direction there can be exchange between all adjacent cells.

The local sediment budget for both typical and cyclonic years is shown in Table 6. The table details the natural resuspension of sediment within each cell as well as the net residual transport into/out of each cell. The table shows that the total resuspension for a cyclonic year is 30% more than for a typical year, with the majority of this increase occurring in the deeper sediment cells (Mid and Off cells) due to the larger waves during the cyclone resuspending more sediment in deeper water. The budget for the typical year shows a loss of 1.5% of the total resuspension mass, while for the cyclonic year it shows a gain of 1.5% of the total resuspension mass. The fact that both of these changes are small compared to the total resuspension mass and that one year represents a gain and the other a loss indicates that the sediment budget in Albatross Bay can overall be considered to be balanced.

The sediment budget shows that a build-up of sediment is predicted within the South Channel sediment cell (SChan), with this varying between 1.2 and 1.4 Mt for the typical and cyclonic years respectively. To show how this sedimentation is spatially represented by the numerical model, the predicted spatial change in bed elevation over the typical and cyclonic wet seasons and the dry season are shown in Figure 29 to Figure 31. The plots show how during both wet season periods the model predicts sedimentation of more than 0.5 m in the South Channel, with the sedimentation starting approximately 4 km to the west of the Embley River entrance. In contrast, during the dry season the sedimentation is significantly lower, with sedimentation in the same location but the depth being less than 0.2 m. It is important to note that the South Channel sediment cell area includes the South Channel as well as areas to the north and south of the channel and so the sedimentation mass shown in Table 6 is larger than the sedimentation just within the dredge area of the South Channel.

The total sedimentation mass within the dredge area of the South Channel sediment cell is 220,000 t for a typical year and 320,000 t for a cyclonic year. The recent bathymetric analysis undertaken as part of the SSM Project found that between 2002 and 2018 the mean annual sedimentation in the South Channel was 360,000 m<sup>3</sup> and the maximum annual sedimentation was 840,000 m<sup>3</sup> (PCS, 2018a). If a conversion of 0.7 t/m<sup>3</sup> is assumed, as suggested by McCook et al (2015) for maintenance dredge sediment, then the mean mass of sediment deposited was 250,000 t and the maximum mass deposited was approximately 600,000 t, although since the capital dredging in 2012 the maximum mass deposited has been approximately 370,000 t. Based on this, the local sediment budget appears to agree relatively well with the historical sedimentation that has occurred in the South Channel.

The local sediment budget provided in Table 6 shows that during both typical and cyclonic years, the Inner Harbour sediment cell (InHarb) is predicted to have a small loss of sediment. The plots of the spatial change in bed level (Figure 29 to Figure 31) show that during the dry season and typical wet season erosion is predicted in the dredged areas of the Inner Harbour. During a cyclonic wet season, the model predicts more potential for sedimentation within the dredged areas, with the main areas of sedimentation predicted to be at the eastern end of the approach channel and the northern area of the departure channel. The trends in the model results generally agree with the changes shown by the bathymetric analysis, with the majority of the dredged areas of the Inner Harbour experiencing small amounts of erosion and accretion being limited to the eastern end of the approach channel and areas of the northern part of the departure channel.

**Table 6. Local annual sediment budget for typical and cyclonic years.**

Region	Area (km <sup>2</sup> )	Typical Year		Cyclonic Year	
		Resuspension (t)	Net Transport (t)	Resuspension (t)	Net Transport (t)
OffAlbN	20	2,520,000	-840,000	4,310,000	-640,000
InAlbNN	19	1,680,000	60,000	1,950,000	30,000
Pine	28	3,340,000	40,000	3,520,000	60,000
Mission	78	2,750,000	200,000	2,960,000	210,000
AlbDMPA	46	490,000	-20,000	680,000	-120,000
MidAlbN	66	1,120,000	-100,000	1,660,000	-190,000
InAlbN	46	1,900,000	-400,000	2,910,000	-450,000
SChan	49	1,210,000	840,000	1,380,000	1,010,000
InHarb	82	2,040,000	-290,000	2,220,000	-100,000
UpEmb	215	6,840,000	-280,000	7,290,000	-300,000
InAlbS	209	1,440,000	0	2,390,000	30,000
MidAlbS	109	670,000	0	1,260,000	-50,000
OffAlbS	79	2,060,000	1,010,000	4,570,000	1,860,000
InAlbSS	100	1,400,000	-680,000	2,170,000	-750,000
<b>Total</b>	<b>1,145</b>	<b>29,460,000</b>	<b>-460,000</b>	<b>39,270,000</b>	<b>600,000</b>



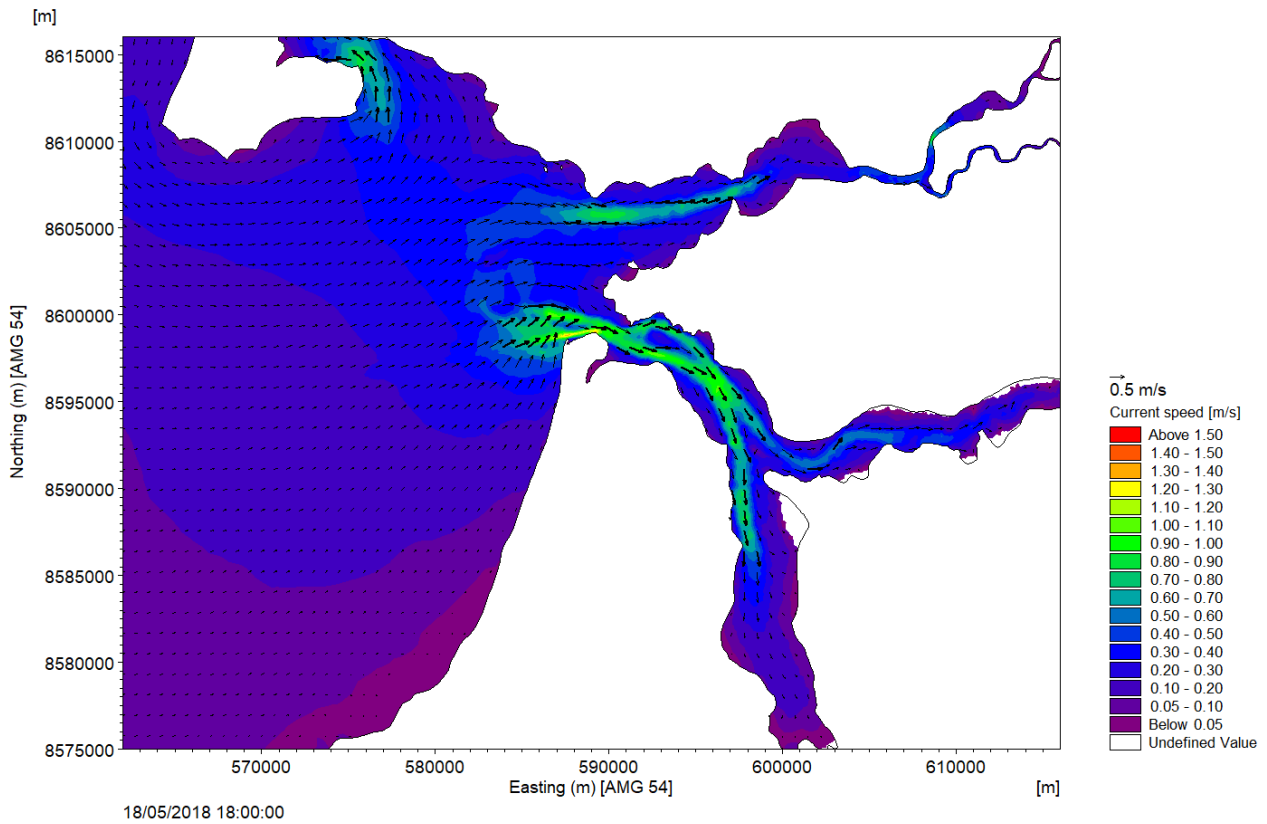


**Figure 26. Modelled peak spring current speed in Albatross Bay during a flooding tide.**

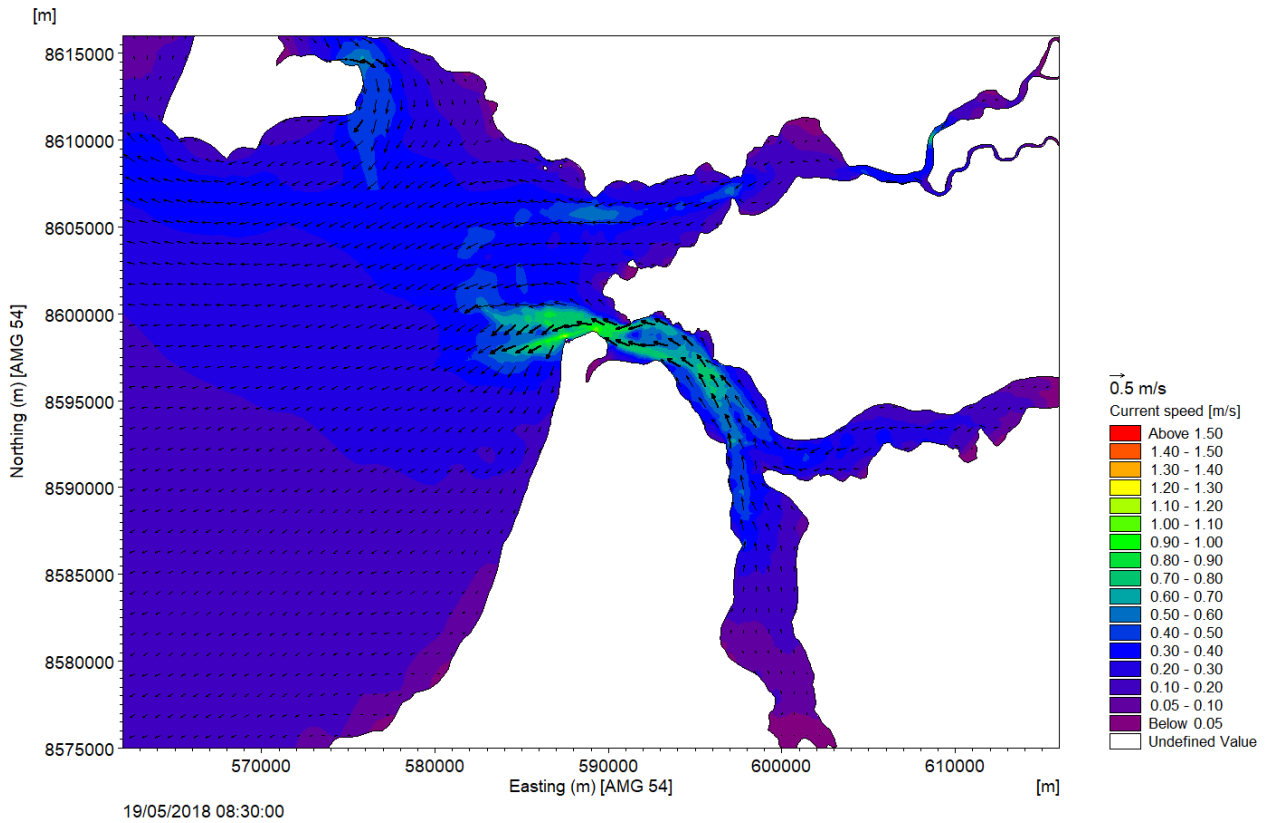


Figure 27. Modelled peak spring current speed in Albatross Bay during an ebbing tide.

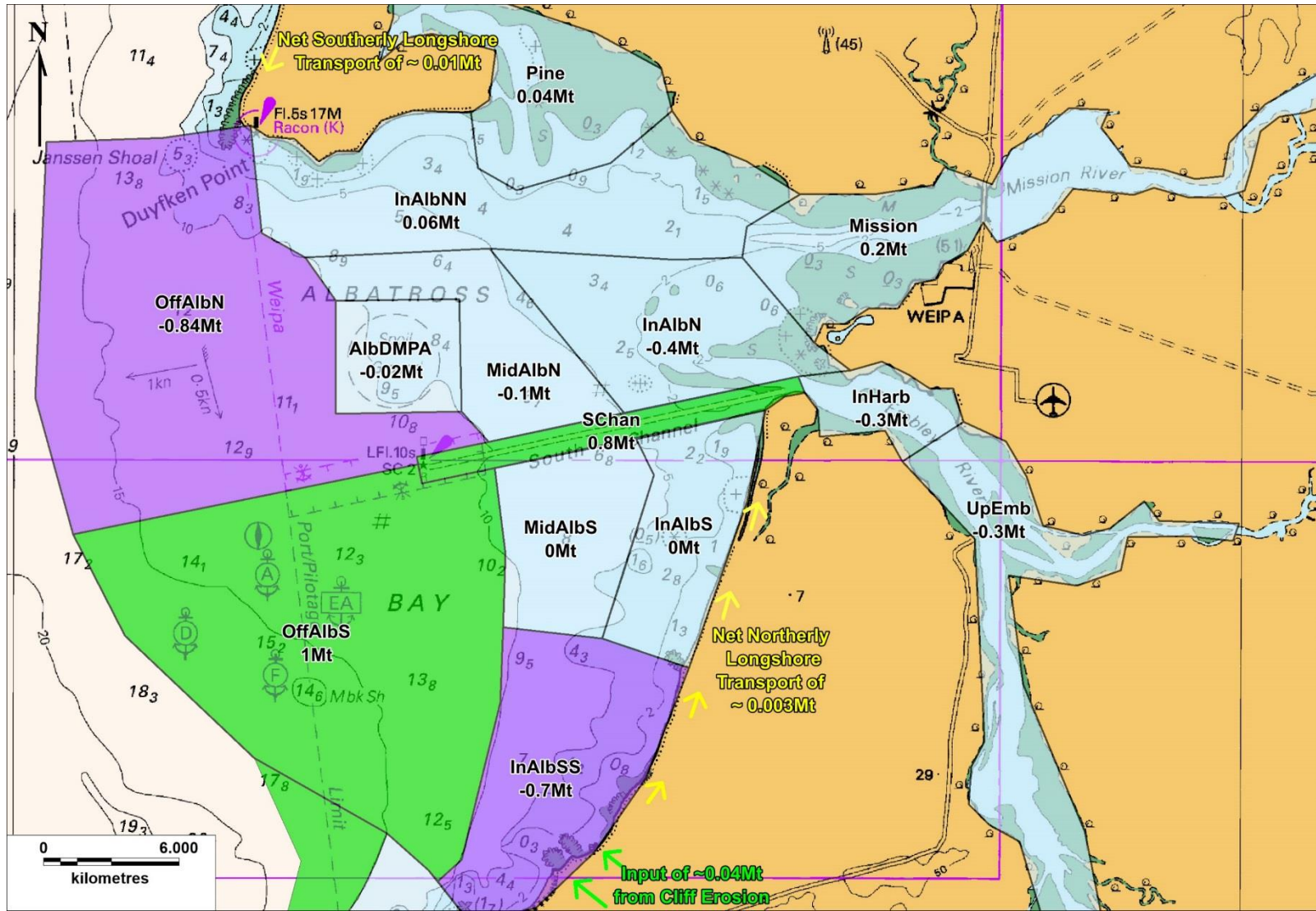
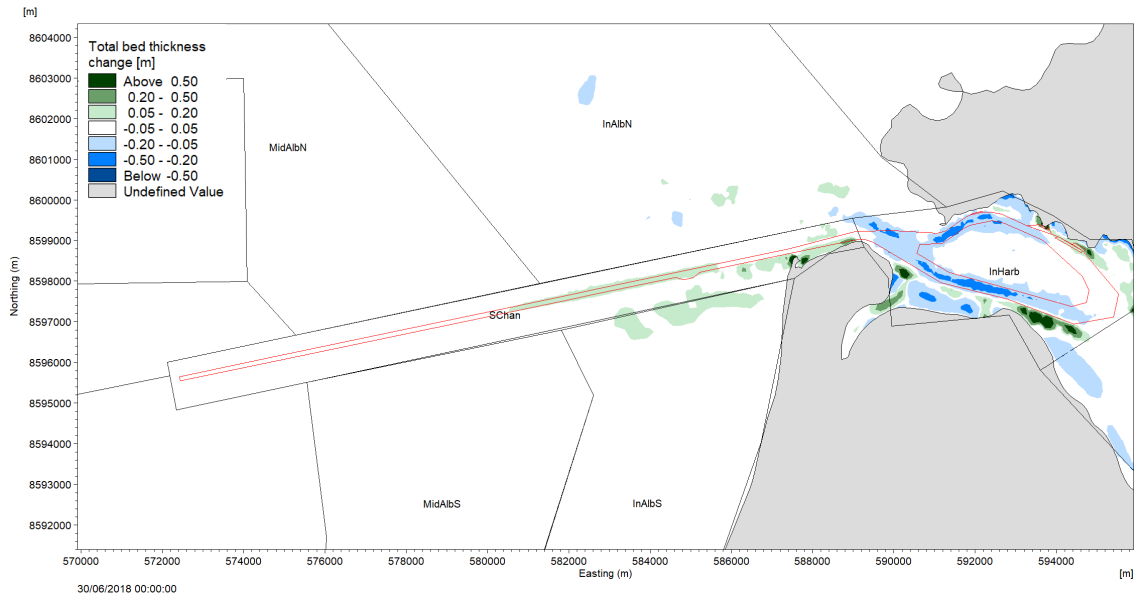
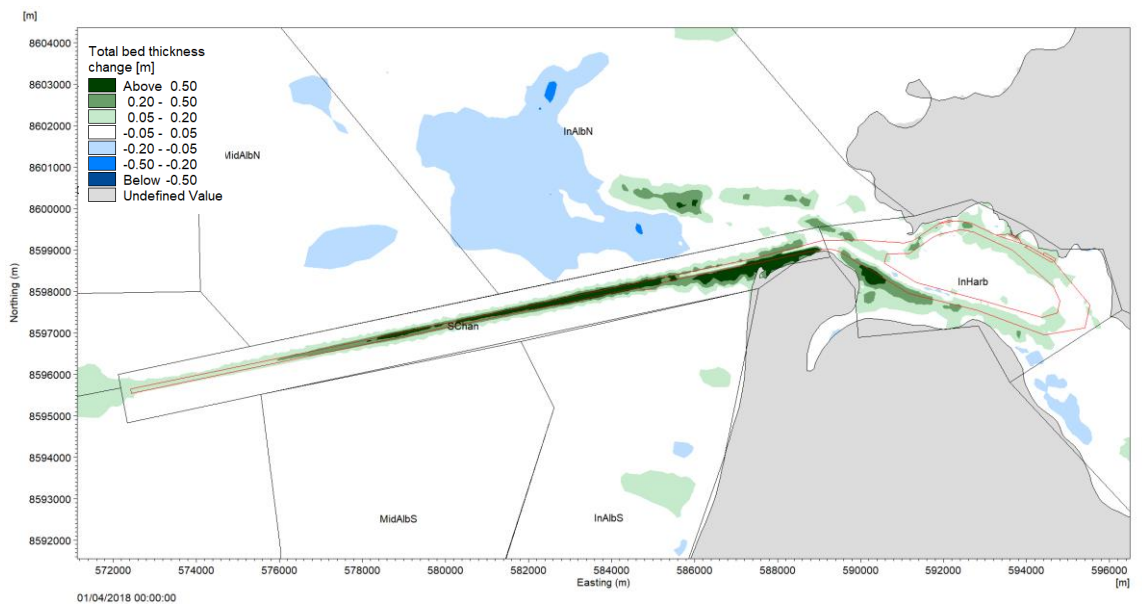


Figure 28. Local sediment budget for the Port of Weipa for a typical year. Values represent annual net transport (i.e. loss or gain of sediment).



**Figure 29. Modelled bed level change around the Port of Weipa over a 3 month dry season period.**



**Figure 30. Modelled bed level change around the Port of Weipa over a 3 month cyclonic wet season period.**

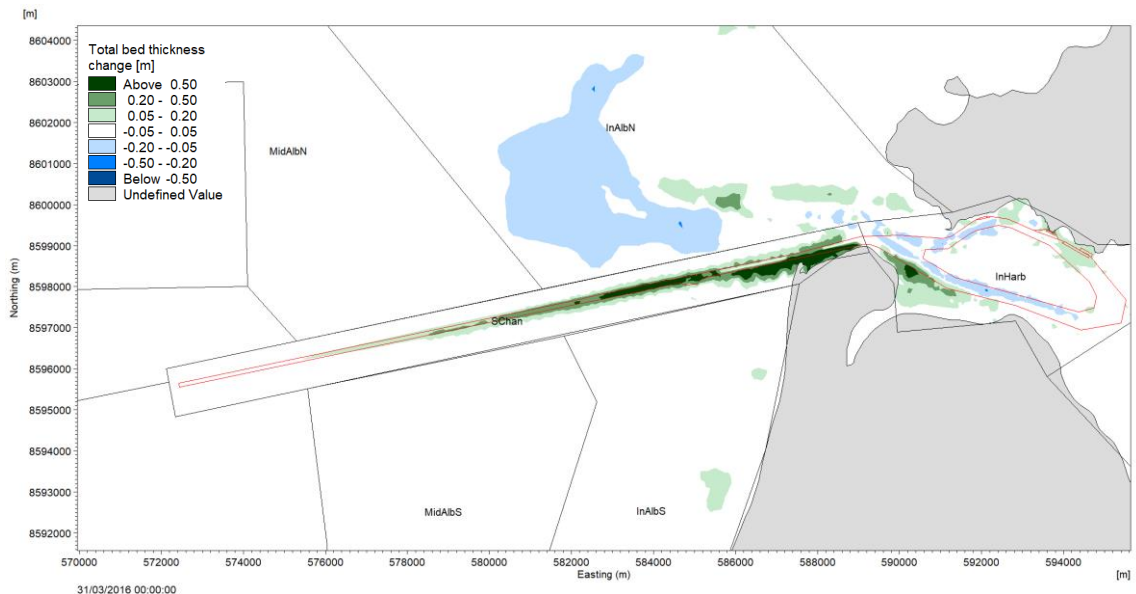


**Figure 31. Modelled bed level change around the Port of Weipa over a 3 month typical wet season period.**

The local sediment budget presented in Figure 28 and Table 6 provides a good summary of the resuspension and sedimentation that occurs in the region, but it isn't possible to derive the gross sediment transport which naturally occurs around the Port of Weipa. A series of transects have been used to calculate the gross and net transport of suspended sediment (Figure 32 and Table 7). The fact that the net transport is less than 10% of the gross transport at all locations highlights the limited residual transport which occurs in the region.

The table shows that over 10 Mt/yr of suspended sediment is transported backwards and forwards past the South Channel (11.4 Mt/yr during a cyclonic year), with a net residual transport of less than 10% of the gross occurring in a southerly direction. If the gross sediment transport is compared to the mean annual sedimentation in the South Channel of approximately 0.25 Mt/yr, then it can be calculated that 2 – 3% of the gross sediment transported backwards and forwards past the South Channel is deposited within the channel.

Table 7 also shows that approximately 6 Mt/yr of suspended sediment is transported through the Embley River mouth, with a net export of suspended sediment from the estuary of approximately 5% of the gross transport. Inside the Inner Harbour there is a slight dominance in transport to the south of Cora Bank, with the gross transport in the Approach Channel being 3 Mt/yr compared to 2.2 Mt/yr in the Departure Channel.

**Table 7. Gross and net sediment transport rates and directions around the Port of Weipa.**

Transect	Typical Year Transport (t/yr)			Cyclonic Year Transport (t/yr)		
	Gross	Net	Net Direction	Gross	Net	Net Direction
SCh_Long	10,430,000	-950,000	South	11,360,000	-1,040,000	South
SCh_Cross	1,900,000	160,000	West	2,030,000	80,000	West
Jackson_Ch	3,660,000	230,000	West	3,840,000	130,000	West
EmMouth	5,780,000	420,000	West	6,000,000	280,000	West
Em_App	2,950,000	100,000	West	3,000,000	40,000	West
Em_Dep	2,230,000	120,000	West	2,300,000	100,000	West

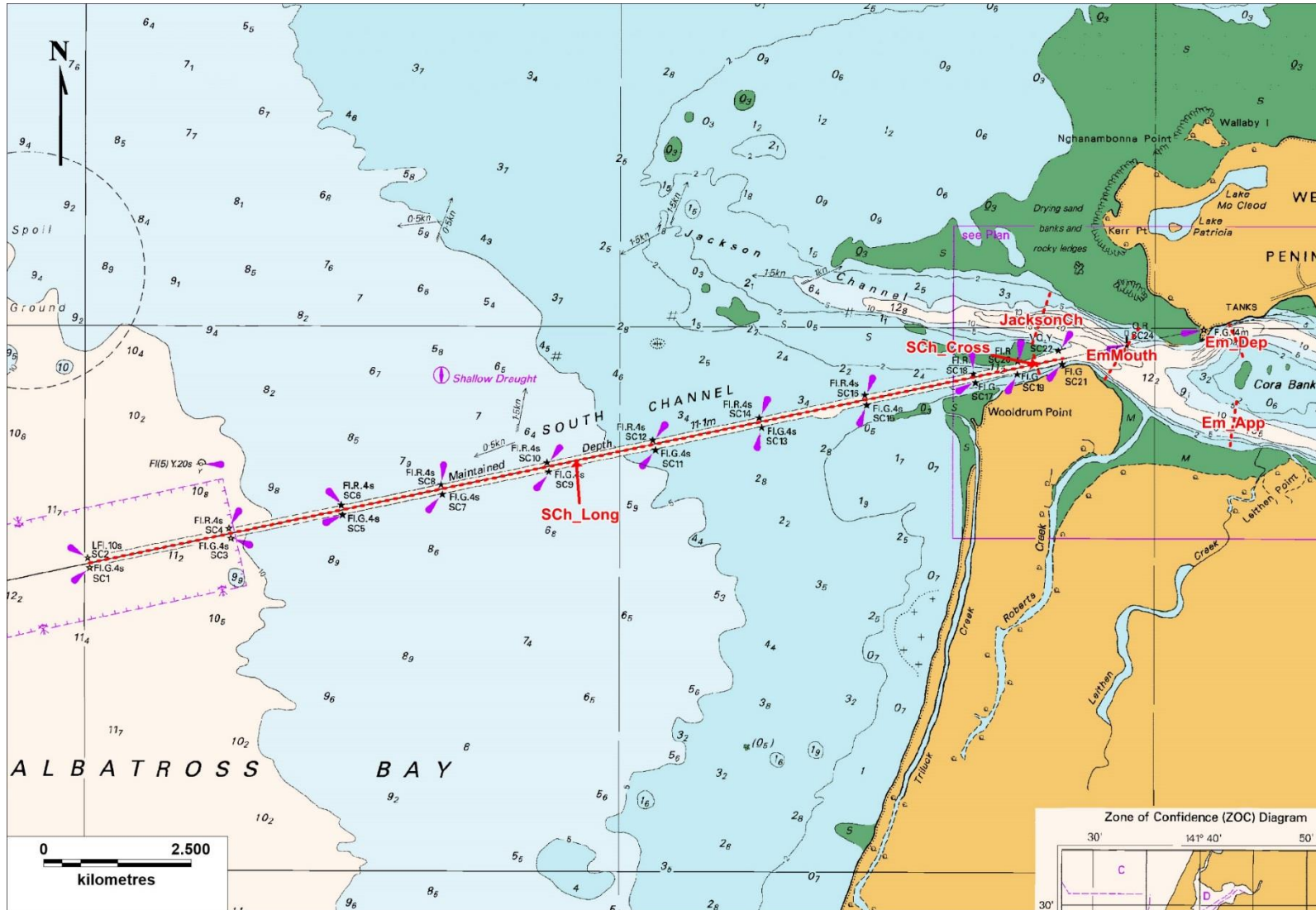


Figure 32. Transect locations for Port of Weipa local sediment budget.

### 3.3.1. Transport from DMPA

The bathymetric analysis found that the Albatross Bay Dredge Material Placement Area (DMPA) was partially retentive, with approximately 60% of the sediment placed at the site being retained and the remaining 40% being resuspended and transported away from the DMPA (PCS, 2018a). To better understand the fate of the dredged sediment which is transported away from the DMPA, the sediment transport model has been used. The model was setup so that the only sediment in the whole model was on the seabed at the Albatross Bay DMPA. It was assumed that the sediment was loosely consolidated with the same erosion threshold as the loosely consolidated surface layer of natural seabed sediment in the surrounding areas. A critical erosion threshold of 0.2 N/m<sup>2</sup> was used, based on Whitehouse et al. (2000). The model was run for the dry season, typical wet season and the cyclonic wet season.

Results from the model simulations are summarised in Table 8. The table shows that the model predicts significantly less erosion during the dry season than the wet season, with the total annual loss from the DMPA being less than 10,000 t. Changes during a typical and cyclonic wet season were more significant, with the changes the greatest during the cyclonic wet season. During both the typical and cyclonic wet season, the results show that between 3 and 4% of the sediment eroded from the DMPA is subsequently deposited within the South Channel.

The spatial distribution of the changes during the cyclonic wet season are shown in Figure 33. The plot shows that during the cyclonic wet season there was erosion over the entire DMPA, which equated to 185,000 t<sup>4</sup> of sediment being lost from the DMPA. The plot shows the deposition in the South Channel occurs in the western third of the South Channel with sedimentation of up to 0.05 m. It is important to note that the plot only shows sediment thicknesses of more than 0.01 m to highlight where the thickest deposits of sediment occur. A sediment layer of less than 0.01 m was also deposited around the Albatross Bay DMPA and within Albatross Bay in a southerly direction. Although the results show that some of the sediment placed at the Albatross Bay DMPA can be subsequently redeposited in the South Channel it is important to also consider the following:

- the results show that erosion of the Albatross Bay DMPA only occurs during large wave events during the wet season, when significant erosion would also be expected in the adjacent areas. Typically, the dredging and placement at the DMPA has occurred towards the start of the dry season, and so the fact that limited erosion occurs during these conditions shows that some consolidation of the sediment will occur over the dry season which will act to limit erosion during the subsequent wet season;
- the Albatross Bay DMPA is not significantly shallower than the surrounding areas (some peaks are 0.5 to 1 m above the natural seabed elevation). As such, if the DMPA was not located here then some erosion of the natural seabed would still be expected during large wave events. The erosion rate is likely to only be slightly higher with the DMPA in place due to the shallower peaks associated with the DMPA; and
- less than 5% of the sediment eroded from the Albatross Bay DMPA was returned to the South Channel, with the remaining sediment being thinly distributed within Albatross Bay. This shows how the sediment lost during any disturbance events (incl. normal wet seasons and cyclones) from the Albatross Bay DMPA (and similarly from any areas of adjacent seabed outside the DMPA) becomes redistributed within Albatross Bay and is subsequently re-assimilated back into the ambient seabed sediment.

<sup>4</sup> for approximate conversion to m<sup>3</sup> divide by 0.7 t/m<sup>3</sup> (i.e. 185,000 t = 264,300 m<sup>3</sup>) (McCook et al., 2015).

**Table 8. Loss of sediment from Albatross Bay DMPA and gain in the South Channel.**

	Loss (-ve) or Gain (+ve) of sediment (t)		
	Dry Season	Typical Wet Season	Cyclonic Wet Season
Albatross Bay DMPA	-9,000	-110,000	-185,000
South Channel	0	3,000	7,000
<b>Percentage of loss from DMPA</b>	<b>0%</b>	<b>3%</b>	<b>4%</b>

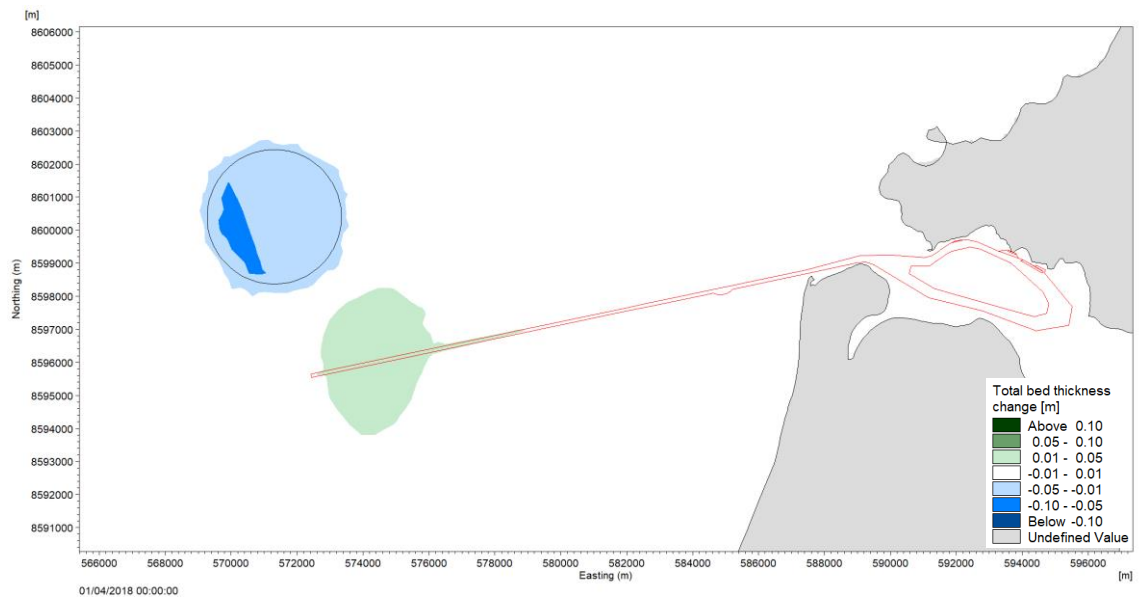


**Figure 33. Bed level change resulting from sediment at the Albatross Bay DMPA over the cyclonic wet season.**



## 4. Summary and Conclusions

This study has the aim of understanding the natural sediment transport processes which occur in the Weipa and Amrun regions. This has included understanding the source of the sediment, sediment transport pathways, processes controlling the sediment transport and the development of a quantitative sediment budget.

Two approaches were adopted to estimate the natural resuspension of fine-grained sediment from the Albatross Bay region to ensure continuity between the approaches. The first approach estimated the annual resuspension through statistical analysis of measured turbidity data, while the second approach estimated annual resuspension using a calibrated sediment transport model. The two approaches provided similar (less than 10% difference) natural annual resuspension estimates for the Albatross Bay region, with the first estimating 38 Mt/yr and the second 35 Mt/yr. The similarity between the two approaches provides confidence that the sediment transport model is able to provide a reliable estimate of the quantitative sediment budget for the region.

The quantitative sediment budget has been presented at both regional and local Port scales. The budget shows the following:

- approximately 45 Mt/yr of sediment is resuspended at the Weipa and Amrun regional scale (covering 10,000 km<sup>2</sup>, approximately 130 km along the coast and 80 km offshore) during a typical year and 70 Mt/yr during a cyclonic year;
- the majority of sediment which is suspended at the Weipa and Amrun regional scale is from the local resuspension of existing fine-grained sediment. Wave action drives the resuspension of existing fine-grained sediment within Albatross Bay and along the open coast to the north and south, while tidal currents and locally generated wind waves drive resuspension within the estuaries;
- there is limited input of new sediment to the sediment budget in the Weipa and Amrun regions (less than 1% of the total annual resuspension mass), with the main sources of new fine-grained sediment being from cliff erosion and river discharges/overland flow;
- there is limited net residual transport of sediment (less than 10% of the gross sediment transport in the Port of Weipa local region) and as such the sediment budget is generally balanced. The suspended sediment is typically either transported north and south along the open coastline, or offshore (west) and onshore (east) in Albatross Bay and the adjoining estuaries;
- significant sedimentation occurs in the South Channel of the Port of Weipa, which is mainly due to the resuspension of existing fine-grained sediment within Albatross Bay due to wave action. The suspended sediment is then repeatedly transported backwards and forwards past the channel with 2 – 3% of the total (gross) suspended sediment becoming trapped. Sedimentation occurs predominantly during the wet season due to the increased SSC resulting from larger waves, with limited sedimentation during the dry season when wave conditions are calm and there is little resuspension of sediment from the seabed;
- limited sedimentation occurs within the dredge areas of the Inner Harbour at Weipa. The results suggest that during cyclonic years some sedimentation can occur at the eastern end of the approach channel and the northern area of the departure channel;
- sediment placed at the Albatross Bay DMPA only has the potential for significant resuspension during large wave events. It is expected that if the DMPA was not there then the natural seabed sediment would be resuspended resulting in a similar mass of sediment being suspended (i.e. the DMPA is not significantly increasing the natural resuspension which would occur in the area); and
- less than 5% of the sediment eroded from the Albatross Bay DMPA was deposited within the South Channel, with the remaining sediment being thinly distributed within Albatross

Bay. This shows how the sediment lost from the Albatross Bay DMPA becomes redistributed within Albatross Bay and is subsequently re-assimilated back into the ambient seabed sediment.

The sediment budget shows that due to the regular reworking of existing fine-grained sediment within Albatross Bay due to wave conditions in the wet season, there is expected to be regular annual sedimentation in the South Channel. As long as the South Channel remains deeper than the adjacent natural seabed (i.e. remains as a navigable channel) it will act as a sediment sink with sedimentation likely to continue. It is therefore concluded that, if no maintenance dredging is undertaken, then ongoing sedimentation in the South Channel is likely to ultimately pose a significant risk to Port operations and safety as the sedimentation will result in the South Channel becoming shallower than the declared depth.

## 5. References

- ABPmer, 2008. Analysis and Modelling Guide, Sediment Budget Analysis. May 2008.
- Advisian, 2018. Port of Weipa: Maintenance dredging sediment characterisation report. Report No. 301001-02056-EN-PLN-0001. April 2018.
- Bates, T.E., Smith, J.W. & Tillman Jr., L.R., 1971. Gulf of Carpentaria bauxite project, ATP 796M. Canadian Superior Mining (Australia) P/L and Ocean Resources N/L, Geological Survey of Queensland library, Company Report 3424.
- BMT WBM, 2018. GBR Quantitative Sediment Budget Assessment. R.B22370.003.02, July 2018.
- Kampuis, J.W., 1991. Alongshore sediment transport rate, Journal of Waterways, Port, Coastal and Ocean Engineering 10, 1-21.
- Hudson, J.P., 1995. The marine geology of the Cape York Peninsula between Weipa and Cape Flattery, Northern Queensland. October 1995.
- McCook, L.J.; Schaffelke, B.; Apte, S.C.; Brinkman, R.; Brodie, J.; Erfteimeijer, P.; Eyre, B.; Hoogerwerf, F.; Irvine, I.; Jones, R.; King, B.; Marsh, H.; Masini, R.; Morton, R.; Pitcher, R.; Rasheed, M.; Sheaves, M.; Symonds, A.; Warne, M.St.J., 2015, Synthesis of current knowledge of the biophysical impacts of dredging and disposal on the Great Barrier Reef: Report of an Independent Panel of Experts, Great Barrier Reef Marine Park Authority, Townsville.
- Michaelsen, P., 1994. Post-glacial sedimentation on the inner shelf, northeast Gulf of Carpentaria. BSc Thesis. Department of Geology, James Cook University, Queensland.
- PCS, 2018a. Port of Weipa: Sustainable Sediment Management Assessment, Bathymetric Analysis. Report No. P007\_R01F1, July 2018.
- PCS, 2018b. Amrun Port: Sustainable Sediment Management Assessment, Bathymetric Analysis. Report No. P007\_R02F1, July 2018.
- RTA, 2011. South of Embley Project, Environmental Impact Statement. Section 6, Marine.
- Shanas, P.R. and Kumar, S.V., 2014. Coastal processes and longshore sediment transport along Kundapura coast, central west coast of India. Geomorphology, vol. 214, 436-451.
- TMR, 2016. Maintenance Dredging Strategy for Great Barrier Reef World Heritage Area Ports. Transport and Main Roads, November 2016.
- Van Rijn, L.C., 1993. Principles of sediment transport in rivers, estuaries and coastal seas. Part I: Edition 1993. Aqua Publications.
- Wang, P., Ebersole, B.A. & Smith, E.R., 2002. Longshore sand transport – initial results from large-scale sediment transport facility. US Army Corps of Engineers. ERDC/CHL CHETN-II-46, March 2002.
- Whitehouse, R.J.S., Soulsby, R.L., Roberts, W. & Mitchener, H.J., 2000. Dynamics of Estuarine Muds. London: Thomas Telford.
- WorleyParsons, 2008. South of Embley Project, Marine modelling and coastal processes. October 2008.
- WorleyParsons, 2013. South of Embley Project, Marine environmental modelling of dredging methods for the proposed port. Report No. 301001-01069-00-EN-REP-0014, February 2013.

# Appendices

## Appendix A – Numerical Model Development

## Appendix A – Numerical Model Development

### A1 Introduction

To assist NQBP with their long term strategic plan for sustainable sediment management at its ports, numerical modelling was undertaken to improve the understanding of sediment transport pathways and quantify transport rates within the Weipa and Amrun regions.

In order to provide the information the sediment budget requires, such as determining where sediment is moving and quantify how much, a suite of numerical models have been developed. This appendix details the data available for the models, the set-up of the models and the calibration and validation process that has been undertaken for each module within the modelling suite.

### A2 Metocean Conditions

It is important to have an understanding of the dominant processes in an area before any numerical models are developed. As part of the bathymetric analysis investigations at the Port of Weipa and Amrun Port, measured data were reviewed to develop an understanding of the dominant coastal processes in the region (PCS, 2018a<sup>1</sup> & 2018b<sup>2</sup>). It was found that wave action was the dominant driver controlling resuspension along the open coast and within Albatross Bay, while within the estuaries (including the Inner Harbour region of the Port of Weipa) tidal currents were the dominant driver controlling resuspension. In both regions the tidal currents are the dominant process controlling the transport of any sediment which was suspended. It is therefore important for the numerical modelling approach to include waves and tidal currents and to be able to demonstrate that the models are providing a realistic representation of the natural conditions.

### A3 Available Data

This section provides details of data that were available to inform the numerical modelling. This includes data that were collected specifically for the Project (some Water Level data, Current data and Water Quality data) as well as additional data collected for other reasons (water level at Humbug Tide Gauge, meteorological and wave). Table 1 provides a summary of the available data while the locations of the sites are shown in Figure 1. The meteorological data have been used as an input to the model, while the other dataset have been utilised in the calibration and validation of the numerical model.

**Table 1. Overview of available data.**

Data Type	Location	Description
Water Level	Humbug Tide Gauge	Archived data recordings available from 1996 – 2018. Predicted data available from 2018 onwards (until recent measured data uploaded).
	ADCP WQ1	Data recorded between 19/04/2018 – 12/07/2018.
	ADCP WQ2	Data recorded between 19/04/2018 – 12/07/2018.
	ADCP WQ3b	Data recorded between 14/06/2018 – 13/07/2018.
Meteorological	Weipa Aero	Wind data available from March 1972 onwards.
Waves	Albatross Bay WRB	Wave data available from May 2008 onwards.

<sup>1</sup> PCS (2018a) Port of Weipa: Sustainable Sediment Management Assessment, Bathymetric Analysis. Report No. P007\_R01F1. July 2018.

<sup>2</sup> PCS (2018b) Amrun Port: Sustainable Sediment Management Assessment, Bathymetric Analysis. Report No. P007\_R02F1. July 2018.

Data Type	Location	Description
Currents (through the water column)	ADCP WQ1	Data recorded between 13/06/2018 – 12/07/2018.
	ADCP WQ2	Data recorded between 19/04/2018 – 12/07/2018.
	ADCP WQ3b	Data recorded between 14/06/2018 – 13/07/2018.
Currents (above the bed)	Marotte WQ1	Data recorded between 15/03/2018 – 15/06/2018
	Marotte WQ2	Data recorded between 18/04/2018 – 15/06/2018
	Marotte WQ4	Data recorded between 15/03/2018 – 01/06/2018
Water Quality	WQ1	Turbidity and SSC data 19/01/2018 – 12/07/2018
	WQ2	Turbidity and SSC data 16/03/2018 – 12/07/2018
	WQ3/WQ3b	Turbidity and SSC data 19/01/2018 – 13/07/2018
	WQ4	Turbidity and SSC data 19/01/2018 – 12/07/2018
	WQ5	Turbidity and SSC data 19/01/2018 – 14/07/2018



*Note: These stations were later used to calibrate and validate the suite of numerical models for this study.*

**Figure 1. Location of sampling stations of available data describing hydrodynamic, meteorological, water quality and sedimentological conditions in the Port of Weipa and Amrun regions.**

## A4 Modelling Approach

This project utilised the modelling software MIKE by DHI. The software includes hydrodynamic, wave and sediment transport modules which can be coupled together. The MIKE 21 Flexible Mesh (FM) modules are based on a flexible mesh approach and have been developed for applications within oceanographic, coastal and estuarine environments (DHI, 2017a<sup>3</sup>).

The hydrodynamic module (HD) is based on the numerical solution of the two-dimensional incompressible Reynolds averaged Navier-Stokes equations, adopting the assumptions of Boussinesq and hydrostatic pressure. The model consists of continuity, momentum, temperature, salinity and density equations and is closed by a turbulent closure scheme (DHI, 2017a<sup>3</sup>).

The spatial discretisation of the primitive equations is performed using a cell-centred finite volume method. The spatial domain is discretised by subdivision of the continuum into non-overlapping elements/cells. In the horizontal plane an unstructured grid is used, which can consist of triangular or quadrilateral elements.

For this study the hydrodynamics of the Weipa and Amrun region have been modelled using a detailed two-dimensional (2D) HD model of the region.

A detailed MIKE spectral wave (SW) model has also been developed which covers the same extent as the HD model. Local wave conditions, in addition to measured winds from Weipa Aero, have been used to drive the SW model.

Decoupled results from the MIKE HD and SW models have been used as inputs to the MIKE sediment transport model.

The modelling approach started with the HD model simulating the 2D flows within Albatross Bay and the Weipa/Amrun region, utilising predicted tidal levels as input conditions to the model boundaries. The SW model was then run using wind data along with offshore wave boundary conditions based on measured wave data from the Albatross Bay WRB. Decoupled results from the HD model, including water depth, current and flux data, in addition to radiation stresses from the SW model were then used to drive the sediment transport model.

Results from the sediment transport model have been post-processed to inform the sediment budget.

## A5 Hydrodynamic model

The following sections provide details on the numerical model setup, calibration and validation of the HD model.

### A5.1 Model setup

The model setup of the hydrodynamic model includes details regarding the domain extent and mesh generation, development of boundary conditions, bathymetry and model sensitivity testing.

#### A5.1.1 Domain extent and mesh generation

The extent of the model domain was carefully selected taking into consideration the location of both Ports and the physical processes within the study area, enabling the same domain to be used for the HD, SW and sediment transport models.

---

<sup>3</sup> DHI, 2017a. MIKE 21 & MIKE 3 Flow Model FM – Hydrodynamic and Transport Module, Scientific Documentation.



The Ports of Weipa and Amrun are located in the Gulf of Carpentaria, on the north-west coast of the Cape York Peninsula in Northern Queensland. The Ports are situated within Albatross Bay, with the Port of Weipa's wharves and berths located in the Embley River and the Port of Amrun sited at the southern end of the Bay on the open coast.

It has been previously documented in the Bathymetric Analysis reports for the Ports (PCS, 2018a & 2018b) that wave action and tidal currents are important processes for sediment mobilisation and transport in the Port regions.

The model geometry took this into consideration when developing the domain extent of the model and the boundary locations. The model domain encompassed Albatross Bay and approximately 80 km of shoreline to the north (to Port Musgrave) and south (to Love River). The domain extended offshore to approximately the -50 m LAT depth contour, resulting in the northern boundary being 73 km in length and the southern boundary 90 km in length. The domain extent, boundary position and length of each boundary are shown in Figure 2.

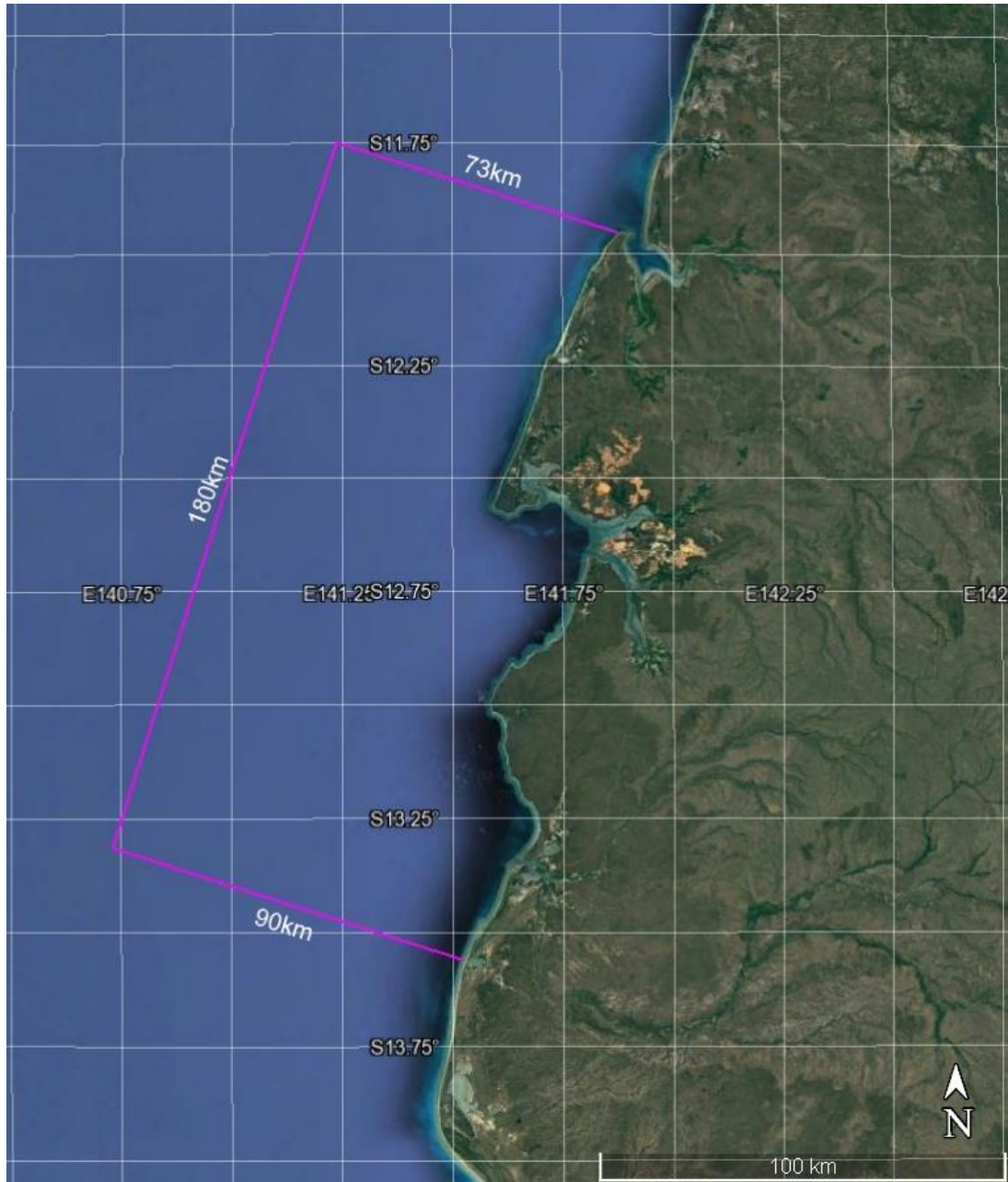
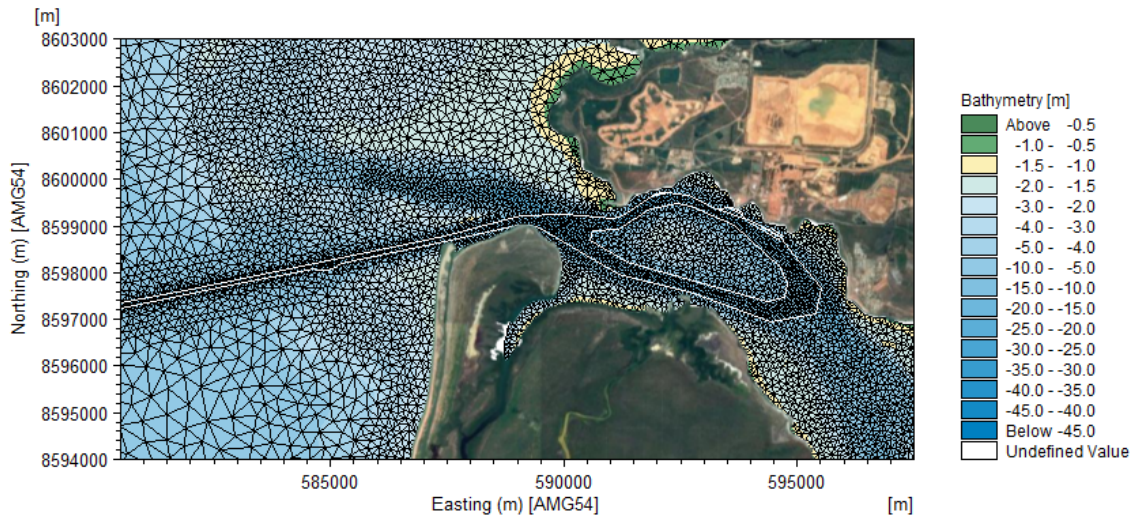
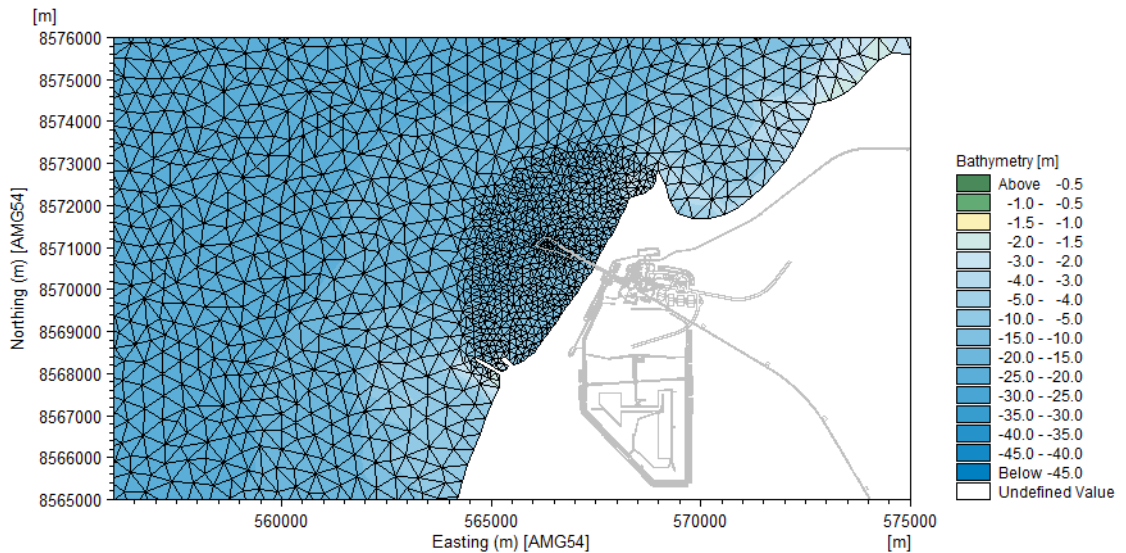


Figure 2. Domain extent, boundary locations and boundary lengths.

The spatial discretisation of MIKE's flexible mesh enabled the model mesh resolution to be varied within the model domain, with higher resolution in areas of interest, such as around the Ports of Weipa and Amrun, and lower resolution in offshore areas. This approach assists with optimising the model simulation times without compromising on representing important physical processes within key study areas. Plots of the mesh configuration are shown in Figure 3 for the Port of Weipa area, and in Figure 4 for the Port of Amrun area. A zoomed out plot of the study area covering both Ports is shown in Figure 5.



**Figure 3. Mesh configuration within the Port of Weipa.**



**Figure 4. Mesh configuration at the Port of Amrun.**

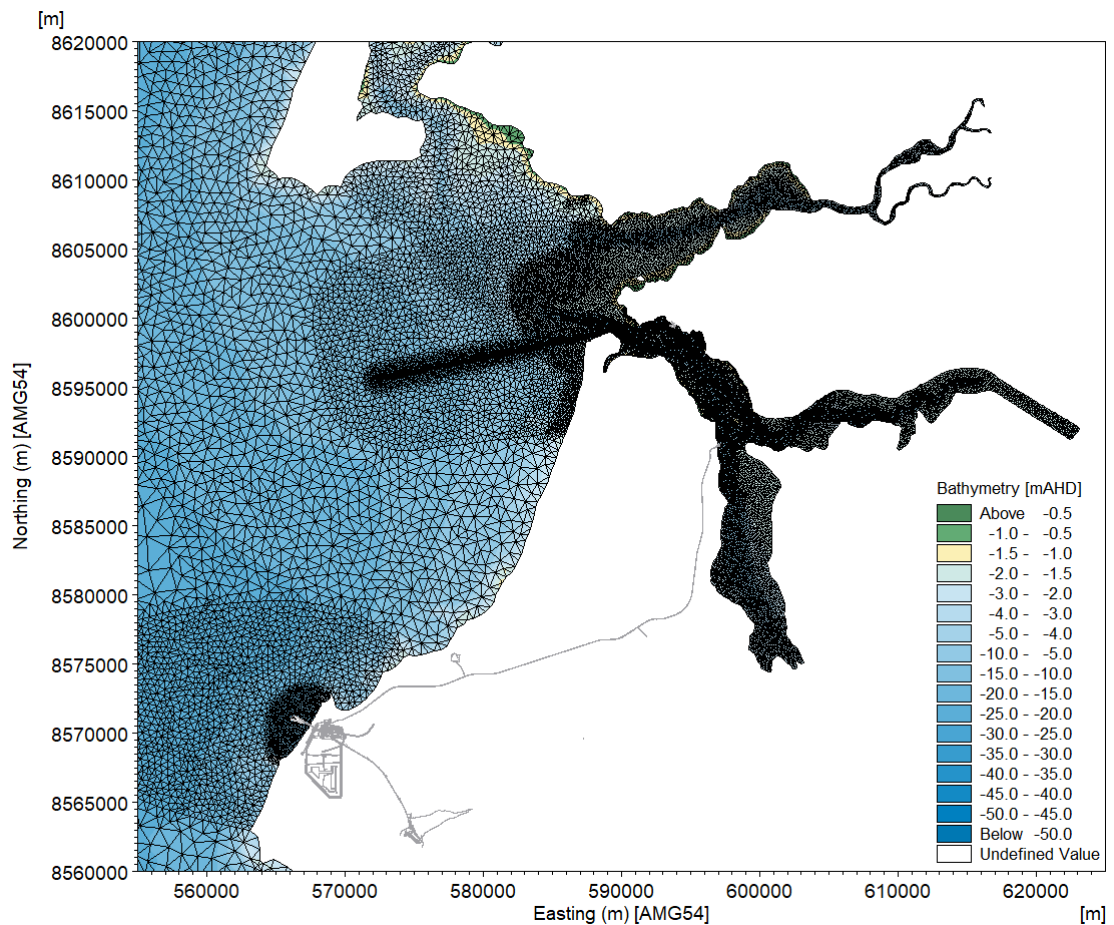


Figure 5. Mesh configuration in the Weipa and Amrun Port regions.

### A5.1.2 Development of boundary conditions

Boundary conditions for all three open boundaries (north, west and south, as shown in Figure 6) were generated using the TPXO 8 Global Inverse Tide Model.

TPXO is a series of fully-global models of ocean tides, which best-fits, in a least-squares sense, the Laplace Tidal Equations and measured altimetry data. The tides are provided as complex amplitudes of earth-relative sea-surface elevation for eight primary (M2, S2, N2, K2, K1, O1, P1, Q1), two long period (Mf, Mm) and 3 non-linear (M4, MS4, MN4) harmonic constituents (plus 2N2 and S1 for TPXO9) (<http://volkov.oce.orst.edu/tides/global.html>). The methods used to compute the model are described in detail by Egbert, Bennett, and Foreman, 1994<sup>4</sup> and further by Egbert and Erofeeva, 2002<sup>5</sup>.

Spatially varying water levels have been used to drive the model on all three open boundaries to account for variations in water level slope, between the nearshore and offshore, and over the length of the offshore boundary. Further modifications to the water levels were applied by including a +20% scaling of the water levels on the open boundaries and by adjusting the location of the data used to provide the forcing conditions along the

<sup>4</sup> Egbert, G., Bennett, A. and Foreman, M. (1994) TOPEX/Poseidon tides estimated using a global inverse model. *Journal of Geophysical Research*, 1994, Volume 99, No C12, pp. 24821 - 24852.

<sup>5</sup> Egbert, G. and Erofeeva, S. (2002) Efficient inverse modeling of barotropic ocean tides. *Journal of Atmospheric and Oceanic Technology*, February 2002, 19:183 - 204.

southern boundary to improve the agreement between measured and modelled water levels within the study area.

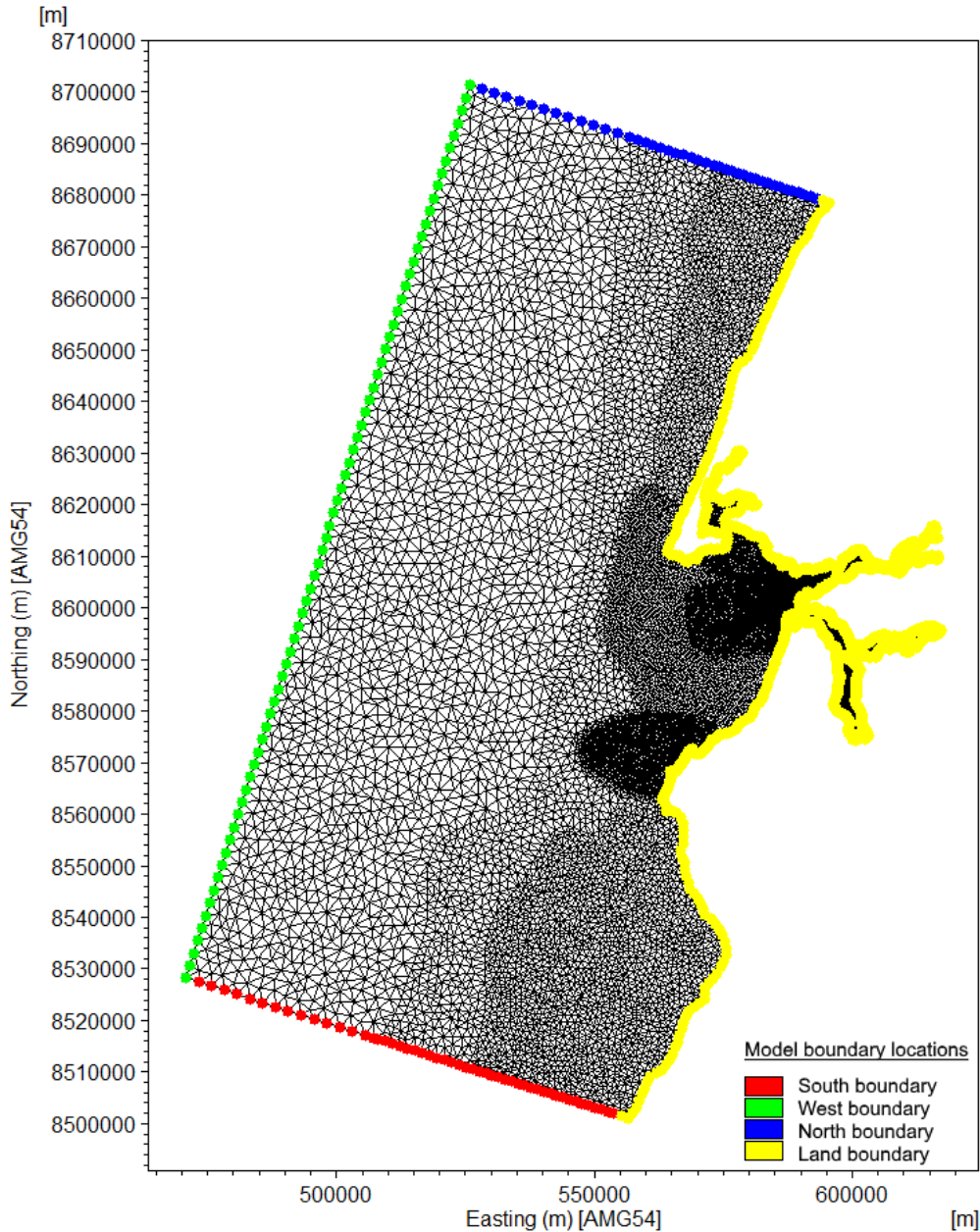


Figure 6. Hydrodynamic model boundary locations, domain extent and mesh configuration.

### A5.1.3 Bathymetry

The bathymetry for the model utilises a selection of data including recent survey data at the Port of Weipa and Amrun Port obtained from NQBP, chart data from the Australian Hydrographic Office (AHO) and, where data gaps existed, water depths were inferred from aerial imagery. A summary of the datasets used and the areas of application is provided in Table 2. For the purposes of the modelling all bathymetric data were adjusted to Australian Height Datum (AHD). An overview of the interpolated soundings covering the extent of the model domain is shown in Figure 7 and for the Weipa and Amrun Port region in Figure 8.

**Table 2. Summary of bathymetric data source and area of application.**

Data type and source	Date of data source	Area of application in model
Survey data from NQBP	2016 and 2017	Humbug Ro-Ro, Hey River, Jackson Bank, Weipa DMPA, Weipa May 2017 pre and June 2017 post dredge survey extents, Triluck Creek, Amrun April 2016 post dredge survey extent including Amrun DMPA.
Chart data from AHO	Sounding dates as per AHO charts 'Approaches to Weipa' and 'Port of Weipa'	All other areas within the model domain outside of the NQBP survey extents, with the exception of a few small areas in the upper reaches of the rivers and some shallow intertidal where chart data was unavailable.
Data inferred from aerial imagery	2018	All other areas where data gaps existed, including the upper reaches of the Embley, Hay, Mission and Pine Rivers, Roberts Creek and Nomenade Creek.

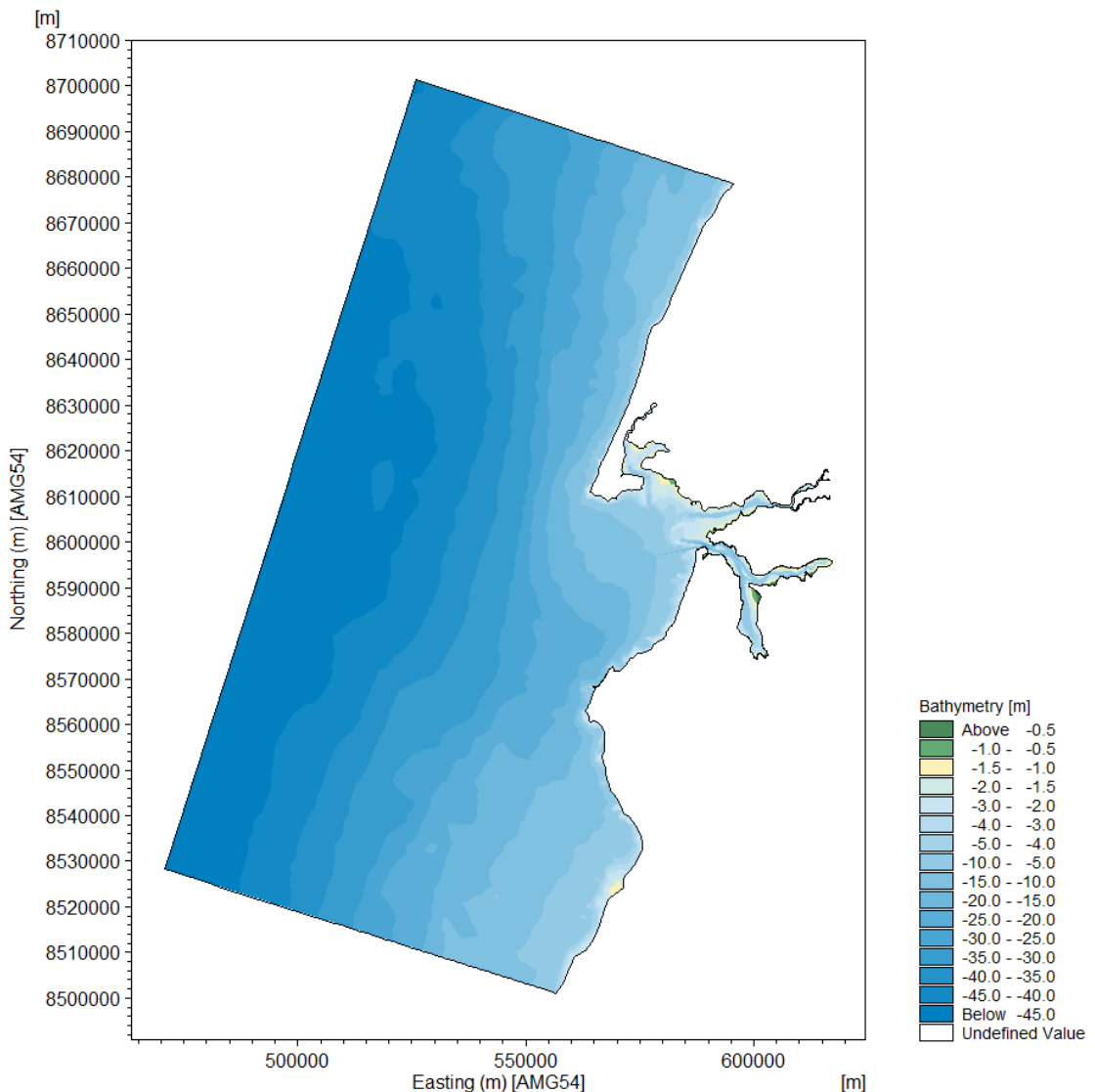


**Figure 7. Model bathymetry within the model domain.**

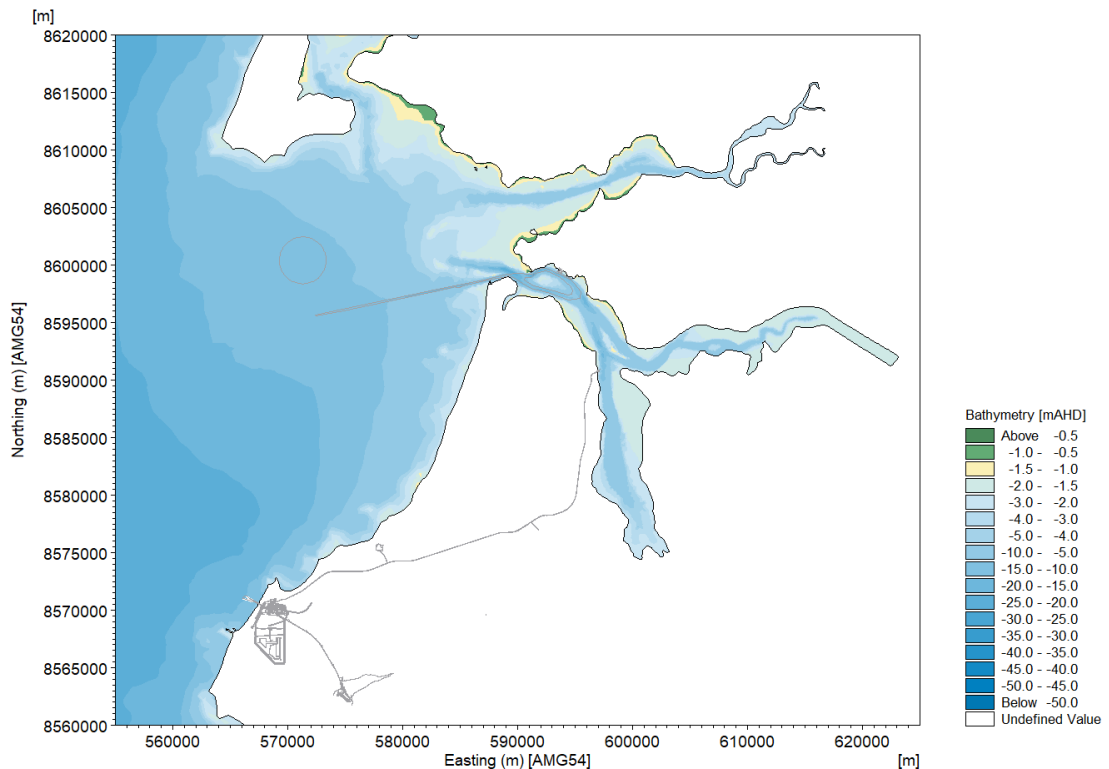


**Figure 8. Model bathymetry within the study area.**

#### A5.1.4 Bed resistance

The model bed resistance is defined as a Manning  $M$  number, this is equivalent to the inverse of the Manning  $n$  number which is more commonly adopted in numerical modelling. To more accurately represent the variation in bed characteristics between the deeper offshore areas and shallower area inside Albatross Bay, a varying bed resistance was applied within the model domain, as shown in Figure 9.

Cowan's<sup>6</sup> method for estimating Manning's bed roughness was used inside the Port of Weipa area, where sandy creeks predominate. In the offshore area, where water depths are deeper, a lower bed resistance value was utilised. Along the offshore boundaries a high roughness value was applied to reduce the potential for any model instabilities as the tidal wave propagates along the open boundaries. It is well documented that seabed habitats (e.g. seagrass meadows or coral reefs) can locally influence the bed roughness (Forsberg et al., 2018<sup>7</sup>; Nunes et al, 2008<sup>8</sup>), but these localised changes would only influence the conditions local to the habitat and would not influence the overall sediment budget. As such, for this assessment they have not been included, but could subsequently be included for future detailed impact assessment studies.

<sup>6</sup> Cowan, W. L., 1956: Estimating hydraulic roughness coefficients. *Agricultural Engineering*, 37: 473-475.

<sup>7</sup> Forsberg, P.L., V.B. Ernstsén, T.J. Andersen, C. Winter, M. Becker, and A. Kroon, 2018. The effect of successive storm events and seagrass coverage on sediment suspension in a coastal lagoon. *Estuarine, Coastal and Shelf Science* 212: 329-340.

<sup>8</sup> Nunes, V. and G. Pawlak, 2008. Observations of Bed Roughness of a Coral Reef. *Journal of Coastal Research* March 24 (2A): 39-50.

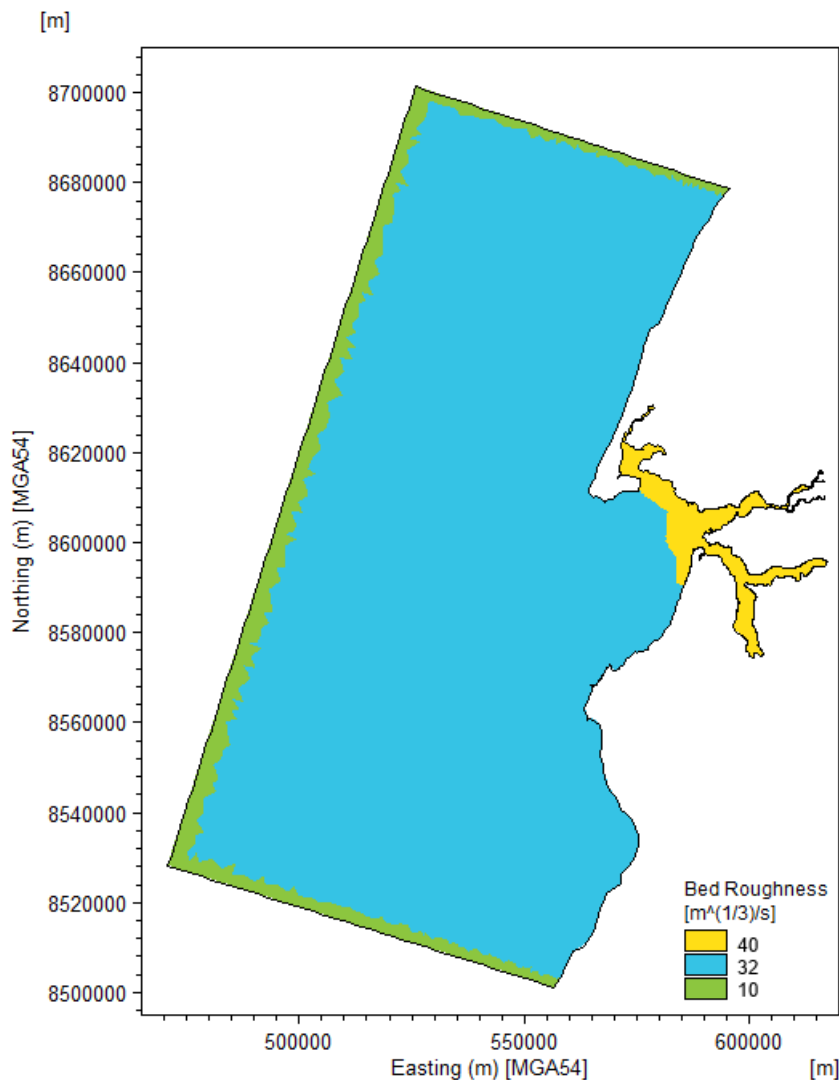


Figure 9. Varying bed resistance in the model domain

## A5.2 Model sensitivity

During the model development, setup and calibration a range of sensitivity testing was undertaken to optimise the model setup based on the available measured data. The sensitivity testing included:

- **Boundary conditions:** offshore tidal boundary conditions from a range of sources were tested to ensure the boundary conditions adopted provided the most accurate representation of the measured water level data available;
- **Bathymetry:** the upstream bathymetry of the estuaries in Albatross Bay (where no bathymetric data were available) was adjusted using an iterative approach to optimise the bathymetry and upstream tidal prism of the estuaries based on the measured water level and current data; and
- **Wind:** sensitivity testing was undertaken to assess the requirement to include wind in the HD model. Tests showed that the inclusion of wind did not change the HD model results at the model calibration and validation sites and so wind was consequently excluded from the HD model (it was included in the wave model, see Section A6).



### A5.3 Model calibration and validation

To ensure that the hydrodynamic model accurately represents the natural conditions in the Weipa and Amrun regions, measured and predicted water level data and measured current speed and direction data have been used to calibrate and validate the hydrodynamic model. The locations of the available data are shown in Figure 1.

Hydrodynamic models are typically calibrated against measured water level and current data at a number of locations throughout the model domain. An assessment of the differences between the measured and modelled values was undertaken to enable the accuracy of the model to be quantified. The calibration of a hydrodynamic model in which tidal forcing dominates (as is the case for the Weipa and Amrun regions), requires at least a spring neap tidal cycle (approximately 14 days) to be simulated by the model.

Details of the data used in the hydrodynamic model calibration and validation are provided in the following sections as well as the final calibration and validation results.

#### A5.3.1 Selection of calibration and validation periods

Typically a numerical model is calibrated for one spring/neap cycle and then validated for a different spring/neap cycle period. This demonstrates that the model is able to replicate the variation in physical processes over different time periods and potentially during periods with different metocean conditions.

Due to the range of instruments used to collect data over the different data collection periods for this project (as discussed in Section A3), it was considered beneficial to select two calibration periods (one wet season and one dry season) and one validation period (dry season) to demonstrate the model performance.

The following calibration and validation periods were selected for the hydrodynamic model:

- Calibration period 1 (wet season) - 20<sup>th</sup> March 2018 to 3<sup>th</sup> April 2018;
- Calibration period 2 (dry season) – 10<sup>th</sup> May 2018 to 24<sup>th</sup> May 2018; and
- Validation period (dry season) – 17<sup>th</sup> June 2018 to 1<sup>st</sup> July 2018.

These periods were selected to enable the model performance to be assessed over the data collection periods and specifically to ensure that the model can replicate conditions during both the wet and dry seasons. The calibration and validation periods selected were 14 days in duration to ensure that a full 14 day spring-neap cycle was covered.

#### A5.3.2 Calibration and validation standards

Owing to the inherent complexities within the natural environment there is a degree of uncertainty which can be associated with model results. A model can only be as good as the data used for the model setup; therefore, confidence in the model is achieved by using the highest quality data available for calibration of the model and using a separate, independent dataset to validate the model outcome.

For quality control in the hydrodynamic model calibration, performance criteria have been defined to demonstrate that the model is capable of accurately representing the natural processes. For this project the guidelines laid down by the UK Foundation for Water Research have been considered. These guidelines distinguish between models of coastal waters and estuarine waters. For coastal waters such as the Weipa and Amrun regions, the following performance criteria have been defined, based on Evans (1993)<sup>9</sup>, and can be expressed in percentage terms as:

---

<sup>9</sup> Evans, G. P. (1993) A Framework for Marine and Estuarine Model Specification in the UK. Report Number FR 0374, Foundation for Water Research, March 1993.

- Modelled water levels should be within 10% of the tidal range over a spring neap tidal cycle;
- Timing of high water and low water should be within 15 minutes; and
- Modelled peak current speeds should be within  $\pm 10 - 20\%$  of measured speeds over a spring neap tidal cycle.

These standards provide a good basis for assessing model performance, but experience has shown that sometimes they can be too prescriptive, and it is also necessary for visual checks to be undertaken. Under certain conditions, models can meet statistical calibration standards but appear to perform poorly. Conversely, seemingly accurate models can fall short of the guidelines. Consequently, a combination of both statistical calibration standards and visual checks has been used to ensure that the model is representative of the natural environment.

### A5.3.3 Model calibration and validation results

The following sections present the results and performance statistics for the calibration and validation periods selected. The results are presented as timeseries plots showing measured/predicted and modelled data for water levels, current speed and direction at the calibration and validation locations shown in Figure 1. A quantitative evaluation of the model performance is provided in the form of the following statistics:

- For water levels:
  - Mean High Water (HW) level difference (modelled – observed) (m);
  - Mean Low Water (LW) level difference (modelled – observed) (m);
  - Mean HW level difference as a percentage of the tidal range (m);
  - Mean LW level difference as a percentage of the tidal range (m);
  - Root Mean Square (RMS) of HW level difference;
  - RMS of LW level difference;
  - Mean HW phase difference (mins); and
  - Mean LW phase difference (mins).
- For currents:
  - Mean ebb speed difference (modelled - observed) (m/s);
  - Mean flood speed difference (modelled - observed) (m/s);
  - Mean ebb percentage difference relative to maximum observed speed; and
  - Mean flood percentage difference relative to maximum observed speed;
  - RMS of ebb speed difference;
  - RMS of flood speed difference;
  - Mean ebb direction difference (degrees); and
  - Mean flood direction difference (degrees).

For calibration period 1 the predicted water levels at Humbug Point (in the Port of Weipa) were compared with model results at WQ1/ADCP1 (located close to Humbug Point). Modelled current speeds and directions were compared against Marotte current data collected above the bed at WQ1 and WQ4. Note: For the purposes of the HD calibration, where a WQ precedes the site name, this refers to a Marotte device being deployed at this location as opposed to an ADCP device. Predicted water levels were also compared at Pennefather River, Humbug Point and Archer River, to show the change in tidal signal characteristics from north to south within the model domain.

For calibration period 2 predicted water levels at Humbug Point were compared with the model at WQ1/ADCP1. Measured water levels at ADCP2 were also compared with model results. As with calibration period 1, modelled current speeds and directions were also compared against Marotte current data collected above the bed at WQ1, WQ2 and WQ4. Modelled currents were also compared with measured ADCP current data collected mid depth at ADCP2.

For the validation period, measured water levels and currents at ADCP1, 2 and 3b have been compared with model results. The statistical results are provided in the following sections. It should be noted that where the text for tabulated statistical results are shown in blue, this indicates that the model is not meeting the calibration standards specified in Section A5.3.2. For these occurrences an explanation has been provided to explain the reasons.

### Calibration period 1

The water level statistics for calibration period 1 are presented in Table 3 and current statistics in Table 4, with time series plots shown in Figure 10.

The statistical results show that the model is performing reasonably well and meeting all the calibration and validation standards, with the exception of the mean ebb percentage difference relative to maximum observed speed at WQ4, which is just outside of the criteria. The timeseries plots in Figure 10 show that when the tidal signal exhibits more diurnal characteristics, the model tends to under predict the peak ebb current speed, both at WQ1 and WQ4. During the diurnal tidal phase there also tends to be a greater difference between modelled and measured ebb current directions. These discrepancies may be due to minor differences in how ebb flows are diverted around Cora Bank, or more likely to be due to discrepancies between the actual and model bathymetry, channel geometry and tidal prism in the mid to upper reaches of the Embley and Hey Rivers. It is expected that the model calibration could be improved in the future if more reliable bathymetric data was collected in these areas.

**Table 3. Water level statistics for calibration period 1.**

Water level statistical description	Station name
	WQ1/Humbug Point
Mean HW level difference (modelled - observed) (m)	0.02
Mean LW level difference (modelled - observed) (m)	-0.01
Mean HW level difference as percentage of tidal range	1.7
Mean LW level difference as percentage of tidal range	-0.6
RMS of HW level difference (m)	0.1
RMS of LW level difference (m)	0.1
Mean HW phase difference (mins)	6
Mean LW phase difference (mins)	-13

*Note: The differences in phase of the high and low waters were derived by subtracting the time of the measured value from the time of the model value. A negative value therefore indicates that the model is early compared to the measured data.*

**Table 4. Current statistics for calibration period 1.**

Current statistical description	Station name	
	WQ1	WQ4
Mean ebb speed difference (modelled - observed) (m/s)	-0.07	-0.16
Mean flood speed difference (modelled - observed) (m/s)	-0.01	-0.05
Mean ebb % difference relative to max. observed speed	-12	-24
Mean flood % difference relative to max. observed speed	-1	-4
RMS of ebb speed difference (m/s)	0.10	0.18
RMS of flood speed difference (m/s)	0.13	0.13
Mean ebb direction difference (deg)	14	7
Mean flood direction difference (deg)	-3	1

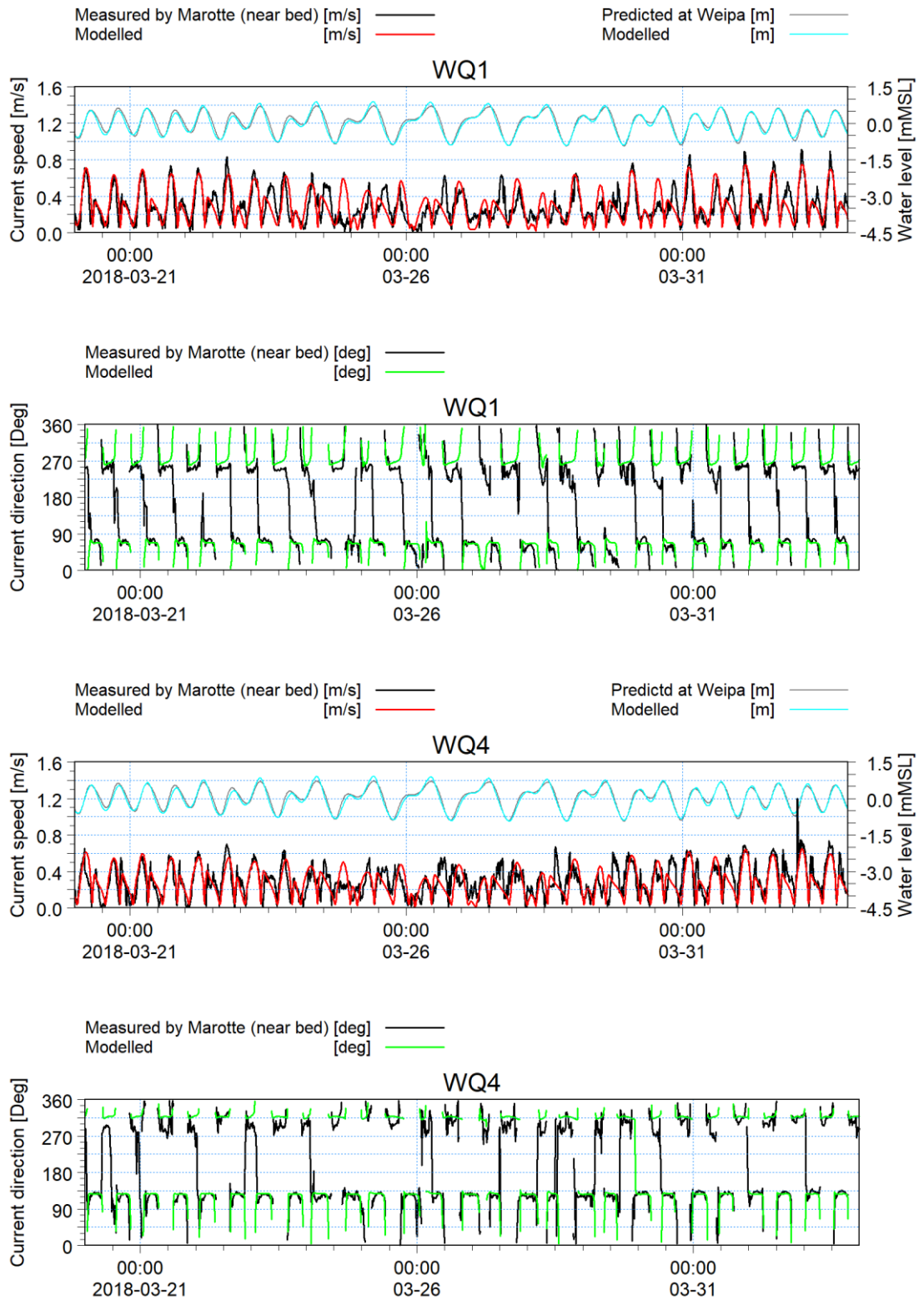
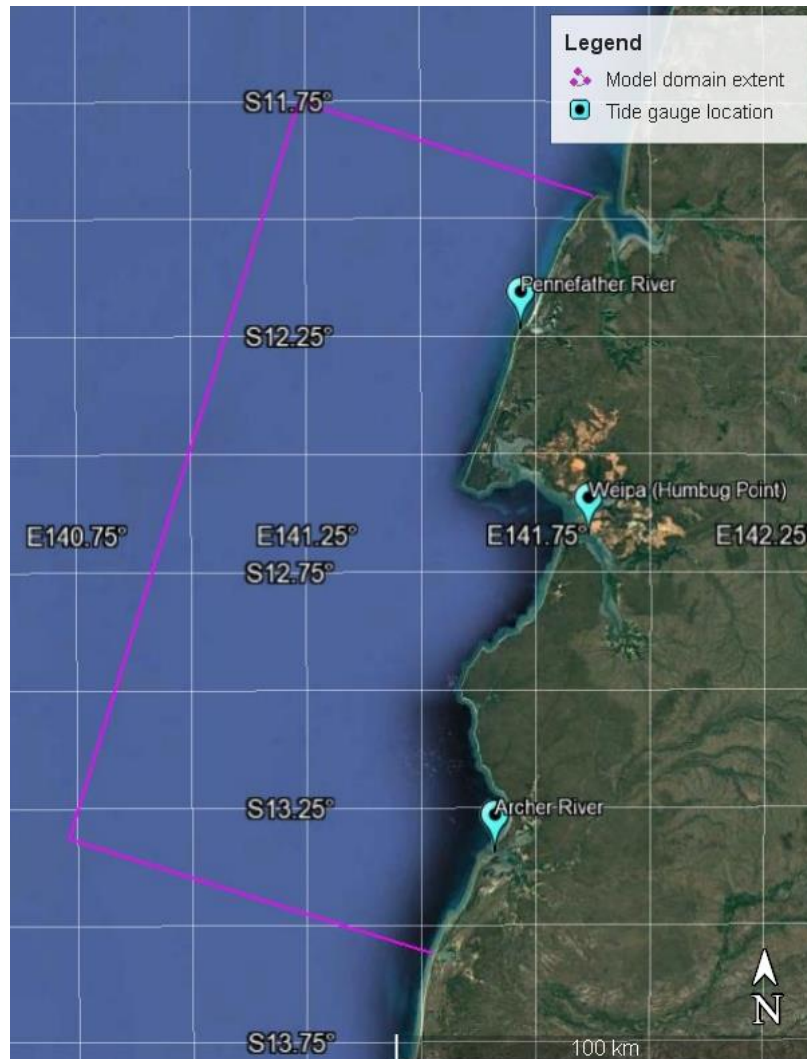


Figure 10. Comparisons in water level, current speed (measured using the Marotte current meters) and current direction data for calibration period 1 at WQ1 and WQ4.

Given the size of the model domain, extending approximately 180 km along the shoreline, it is considered beneficial to demonstrate the model's ability to replicate the variations in tidal signal across the domain. Three tide gauge stations within the model domain were selected including Pennefather River, Humbug Point (Weipa) and Archer River, approximate locations of which are shown in Figure 11.



**Figure 11. BoM predicted water level stations used to calibrate the model.**

The predicted and modelled water levels are compared at the three tide gauge stations in Figure 12. The bottom plot in Figure 12 shows how the tidal signal changes, exhibiting a greater semi-diurnal component further north towards Pennefather River and the northern model boundary. The variation in tidal range and semi-diurnal/diurnal tidal characteristics are well replicated by the model with mean HW and LW differences less than 0.05 m and RMS errors of 0.1 m.

An offset in the phasing of the tide at both the Pennefather and Archer Rivers is evident between the modelled and predicted data presented in Figure 12. This is most likely to be due to a discrepancy in the tide gauge locations specified by BoM. The tide gauges may have been located further upriver, as opposed to on the coast, which could account for the phase difference allowing time for the tidal wave to propagate up the river.

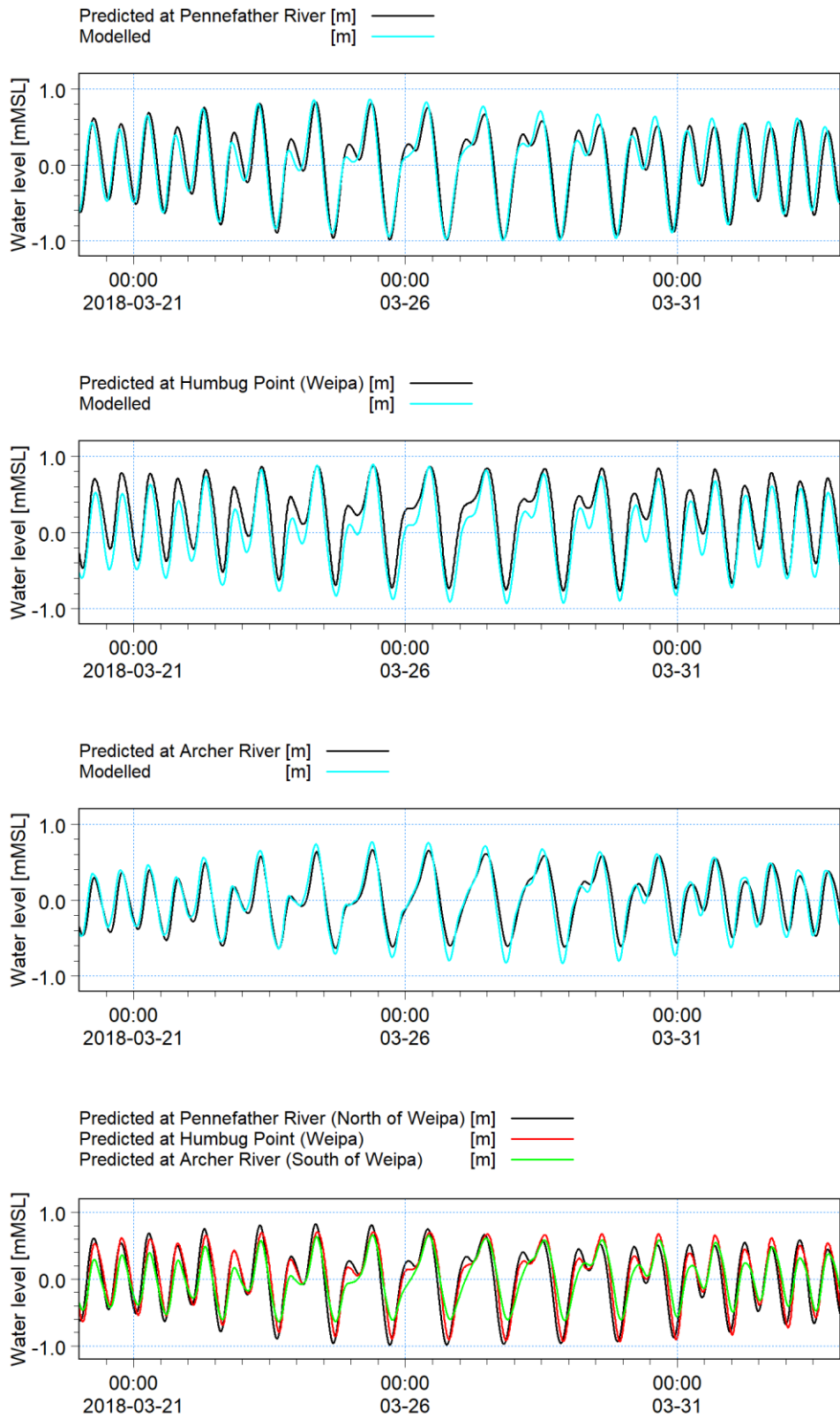


**Figure 12. Comparison of predicted and modelled water levels within the model domain for calibration period 1.**

## Calibration period 2

The water level statistics for calibration period 2 are presented in Table 5 and current statistics in Table 6, with plots comparing the time series data in Figure 13, Figure 14 and Figure 15.

The statistical results show that the model is performing well at ADCP1 and ADCP2 for water levels, with all calibration criteria being met. For the current statistics, discrepancies outside of the recommended calibration criteria are again noted for the ebb phase of the tide, both for speed and direction. In these instances the model is under predicting ebb current speeds at WQ1 but over predicting ebb current speeds at ADCP2, particularly during the more diurnal phase of the tidal cycle. This can most likely be attributed to differences in the shape of the tidal signal, which are more evident during the diurnal phase of the tide, which is particularly shown at ADCP1 on the 20<sup>th</sup>, 22<sup>nd</sup> and 23<sup>rd</sup> of May.

During the tidal period, which exhibits more diurnal characteristics, the data show that the first ebb tide of the cycle is more like a period of slack water as opposed to an ebb period, indicated by the flat appearance of the tidal signal. Current speeds during this period are low as there is little movement in the volume of water at this point within the Embley River. On the subsequent ebb tide the gradient of the tidal curve is large, resulting in higher current speeds. The model is not able to accurately represent this trend. During the first ebb tide/slack water, the tidal signal within the model at ADCP1 has a larger gradient than the measured data, which results in higher current speeds than the measured data. This has a knock-on effect for the subsequent ebb tide as there is slightly less volume of water in the estuary at this point in the tide, resulting in lower current speeds for the second ebb tide.

The variations in the tidal signal cause the difference between measured and modelled ebb current speeds. It is evident that these local tidal harmonic characteristics are not well accounted for within the predicted water level conditions, which are also what is used to drive the model. Despite this limitation it should be noted that for the majority of the time the model is performing well and replicating the physical process at each of the calibration locations.

**Table 5. Water level statistics for calibration period 2.**

Water level statistical description	Station name	
	ADCP1	ADCP2
Mean HW level difference (modelled - observed) (m)	0.00	0.08
Mean LW level difference (modelled - observed) (m)	-0.02	0.06
Mean HW level difference as percentage of tidal range	-0.2	9.6
Mean LW level difference as percentage of tidal range	-2.1	6.8
RMS of HW level difference (m)	0.1	0.2
RMS of LW level difference (m)	0.1	0.1
Mean HW phase difference (mins)	12	-15
Mean LW phase difference (mins)	-5	0

*Note: The differences in phase of the high and low waters were derived by subtracting the time of the measured value from the time of the model value. A negative value therefore indicates that the model is early compared to the measured data.*



**Table 6. Current statistics for calibration period 2.**

Current statistical description	Station name			
	WQ1	WQ2	WQ2/ ADCP2	WQ4
Mean ebb speed difference (modelled - observed) (m/s)	-0.13	0.10	0.08	-0.03
Mean flood speed difference (modelled - observed) (m/s)	-0.03	0.07	-0.02	0.03
Mean ebb % difference relative to max. observed speed	-18	25	17	-7
Mean flood % difference relative to max. observed speed	-4	12	-3	4
RMS of ebb speed difference (m/s)	0.14	0.14	0.11	0.06
RMS of flood speed difference (m/s)	0.10	0.08	0.05	0.08
Mean ebb direction difference (deg)	4	-7	8	19
Mean flood direction difference (deg)	-8	-8	2	-12

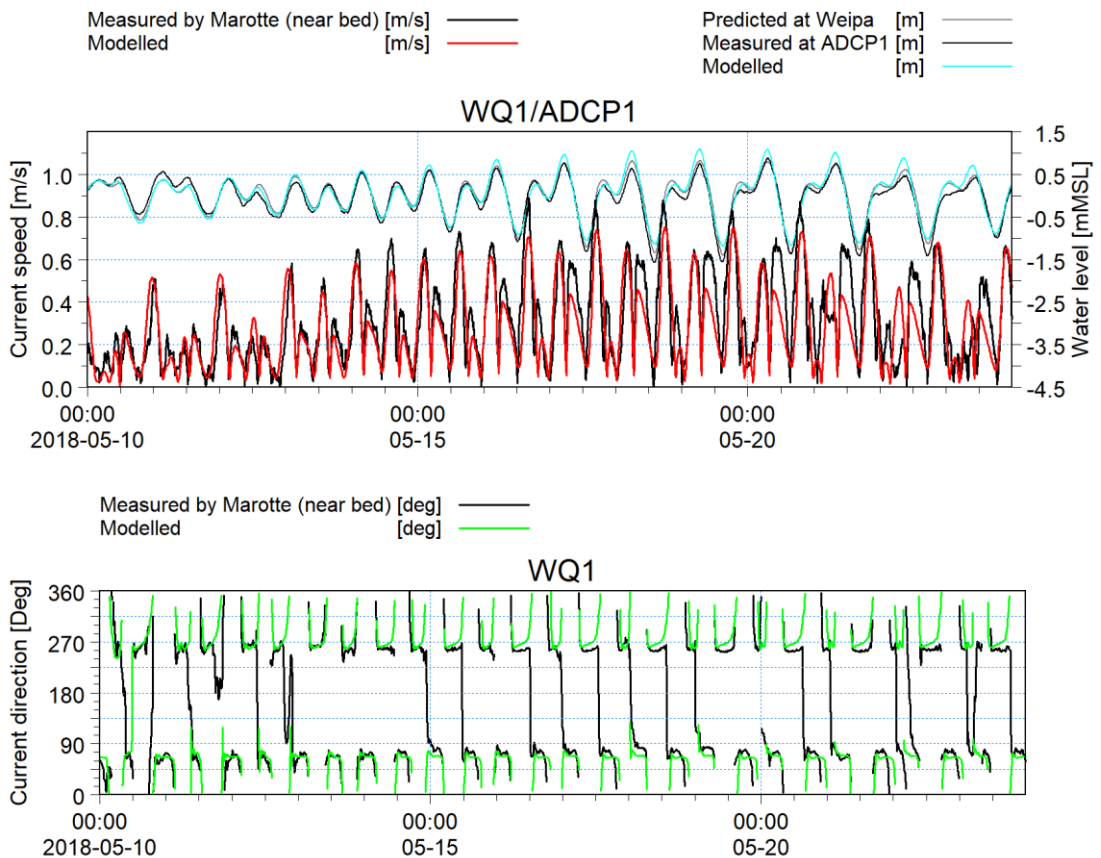


**Figure 13. Comparisons in water level, current speed (measured using ADCP and Marotte current meters) and current direction data at WQ1/ADCP1 for calibration period 2.**

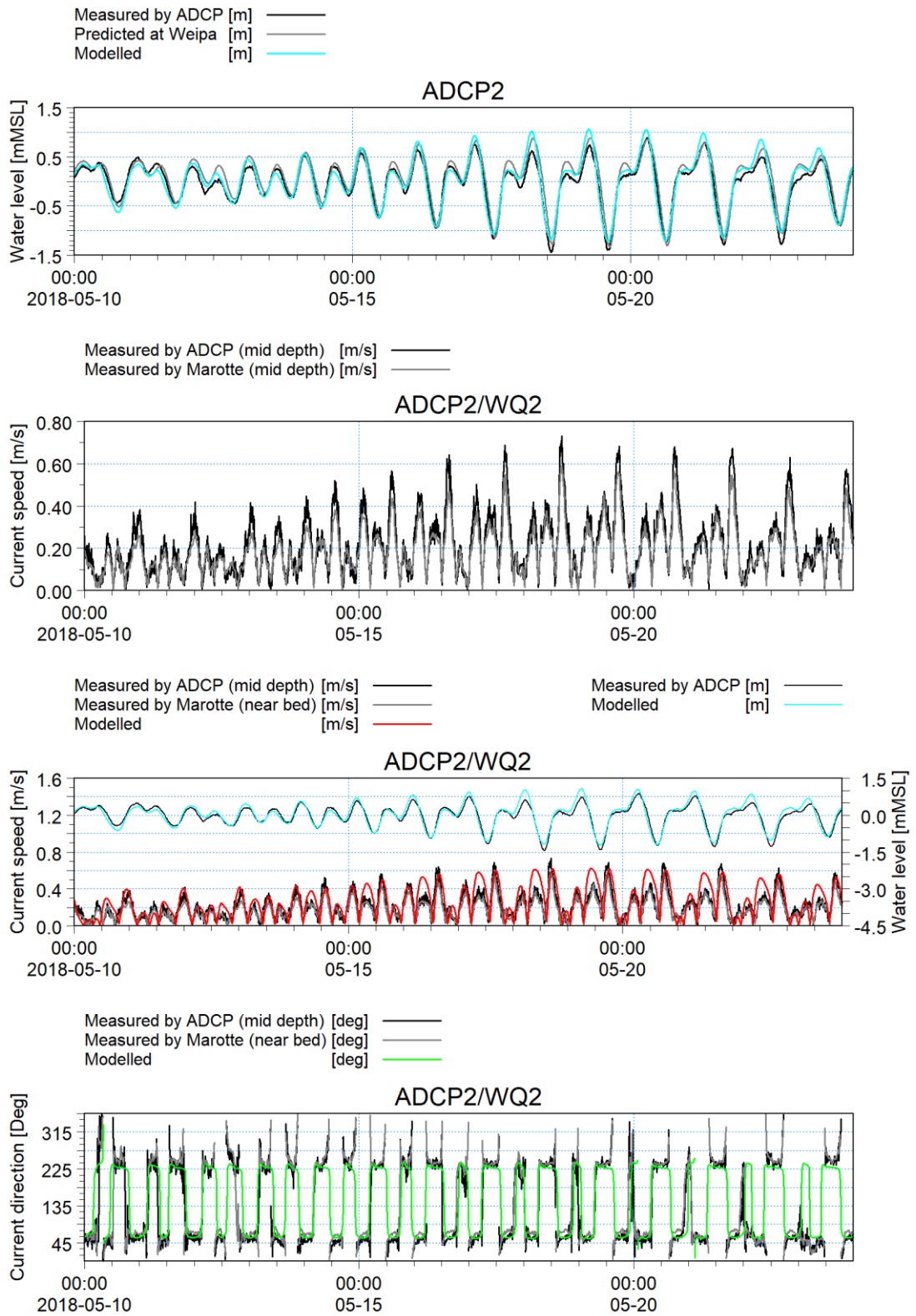
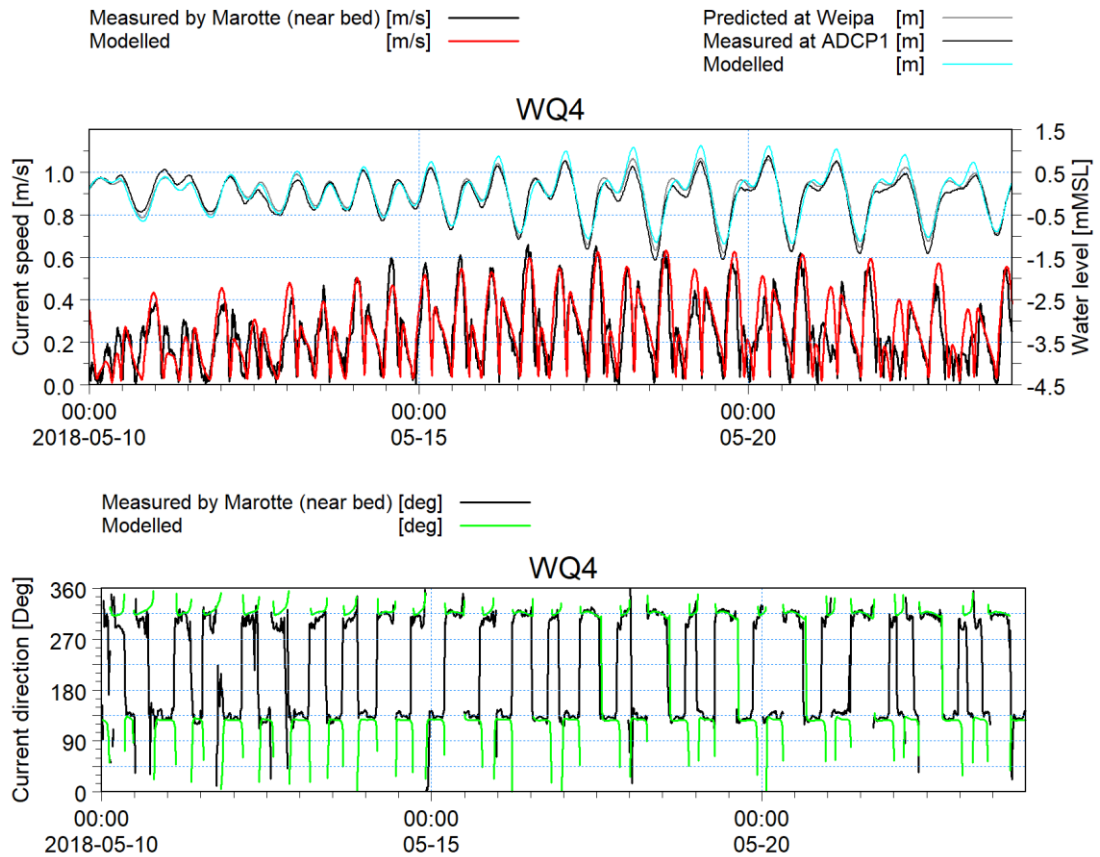


Figure 14. Comparisons in water level, current speed (measured using ADCP and Marotte current meters) and current direction data at WQ2/ADCP2 for calibration period 2.



**Figure 15. Comparisons in water level, current speed (measured using a Marotte current meter) and current direction data at WQ4 for calibration period 2.**

### Validation period

The water level statistics for the validation period are presented in Table 7 and current statistics in Table 8, with plots of the timeseries data shown in Figure 16. Comparisons in water level, current speed and current direction data at ADCP1 and 2 for the validation period. are shown in Figure 16 and Figure 17.

The statistical results show that the model is generally providing a reasonable representation of the measured hydrodynamic conditions. The model is replicating the variation in water levels within the calibration criteria at all three ADCP locations (ADCP1 and 2 at Weipa and ADCP3b at Amrun). It is noted under Table 7 that there is typically more noise in the measured data collected during the validation period and consequently this made it more difficult to compare with modelled data, this is particularly evident at ADCP3b. Consequently, statistics were also calculated at WQ1 using predicted data, as was adopted for the calibration period when no measured data were available, to assist with assessing model performance. Comparison between predicted and modelled water levels at WQ1/Humbag Point and ADCP1 shows that the model performance is improved relative to the comparison between modelled and measured water levels, with the HW difference being less than 12% of the tidal range and the phase differences reduced to be less than 10 minutes.

As with the calibration periods, similar observations can be made with regard to the differences in the shape of the tidal curve between modelled and measured data during the validation period, particularly on the ebb stage of the tide during the diurnal phase. This accounts for the over estimation in some peak ebb current speeds at ADCP 1 and 2.

Visual inspection of the timeseries plots assists in providing confidence that the model is replicating variations in water levels, current speeds and directions well. At ADCP3b there is a significant amount of noise in the data, however, it is noted that there is an offset when the currents are orientated towards the southwest. This can most likely be attributed to variations in local bathymetry which have not been accounted for within the model due to lack of more detailed bathymetric survey data in the area, particularly in the vicinity of the rock features.

**Table 7. Water level statistics for validation period.**

Water level statistical description	Station name			
	*WQ1 / Humbug	ADCP1	ADCP2	ADCP3b
Mean HW level difference (modelled - observed) (m)	0.11	0.14	0.12	0.13
Mean LW level difference (modelled - observed) (m)	0.03	0.04	-0.02	-0.01
Mean HW level difference as percentage of tidal range	11.6	14.7	14.5	14.4
Mean LW level difference as percentage of tidal range	3.5	4.6	-2.5	-0.9
RMS of HW level difference (m)	0.2	0.2	0.2	0.2
RMS of LW level difference (m)	0.1	0.1	0.1	0.1
Mean HW phase difference (mins)	4	-29	-40	-18
Mean LW phase difference (mins)	5	6	-9	8

*Note: The differences in phase of the high and low waters were derived by subtracting the time of the measured value from the time of the model value. A negative value therefore indicates that the model is early compared to the measured data.*

*Note2:\* Due to noise in the measured data the statistical results calculating mean HW and LW phase differences were considered unreliable at the ADCP locations. Consequently, the model data was also compared against predicted water level data at WQ1/Humbug Point to provide an indication of model performance at this location.*

**Table 8. Current statistics for validation period.**

Current statistical description	Station name		
	ADCP1	ADCP2	ADCP3b*
Mean ebb speed difference (modelled - observed) (m/s)	-0.06	0.10	-
Mean flood speed difference (modelled - observed) (m/s)	0.05	0.05	0.02
Mean ebb % difference relative to max. observed speed	-11	20	-
Mean flood % difference relative to max. observed speed	6	8	10
RMS of ebb speed difference (m/s)	0.07	0.12	-
RMS of flood speed difference (m/s)	0.15	0.08	0.04
Mean ebb direction difference (deg)	8	20	-
Mean flood direction difference (deg)	-1	7	26

*Note:\* The measured data at ADCP3b did not show a consistent ebb current and so no statistics are presented for the ebb current.*

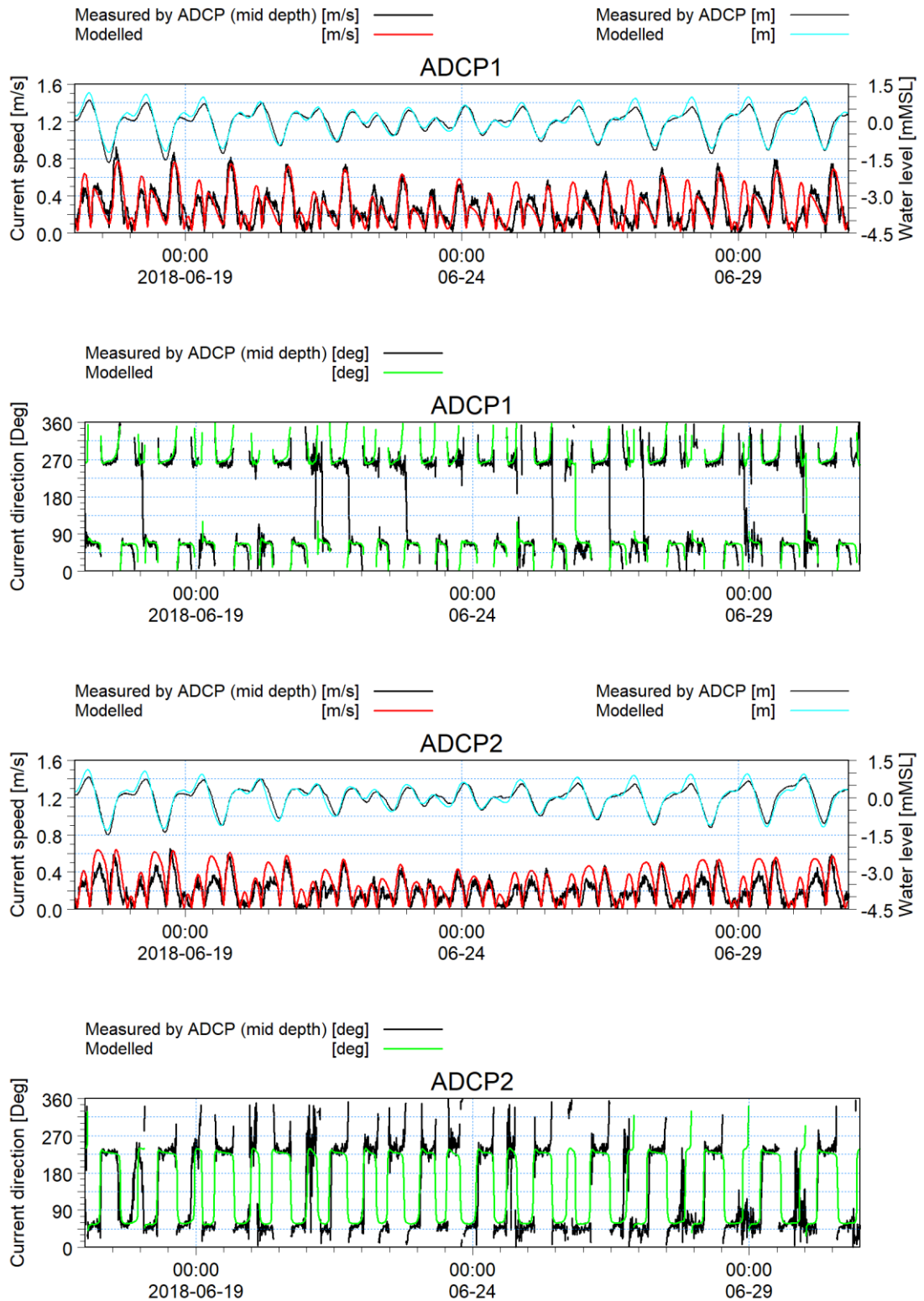


**Figure 16. Comparisons in water level, current speed and current direction data at ADCP1 and 2 for the validation period.**

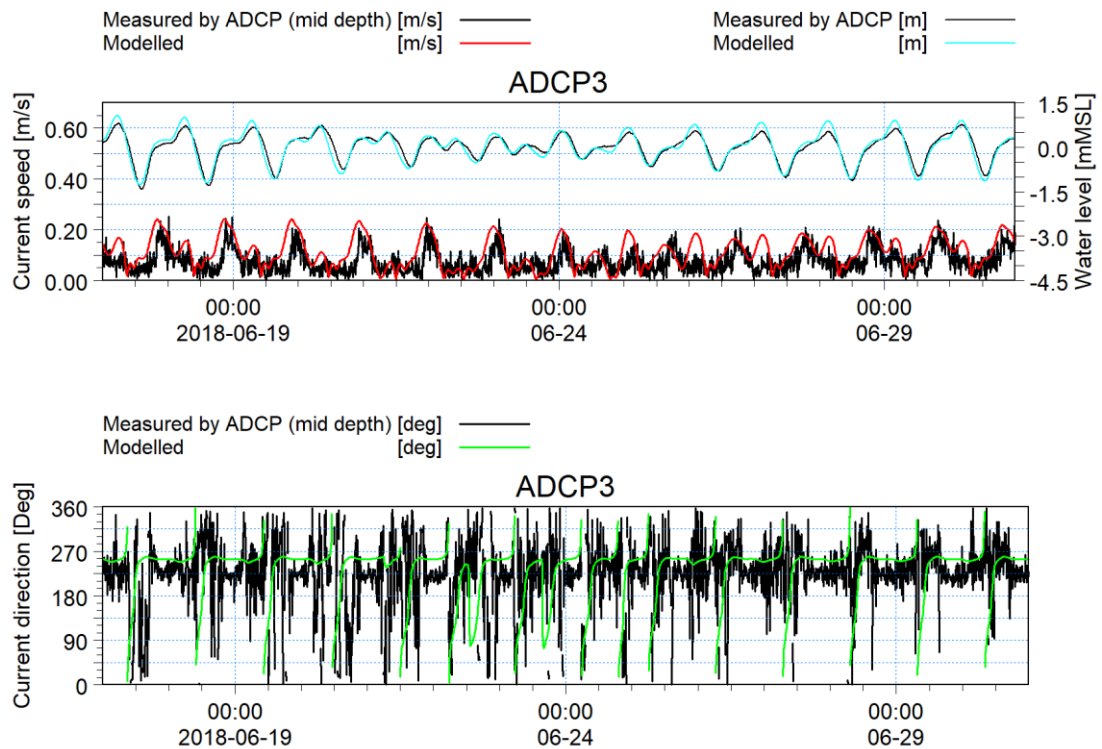


Figure 17. Comparisons in water level, current speed and current direction data at ADCP3b for the validation period.

#### A5.3.4 Model calibration and validation summary

Statistics and timeseries plots of water levels, current speeds and current directions have been presented, comparing both modelled and measured/predicted data at various sites within the project study area over the calibration and validation periods.

The results show that the hydrodynamic model is able to replicate the physical processes within the study area well, generally achieving the stringent standards outlined in Section A5.3.2, during the calibration and validation periods.

The model is able to reproduce the general variation in semi-diurnal and diurnal tidal characteristics within the model domain well, with the exception of being able to replicate the intricacies of the mid tide slack water phenomena, which occurs inside the Embley River during the diurnal ebb tidal phase. The timing of high and low waters, in addition to variations in current magnitude and direction, are also typically well captured by the model.

Although not explicitly discussed earlier, the RMS deviation values show some variability between the modelled and measured water levels through the calibration and validation periods but otherwise show consistency in the modelled water levels and currents relative to the measured data.

Given the proposed application of this model, the calibration and validation exercise undertaken demonstrates that the model is sufficiently well calibrated for this type of study. The calibrated hydrodynamic model has subsequently been used to provide inputs to the sediment transport modelling, which in turn has been used to improve the understanding of sediment transport pathways and quantify transport rates within the Weipa and Amrun regions. Details associated with the sediment transport model are discussed in Section A7.

## A6 Wave model

The wave model utilises the same mesh and bathymetry as the hydrodynamic model described in the previous sections. In addition, the spatially varying water level from the hydrodynamic model was applied to the spectral wave model to ensure any influence from the varying water levels on the wave conditions was included.

### A6.1 Wave boundary conditions

Sensitivity testing was undertaken to determine the most appropriate wave boundary conditions to apply to the model. Boundary conditions were developed based on a global wave model (WaveWatch III) and based on the measured wave conditions at the Albatross Bay waverider buoy (WRB). It was found that boundary conditions derived from the Albatross Bay WRB resulted in the best model calibration.

During the dry season the wave direction measured at the Albatross Bay WRB shows that the waves are travelling away from the shoreline. These waves are generated by local winds from a south-east to easterly direction and so cannot be represented by an offshore wave boundary. Therefore, local wind conditions from the Bureau of Meteorology Weipa Airport weather station were included in the model to allow the generation of these local wind waves within the estuaries, Albatross Bay and further offshore.

### A6.2 Model calibration and validation

The wave model was calibrated to measured wave conditions at the Albatross Bay WRB for the wet season period from the start of January to the end of March 2018. This period was selected as it includes a range of wave conditions, including a large tropical cyclone (TC Nora), and water quality data was also collected over the period meaning that it can be used to calibrate the sediment transport model (see Section A7). Following the model calibration, the wave model was validated to measured wave conditions at the Albatross Bay WRB for the 2018 dry season (start of April to end of June 2018).

The measured and modelled wave conditions during the model calibration and validation periods are shown in Figure 18 and Figure 19, respectively. In addition, a quantitative comparison of measured and modelled wave height percentiles is shown for the validation and calibration periods in Table 9. The plots and table show that the wave model provides a realistic representation of the measured wave conditions (wave height, period and direction) at the Albatross Bay WRB during both the wet and dry seasons. The correlation between the measured and modelled wave height over the calibration and validation periods is shown in Figure 20. The plot shows a good correlation up to an  $H_s$  of 3 m, and then the model starts to underestimate the wave heights. These extreme wave heights all occurred during TC Nora and given the complexities associated with accurately representing wave conditions during a tropical cyclone, the underestimation is not considered to be an issue of major concern.

**Table 9.  $H_s$  calibration and validation percentile statistics at Albatross Bay WRB.**

Percentile	Calibration Period		Validation Period	
	Measured $H_s$ (m)	Modelled $H_s$ (m)	Measured $H_s$ (m)	Modelled $H_s$ (m)
5 <sup>th</sup> Percentile	0.14	0.09	0.14	0.09
10 <sup>th</sup> Percentile	0.18	0.15	0.17	0.11
20 <sup>th</sup> Percentile	0.24	0.25	0.22	0.18
50 <sup>th</sup> Percentile	0.44	0.53	0.30	0.32
80 <sup>th</sup> Percentile	0.81	0.84	0.42	0.50
90 <sup>th</sup> Percentile	1.04	1.05	0.54	0.62
95 <sup>th</sup> Percentile	1.28	1.31	0.63	0.71
99 <sup>th</sup> Percentile	2.18	2.32	0.77	0.82



**Figure 18. Comparison between measured and modelled wave conditions at the Albatross Bay WRB during the calibration period.**





**Figure 19. Comparison between measured and modelled wave conditions at the Albatross Bay WRB during the validation period.**

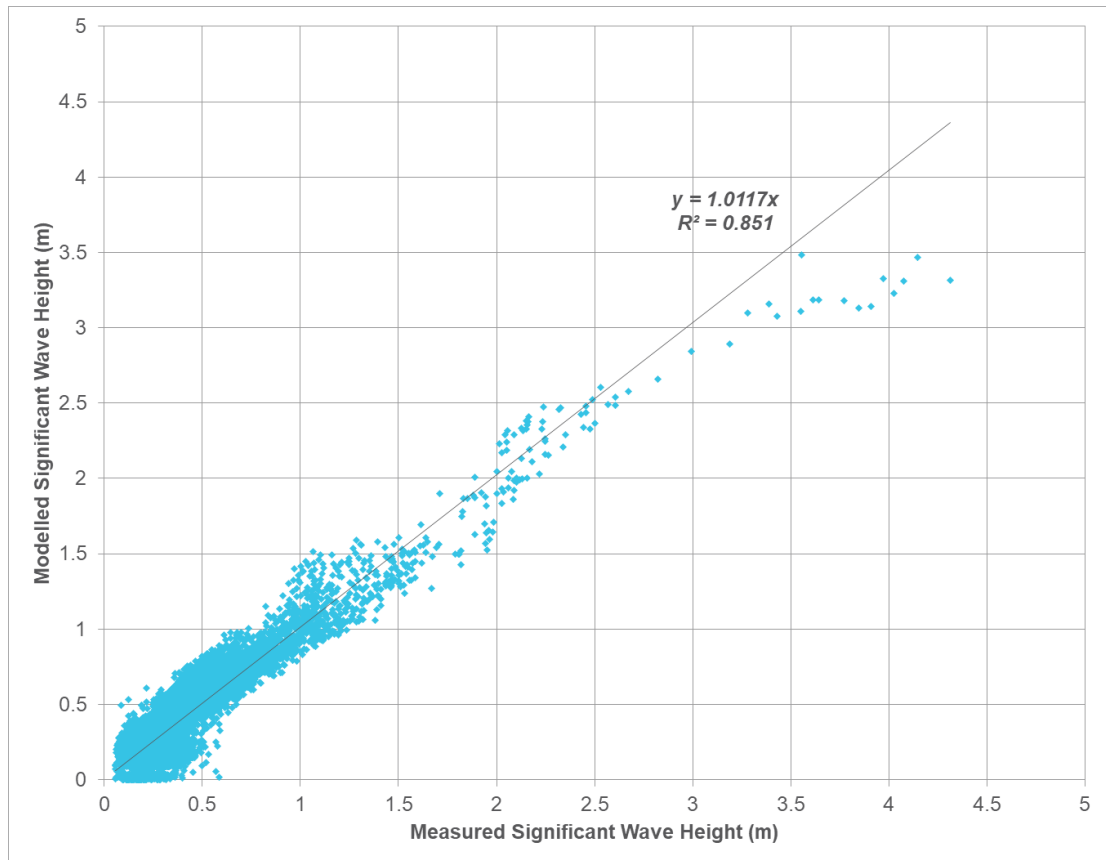


Figure 20. Correlation between measured and modelled  $H_s$  at Albatross Bay WRB.

## A7 Sediment transport model

The sediment transport model utilises the same model mesh and bathymetry as the hydrodynamic and wave models described in the previous sections. The sediment transport model is driven by the hydrodynamic and wave models, with the results from these models directly influencing when sediment can be resuspended or deposited and where the sediment is transported. The sediment transport model of the natural conditions at Weipa and Amrun was set up in two-dimensional depth averaged mode as the underlying equations were all derived in two dimensions.

### A7.1 Model set up

The sediment transport model for the Weipa and Amrun port regions was configured so that the sediment on the seabed that was available for resuspension and transport was representative of the majority of the sediment in region. Three separate sediment types were included in the model: medium to coarse silt, very fine to medium silt and clay.

The model was run with no sediment in suspension at the start to allow the model to naturally resuspend sediment based on the metocean conditions. There was no additional input of suspended sediment at the model boundaries, which meant that the only sediment in the numerical model was the sediment on the seabed at the start of the simulation. The initial map of bed sediment adopted for the model simulations was defined by running the model over a three month wet season (as this is when the majority of sediment transport occurs) simulation multiple times to redistribute the bed sediment towards a dynamic equilibrium state representative of the natural environment. In areas where the sediment is known to be predominantly sand or gravel, no bed sediment was included in the initial map of bed sediment. The model was also setup to include flocculation when the SSC exceeds 10 mg/l,

this process is expected to occur naturally in the area and so it is important to include it in the model (DHI, 2017b<sup>10</sup>).

Sensitivity testing was undertaken as part of the model calibration process to determine the optimum parameter settings to adopt in the model to represent the measured water quality data. As part of the sensitivity testing the following parameters were defined to control when erosion (resuspension) and deposition occur:

- Critical shear stress for erosion = 0.2 N/m<sup>2</sup>; and
- Critical shear stress for deposition = 0.1 N/m<sup>2</sup>.

## A7.2 Model calibration and validation

Due to the inherent complexities associated with sediment transport modelling (including having to accurately represent the hydrodynamic and wave conditions and the properties of the sediment on the bed and in the water column), quantitative comparisons between measured and modelled data are not commonly adopted. The typical approach is for the modelled data to be compared graphically with measured data at specific sites for both the calibration and validation periods to demonstrate that the numerical model is able to approximately replicate the spatial and temporal patterns shown in the measured SSC.

Demonstrating that the model can replicate the overall spatial and temporal patterns in SSC provides confidence that the model is representing the key processes which mobilise the sediment as well as the processes which transport the sediment. Recently, the best practise approach for sediment transport modelling has been to adopt a quantitative validation method when sufficient measured data are available (Los & Blaas, 2010<sup>11</sup>). The quantitative validation approach has been adopted for this assessment, with the OSPAR cost function (CF), or normalised mean absolute error, applied to quantify the performance of the sediment transport model (Los et al, 2008<sup>12</sup>).

As with the wave model, the sediment transport model was calibrated for the 2018 wet season period (January to March inclusive) and validated for part of the 2018 dry season (April to June inclusive). The wet season was selected as the calibration period as this was when the measured turbidity was most variable due to the changeable wave conditions and so allowed the model parameters to be adjusted to best represent the sediment transport for a range of wave conditions. The calibration and validation periods were selected as they represent a range of metocean and water quality conditions, including large waves and strong winds resulting in high turbidity during a tropical cyclone as well as periods with offshore winds and small waves resulting in low turbidity during periods of the dry season. In addition, measured turbidity data (which were subsequently converted to SSC based on correlations derived from water samples) were available over these periods at up to five monitoring sites.

The measured and modelled SSC at four of the monitoring sites<sup>13</sup> during the wet season calibration period are shown in Figure 21 to Figure 24. The plots show that the model is able to provide a realistic representation of the variability in SSC during the wet season and during cyclonic conditions both over time due to variable metocean conditions and between the sites due to their local environmental conditions. The graphical comparison between the measured and modelled SSC presented here demonstrates that the model can be considered to be well calibrated. This provides confidence that the model is representing the key processes (tidal currents and waves) that mobilise sediment from the seabed in the

<sup>10</sup> DHI, 2017b. MIKE 21 & MIKE 3 Flow Model FM – Mud Transport Module, Scientific Documentation.

<sup>11</sup> Los, F.J & Blaas, M., 2010. Complexity, accuracy and practical applicability of different biogeochemical model versions. *Journal of Marine Systems* 81, 44-74.

<sup>12</sup> Los, F.J., Villars, M.T. & Van der Tol, M.W.M., 2008. A 3-dimensional primary production model and its applications to the North Sea. *Journal of Marine Systems* 74, 259-294.

<sup>13</sup> Insufficient reliable data was available at WQ1 to allow a comparison to be made, for further details see Section 2.3 of the main report.

Weipa and Amrun regions as well as the processes that transport and subsequently deposit the sediment.

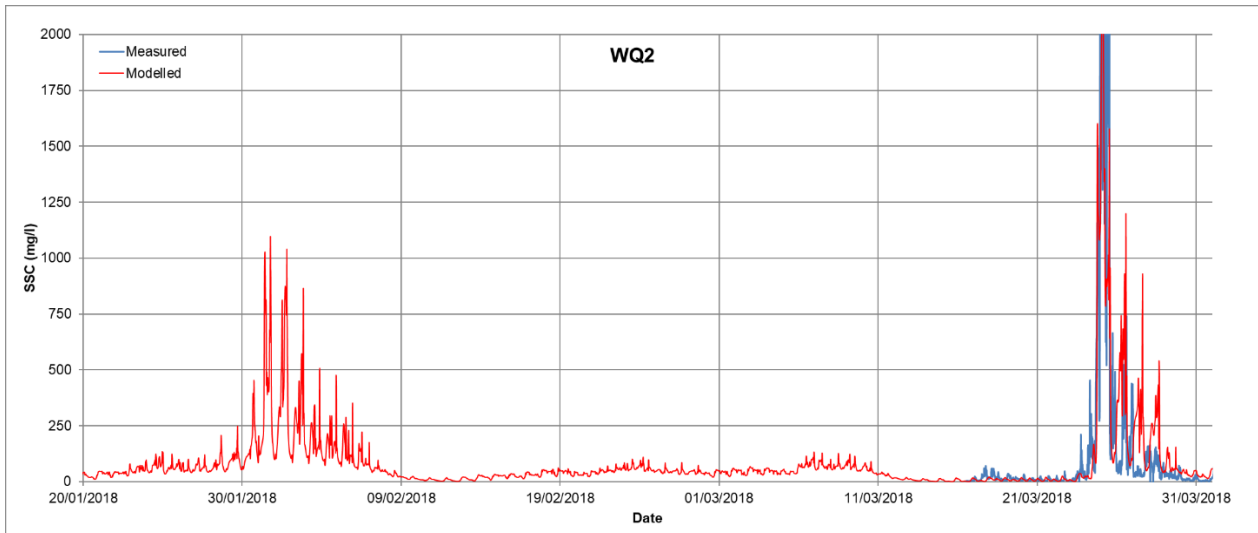


**Figure 21. Measured and modelled SSC at WQ2 during the wet season model calibration period. Note: measured data were only available from 16/03/2018.**

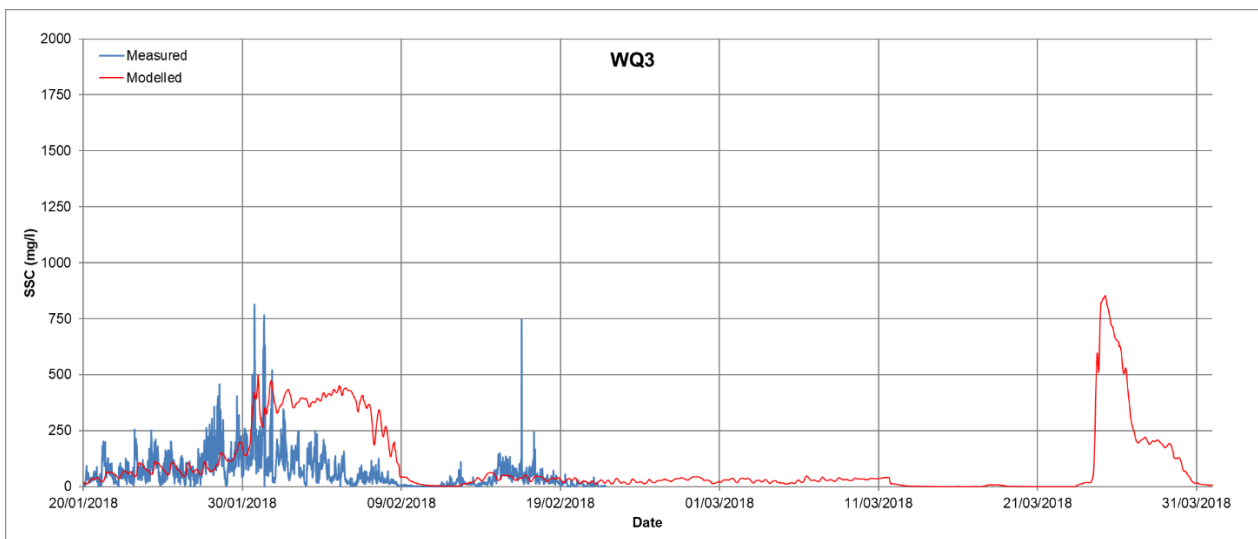


**Figure 22. Measured and modelled SSC at WQ3 during the wet season model calibration period. Note: measured data were only available up to 22/02/2018.**

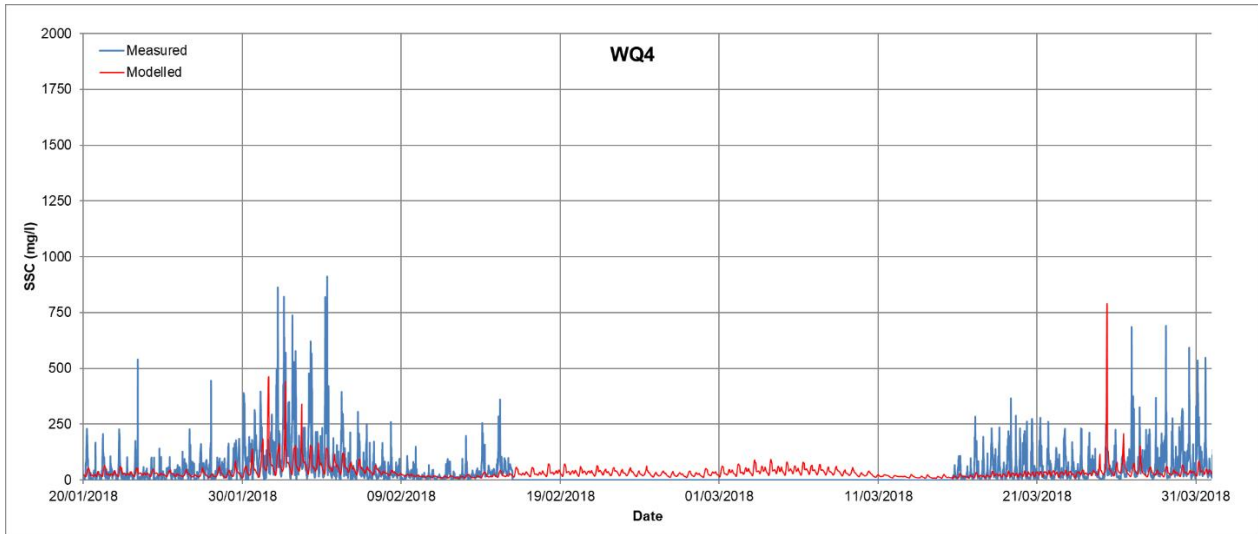


**Figure 23. Measured and modelled SSC at WQ4 during the wet season model calibration period. Note: measured data were only available from 16/02/2018 to 15/03/2018.**

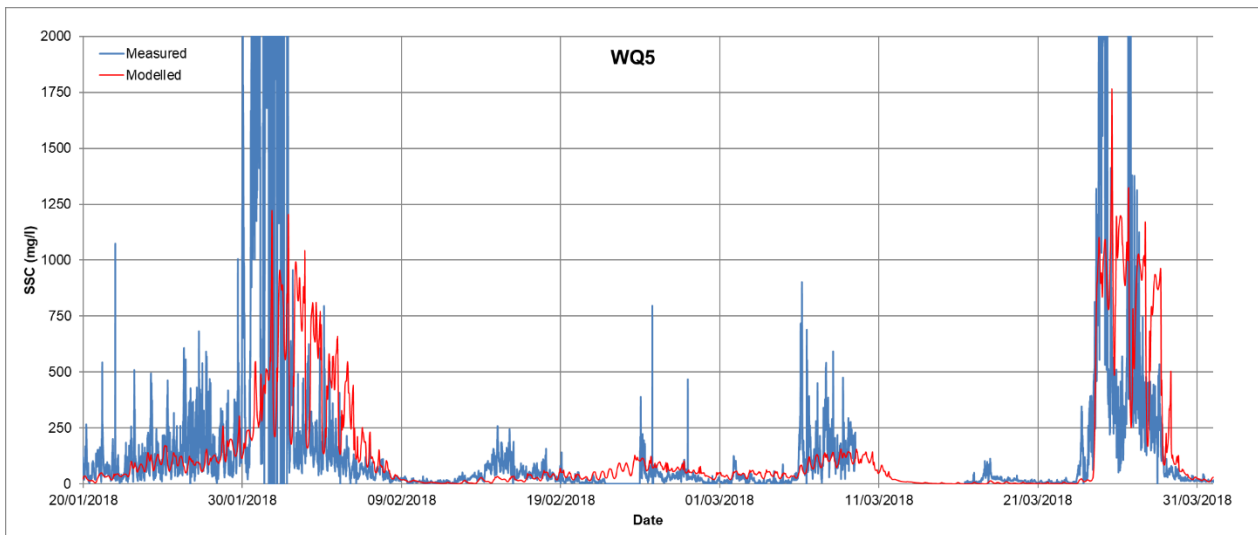


**Figure 24. Measured and modelled SSC at WQ5 during the wet season model calibration period.**

Following the model calibration during the 2018 wet season period, the model was setup with the same parameters as adopted during the calibration period to simulate the sediment transport during the 2018 dry season validation period. The modelled SSC is compared graphically with the measurements at the five monitoring sites over the validation period in Figure 25 to Figure 29. The visual comparison indicates that the model agrees well with the measured data, with the only noticeable limitation of the model being that it is not able to replicate the short duration (minutes to hours) spikes in SSC that occur at some of the sites (WQ4 and WQ5). However, the modelled SSC provides a good representation of the longer term average (e.g. 12 hourly averaged) changes in SSC that occur at these locations, which is considered to be more important to represent a quantitative sediment budget. The OSPAR CF has been calculated for all sites except for WQ3b where there was insufficient measured data. The CF value adopts the normalised mean absolute error to express the goodness of fit in terms of the standard deviation of the measured data, with  $CF < 1$  being classified as 'very good',  $1 < CF < 2$  as 'good',  $2 < CF < 3$  as 'reasonable' and any CF beyond this upper limit

classified as ‘poor’ (Los & Blaas, 2010<sup>14</sup>). The following CF values were calculated for the validation period:

- WQ1 = 1.3;
- WQ2 = 1.1;
- WQ4 = 0.6; and
- WQ5 = 0.6.

Based on these the sediment transport model performance can be considered to be between very good and good for the validation period. The validation is therefore providing confidence that the model is able to represent the key processes (tidal currents and waves) that mobilise sediment from the seabed in the Weipa and Amrun regions as well as the processes that transport and subsequently deposit the sediment over the dry season.

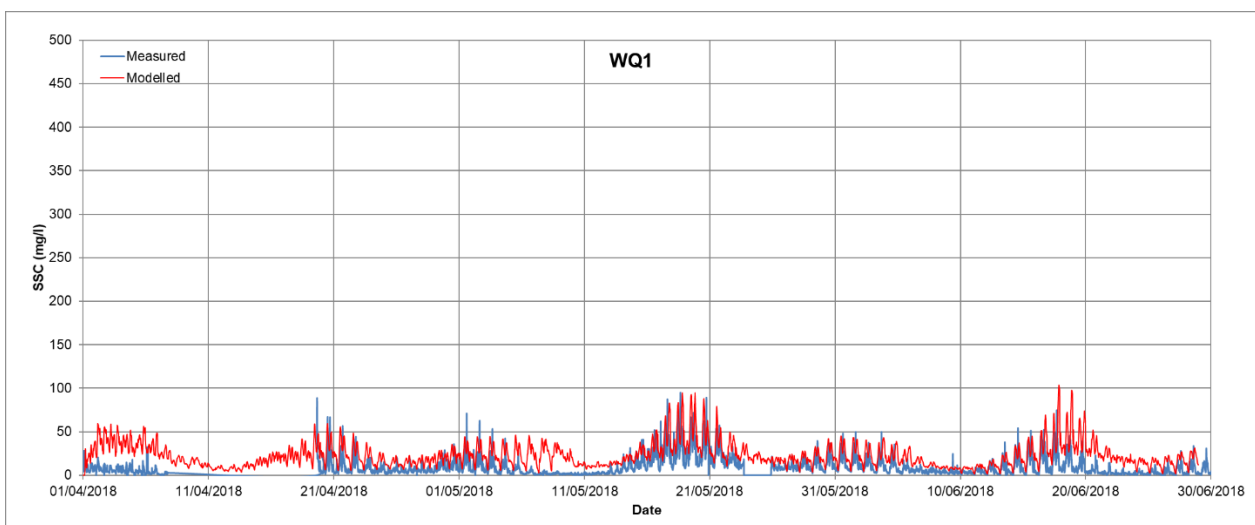


Figure 25. Measured and modelled SSC at WQ1 during the dry season model validation period.

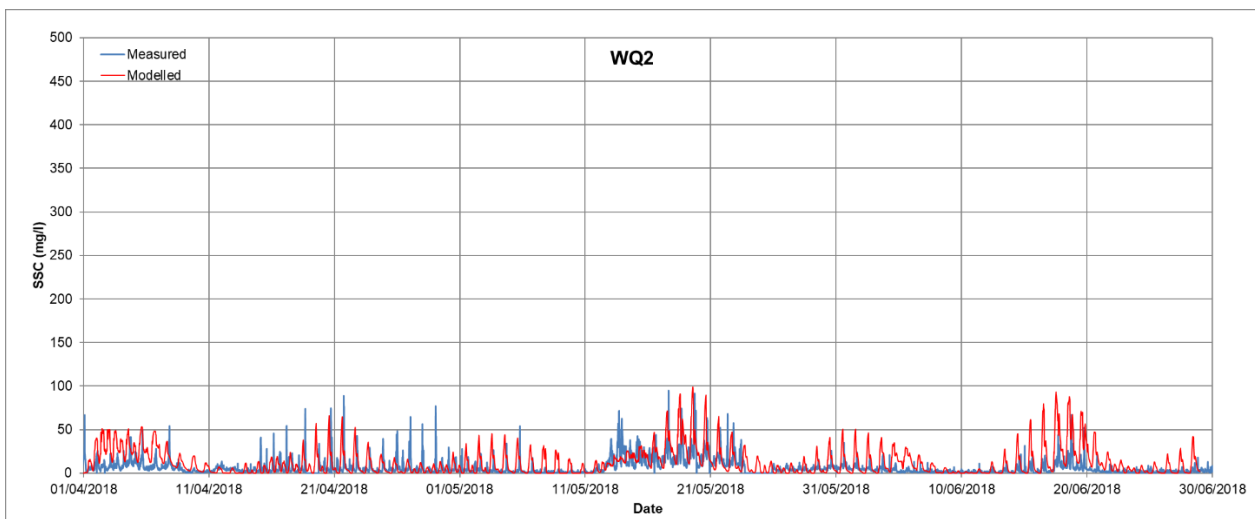
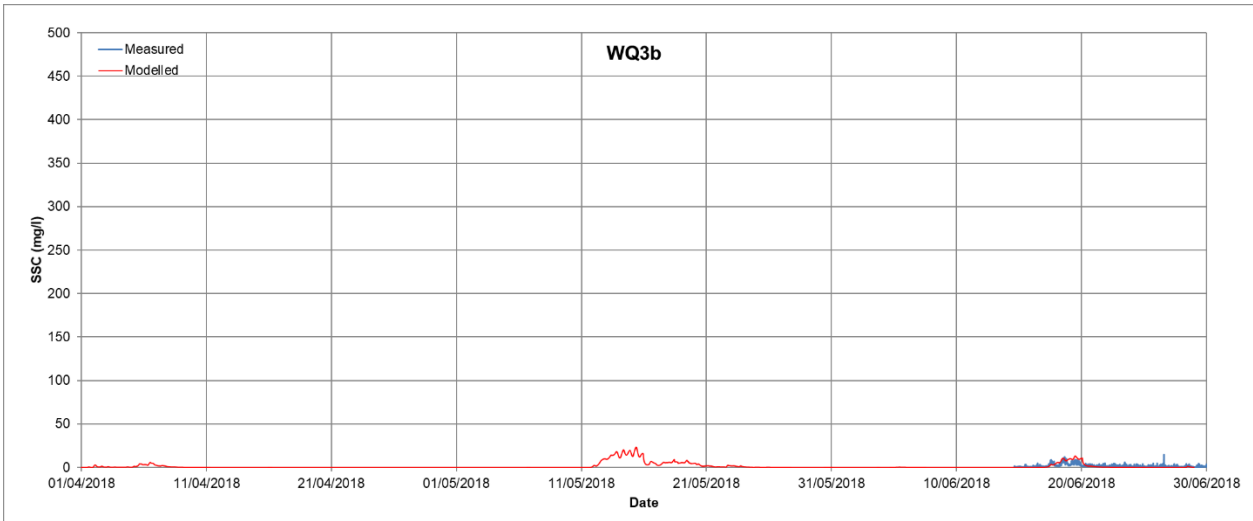
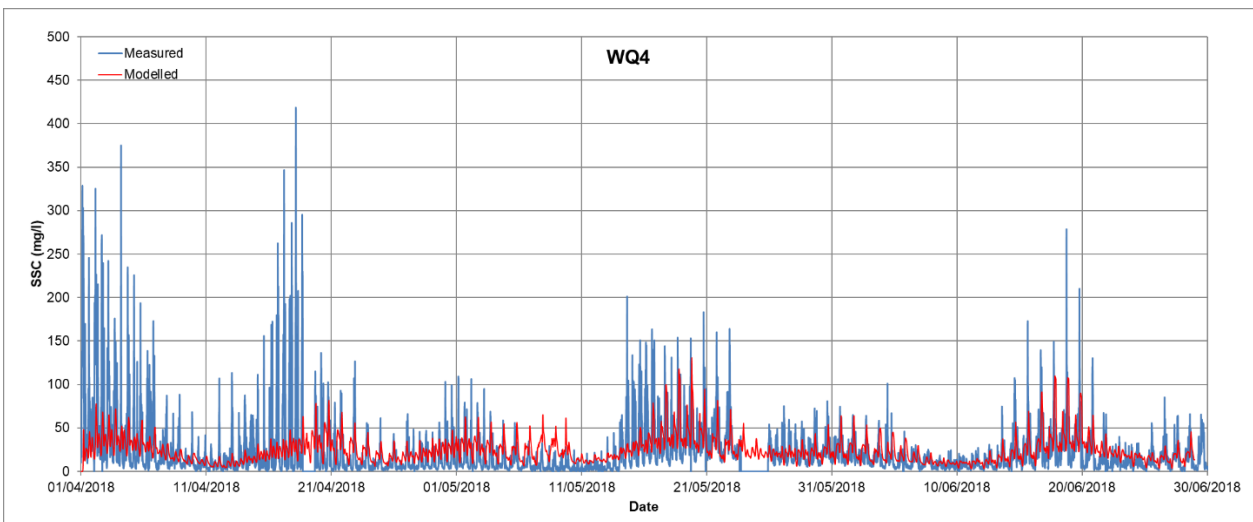


Figure 26. Measured and modelled SSC at WQ2 during the dry season model validation period.

<sup>14</sup> Los, F.J & Blaas, M., 2010. Complexity, accuracy and practical applicability of different biogeochemical model versions. *Journal of Marine Systems* 81, 44-74.



**Figure 27. Measured and modelled SSC at WQ3b during the dry season model validation period. Note: measured data were only available from 14/06/2018**



**Figure 28. Measured and modelled SSC at WQ4 during the dry season model validation period.**

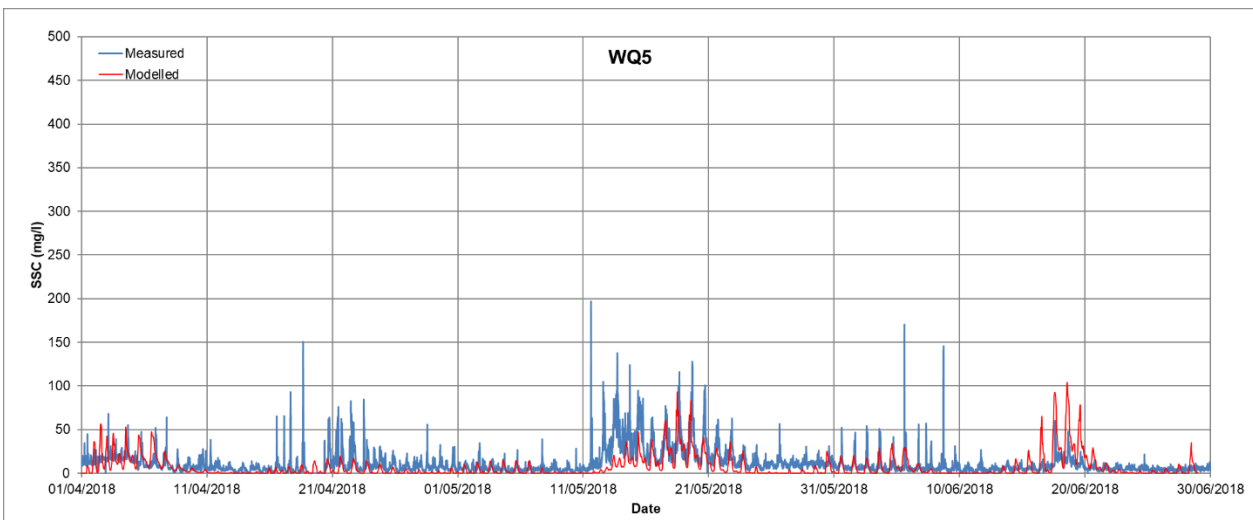


**Figure 29. Measured and modelled SSC at WQ5 during the dry season model validation period.**

## A8 Summary

This appendix has provided details of the setup, calibration and validation of a suite of numerical models used to inform the quantitative sediment budget. Hydrodynamic, wave and sediment transport models of the Weipa and Amrun region have been developed for the Project.

The calibration and validation of the hydrodynamic and wave models has demonstrated that they are generally able to accurately represent the tidal and wave conditions in the region. In addition, the calibration and quantitative validation of the sediment transport model compared to the measured water quality data provides further evidence that the model is accurately representing the key processes that mobilise sediment from the seabed in the Weipa and Amrun regions as well as the processes that transport and subsequently deposit the sediment.

It can therefore be concluded that the suite of models developed can be used as a tool to provide an estimate of the sediment budget for the Weipa and Amrun regions.